COMPUTER OPTIMIZATION OF WATER-AUGMENTED TURBOFAN CONCEPT AND DEVELOPMENT OF A TEST FACILITY FOR TWO-PHASE FLOW

Randolph Grant Watson

United States
Naval Postgraduate School

THESIS

COMPUTER OPTIMIZATION OF WATER-AUGMENTED TURBOFAN CONCEPT
AND
DEVELOPMENT OF A TEST FACILITY FOR TWO-PHASE FLOW

by

Randolph Grant Watson

June 1969

Computer Optimization of Water-Augmented Turbofan Concept and Development of a Test Facility for Two-Phase Flow

by

Randolph Grant Watson
Lieutenant, United States Navy
B.S.A.E., University of Illinois, 1962

Submitted in partial fulfillment of the
requirements for the degree of

AERONAUTICAL ENGINEER

from the

NAVAL POSTGRADUATE SCHOOL
June 1969

ABSTRACT

A turbofan engine propulsion system in which large amounts of water are injected into the fan discharge duct is investigated with the goal of increasing both the thrust and propulsive efficiency while retaining the light-weight qualities of a standard turbofan engine. A parametric computer analysis is used to examine the effect of several variables, including water-to-gas generator air ratio, water injection velocity, fan duct pressure loss, and fan duct thermal and dynamic nonequilibrium, upon thrust and propulsive efficiency. In addition, the design parameters of fan pressure ratio and fan bypass ratio are examined for their optimum values, and optimum operating combinations of water-to-gas ratio and water injection velocity are determined.

A test apparatus is developed for the direct measurement of wall friction force in two-phase flows. A computer program is presented to reduce experimental data and compare with pressure drop predicted by two empirical correlations.

TABLE OF CONTENTS

LIST OF FIGURES

TABLE OF SYMBOLS

SYMBOL	MEANING
a	sound speed (ft/sec)
A	area (ft^2)
BR	bypass ratio
Cp	specific heat at constant pressure (ft-lb/slug-deg R)
D	inside pipe diameter (ft)
f	friction factor
FAR	fuel-air ratio
H	enthalpy (ft-lb/slug)
HVF	lower heating value of fuel (BTU/lbm)
ID	inside diameter
K	friction coefficient for valves or fittings
L	test section length (ft)
LVF	liquid volume fraction
M	mach number
MR	mixture ratio
MW	molecular weight
$\dot{m}$	mass flow rate (slug/sec)
P	pressure (lb/ft^2)
ΔP	pressure drop (lb/ft^2)
R	gas constant (ft-lb/slug-deg R)
Re	Reynolds number
S	entropy (ft-lb/slug-deg R)
ST	specific thrust $\dfrac{(lb_f\text{-sec})}{lb_m}$
T	temperature (deg R)
TH	thrust (lb)
V	velocity (ft/sec)
$\bar{V}$	mean velocity (ft/sec)
W	work (ft-lbf/slug)
WGR	water-to-gas generator air ratio
X	specific humidity
γ	ratio of specific heats
η	efficiency

SYMBOL	MEANING
μ	viscosity coefficient (lbm/ft-sec)
ρ	density (slug/ft^3)
Φ	Lockhart-Martinelli correlation parameter
χ	Lockhart-Martinelli flow modulus
Ψ	dimensionless group equal to fL/D $+ \sum K$

SUBSCRIPT	MEANING
A	air
B	burner
c	refers to cool air
C	compressor
D	gas generator diffuser
f	saturated liquid
fg	change by evaporation
fu	fuel
F	fan
FD	fan diffuser
g	saturated vapor
G	actual gas flow
G*	fictitious all-gas flow
h	refers to hot air
i	refers to property at station (i), i = 1,2...
INJ	water injection
I	refers to state reached by isentropic process
L	actual liquid flow
L*	fictitious all-liquid flow
N	gas generator nozzle
p	water injection pump
PR	propulsive
PV	partial vapor
R	velocity recovery
REFA	reference to ambient air
T	total, turbine
TP	two-phase
W	water
V	vapor

ACKNOWLEDGEMENT

The author wishes to express his sincere appreciation to those who assisted in making this report possible. In particular, the continuous encouragement and willingness to assist shown by the author's advisor, Dr. R. D. Zucker, is greatly appreciated. The technicians who so ably assisted in the construction and instrumentation of the two-phase flow test rig also deserve appreciation.

Finally, the author wishes to thank the Office of Naval Research Foundation for the grant which made the project economically possible and the United States Navy for making possible the entire course of study at the Naval Postgraduate School.

I. COMPUTER OPTIMIZATION OF WATER-AUGMENTED TURBOFAN CONCEPT

A. SOURCE AND BACKGROUND

Transportation by water-borne craft is one of the oldest and most economical means known to man. Although many improvements have been made in payload carrying ability, navigational ability and propulsion systems over the centuries, the degree of improvement in the speed of water craft has been quite small. It has become desirable, from both a military and civilian point of view, to find new light-weight propulsion systems for water craft which provide significant increases in speed capability while retaining the load carrying ability and efficiency of previous sea transportation systems.

The feasibility of producing a ship or boat capable of sustained high speeds with relatively large payloads and reasonable efficiency depends largely upon two factors: drag reduction and the availability of a light-weight efficient propulsion system. Drag reduction can be achieved by use of hydrofoils, the captured air bubble concept or recent boundary layer control schemes including blowing, suction and polymer injection. The development of a suitable propulsion system, however, has not be quite so active.

The turbofan provides relatively high thrust and very low system weight compared to more conventional marine propulsion systems. However, in the speed range contemplated for marine craft, 100 knots and below, the propulsive efficiency of the turbofan is too low to allow serious consideration.

Early methods of increasing the thrust and propulsive efficiency in turbojet and turbofan engines centered on injection of water into the compressor or exhaust section. This method of water injection has been used primarily in aircraft applications for short periods only and has several drawbacks for marine applications, among which are stiff requirements on water purity due to machinery corrosiveness and energy transfer losses caused by water evaporation due to mixing with hot gases. A more recent proposal has been to inject large quantities of water into the fan discharge duct of a turbofan engine, thus overcoming the two primary drawbacks mentioned above because the gases are relatively cool and the water contacts no moving machinery. Consequently, sea water can be used in large quantities.

Several investigators have made preliminary studies concerning the feasibility of using water-augmented air-jets for water craft propulsion. Muench and Keith [Ref. 1] conducted a preliminary parametric study of possible propulsive efficiencies and concluded that reasonable efficiencies can be realized. Davison and Sadowski [Ref. 2] applied their analysis to a particular existing turbofan engine design with water injected into the fan discharge duct. Their analysis showed that although efficiencies were slightly lower than for other more conventional marine propulsion systems, the extremely low system weight more than compensated for the efficiency deficit. Quandt [Ref. 3] has assembled some recent theoretical and experimental techniques concerning "the gas-phase-continuous two-phase jet system."

Knudson [Ref. 4] followed the work of Davison and Sadowski in proposing the injection of large amounts of sea water into the fan discharge duct of a turbofan engine to achieve increased thrust and propulsive efficiency. The general arrangement of the water-augmented turbofan engine is presented in Fig. 1. Knudson was the first to consider the effects of velocity slip ratios and temperature ratios between water droplets and air in the fan mixing duct and nozzle. The effects of variation of water- to-gas mass flow ratio and water injection velocity were also examined.

The present analysis undertakes a more detailed computer study which includes the pump work required to inject the water at velocities greater than craft velocity. A wide range of design and operating parameters is examined for the effect on overall thrust and propulsive efficiency. Some minor programing errors were discovered in Ref. 4 and these are corrected in the present analysis.

B. WATER-AUGMENTED TURBOFAN ANALYSIS

The analysis which follows is based on that given by Knudson with appropriate changes and corrections for the present use. The analysis differs from that for a normal "dry" turbofan in the fan mixing duct and fan nozzle sections due to the injection of water. The equations are developed in a manner similar to their use in the computer program.

1. Assumptions

Following general practice in the analysis of turbofan engines the air was assumed to behave as a perfect gas with two constant values of specific heat ratio, γ , 1.4 for the relatively cool sections of the system and 1.33 for the high temperature sections of the engine. In the burner section of the engine the arithmetical mean of the two values of specific heat ratio was used since the air transitioned from the cool to the hot state. It was assumed that no heat was transferred except in the combustion chamber and that no work was transferred other than in the compressor, fan and turbine. The mixing duct area was assumed constant and it was also assumed that only converging nozzles were used in the engine.

Finally, it was assumed that completely dry air entered the system. The external drag of the water inlet scoop was not included in the analysis since this factor is dependent on the actual scoop design employed.

2. Gas Generator Diffuser

The ambient total pressure is determined from

$$P_{TO} = P_{AO}\left(1 + \frac{\gamma_c - 1}{2} M_0^2\right)^{\frac{\gamma_c}{\gamma_c - 1}} \tag{1}$$

and the diffuser efficiency is defined by

$$\eta_D = \frac{P_{T1} - P_{AO}}{P_{TO} - P_{AO}} \tag{2}$$

Thus

$$P_{T1} = P_{AO} + \eta_D (P_{TO} - P_{AO}) \tag{3}$$

The total temperature remains constant through the diffuser and is

$$T_{T1} = T_{TO} = T_{AO}\left(1 + \frac{\gamma_c - 1}{2} M_0^2\right) \tag{4}$$

The total enthalpy is

$$H_{T1} = C_{PC}(T_{T1} - T_{AO}) + H_{REFA} \tag{5}$$

where C_{pc} is the cool temperature specific heat and H_{REFA} is the enthalpy of the air at the ambient static temperature, T_{AO}.

3. Compressor

The ideal (isentropic) temperature at the compressor exit for a specified total pressure ratio, P_{T2}/P_{T1}, is

$$T_{T2I} = T_{T1}\left(P_{T2}/P_{T1}\right)^{\frac{\gamma_c - 1}{\gamma_c}} \tag{6}$$

If the compressor efficiency, η_c , is defined as the ratio of the isentropic compressor work to the actual compressor work, the total enthalpy at the compressor exit is

$$H_{T2} = \frac{C_{pc}(T_{T2I} - T_{T1})}{\eta_c} + H_{T1} \tag{7}$$

and the corresponding total temperature is

$$T_{T2} = \frac{H_{T2} - H_{REFA}}{C_{pc}} + T_{AO} \tag{8}$$

4. Burner

The specific heat in the burner section is taken as

$$C_{pB} = \frac{C_{pc} + C_{ph}}{2} \tag{9}$$

The burner exit total enthalpy is

$$H_{T3} = C_{pB}(T_{T3} - T_{T2}) + H_{T2} \tag{10}$$

where the total temperature at the burner outlet, T_{T3}, is fixed by the maximum allowable turbine inlet total temperature. The energy equation through the burner can be written

$$\dot{m}_c H_{T2} + \dot{m}_{fu}(H_{fu2} + \eta_B HVF) = (\dot{m}_c + \dot{m}_{fu}) H_{T3} \tag{11}$$

where $\dot{m}_C$ is the compressor mass flow rate, $\dot{m}_{fu}$ is the fuel mass flow rate, H_{fu2} is the fuel enthalpy prior to entering the burner, η_B is the burner efficiency, HVF is the heating value of the fuel and H_{T3} is the total enthalpy at the burner outlet. If it is assumed that the fuel injection temperature is equal to the air temperature at the injection point and that the energy needed to vaporize the fuel is included by choosing the lower heating value of the fuel, then the fuel-air ratio can be represented by

$$FAR = \frac{\dot{m}_{Fu}}{\dot{m}_C} = \frac{C_{ph}(T_{T3} - T_{T2})}{\eta_B(HVF) - C_{ph}(T_{T3} - T_{T2})} \tag{12}$$

5 Turbine

The total work output of the turbine must equal the total work input to the other components of the engine.

$$\dot{m}_T(H_{T3} - H_{T4}) = \dot{m}_C(H_{T2} - H_{T1}) + \dot{m}_F(H_{T7} - H_{T6}) + \dot{m}_W W_P$$

where $\dot{m}_T$ is the turbine mass flow rate, $\dot{m}_F$ is the fan mass flow rate, $\dot{m}_W$ is the water mass flow rate and W_P is the water injection pump work per unit mass given by

$$W_P = \frac{V_{W7}^2 - (\eta_R V_0)^2}{2\eta_P} \tag{13}$$

where V_{W7} and V_0 are the water injection velocity and the craft velocity, respectively, η_R is the water intake system velocity recovery factor and η_P is the pump efficiency. The total temperature at the turbine outlet is

$$T_{T4} = T_{T3} - \frac{H_{T3} - H_{T4}}{C_{ph}} \tag{14}$$

If the turbine efficiency is defined as the ratio of actual work output to isentropic work output, then

$$T_{T4I} = T_{T3} - \frac{H_{T3} - H_{T4}}{\eta_T C_{ph}} \tag{15}$$

and

$$P_{T4} = P_{T4I} = P_{T3}\left(T_{T4I}/T_{T3}\right)^{\frac{\gamma_h}{\gamma_h - 1}} \tag{16}$$

6. Gas Generator Nozzle

The nozzle must discharge to atmospheric pressure (unless choked) and thus the ideal static temperature at the nozzle exit is

$$T_{A5I} = T_{T4}\left(P_{A5}/P_{T4}\right)^{\frac{\gamma_h - 1}{\gamma_h}} \tag{17}$$

Under assumption of constant specific heats, the nozzle efficiency can be represented by

$$\eta_N = \frac{T_{T4} - T_{A5}}{T_{T4} - T_{A5I}} \tag{18}$$

Thus, for a given nozzle efficiency, the static temperature at the nozzle exit, T_{A5}, can be found and the nozzle exit velocity can be determined from

$$V_{A5} = \sqrt{2\, C_{ph}(T_{T5} - T_{A5})} \tag{19}$$

The exit mach number is given by

$$M_5 = \frac{V_{A5}}{a_5} = \frac{V_{A5}}{\sqrt{\gamma_h R\, T_{A5}}} \tag{20}$$

If the exit mach number exceeds unity, the computations are adjusted to produce sonic velocity at the exit with the appropriate exit pressure.

7. <u>Fan Diffuser and Fan</u>

The fan diffuser analysis is identical to that of the gas generator diffuser. Similarly, the fan analysis corresponds to the compressor analysis.

8. <u>Fan Mixing Duct Water Injection Analysis</u>

The analysis of the water injection process in the fan mixing duct considers the possibility of variation in the thermal and dynamic equilibrium in the fan mixing duct and the fan nozzle, respectively, and static pressure changes between the water injection plane (fan mixing duct entrance) and the fan mixing duct exit (stations 7 and 8, respectively, in Fig. 1).

The following terms are used throughout the analysis and are defined here for convenience:

Bypass Ratio (BR)	$= \dot{m}_F/\dot{m}_C$
Water to Gas Generator Air Ratio (WGR)	$= \dot{m}_W/\dot{m}_C$
Mixture Ratio (MR)	$= \dot{m}_W/\dot{m}_F$

The mean velocity of the two-phase flow is defined by

$$\dot{m}_F V_A + \dot{m}_W V_W = (\dot{m}_F + \dot{m}_W)\bar{V}$$

and the mean velocity is thus

$$\bar{V} = \frac{V_A + MR(V_W)}{1 + MR}$$

The momentum equation in the mixing duct is

$$(\dot{m}_F + \dot{m}_W)\,d\bar{V} = -A\,dP \tag{21}$$

If the area occupied by the air is $\dot{m}_F/\rho_A V_A$ and the area occupied by the water is $\dot{m}_W/\rho_W V_W$, the total flow area can be written

$$A = \dot{m}_F\left(\frac{1}{\rho_A V_A} + \frac{MR}{\rho_W V_W}\right) \tag{22}$$

Combining equations (21) and (22) and assuming a constant area mixing duct the resulting equation can be integrated yielding

$$\bar{V}_8 = \bar{V}_7 + (P_{A7} - P_{A8})\left(\frac{1}{1+MR}\right)\left(\frac{1}{\rho_{A7} V_{A7}} + \frac{MR}{\rho_{W7} V_{W7}}\right) \tag{23}$$

In order to conduct an energy analysis through the mixing duct it is necessary to consider the effects of vaporization of water. The values H_f, H_{fg}, S_f and S_{fg} were determined for the computer using least squares cubic approximations of the data in the steam tables [Ref. 5] for the temperature range 510-660 degrees Rankine. The equations used are shown at the beginning of the computer program in Appendix II. The values of H_g and S_g are found from the equations

$$H_g = H_f + H_{fg}$$

$$S_g = S_f + S_{fg}$$

The partial pressure of water vapor, P_{PV}, in atmospheres is determined from equation (12) in Ref. 5.

$$\log_{10}(P_{PV}) = \log_{10}(P_c) - \frac{\bar{X}}{T}\cdot\left[\frac{A + B\bar{X} + C\bar{X}^3}{1 + D\bar{X}}\right] \tag{24}$$

The specific humidity, X, of the mixture is defined as the ratio of the mass of the water vapor to the mass of the dry air in the duct. Using the perfect gas relations for air and water vapor it can be shown that

$$X_8 = \left(\frac{P_{PV8}}{P_{A8} - P_{PV8}}\right)\left(\frac{MW_V}{MW_A}\right)\left(\frac{T_{A8}}{T_{V8}}\right) \tag{25}$$

where MW is the molecular weight and subscripts V and A signify water vapor and air, respectively. The vapor temperature is assumed equal to the air temperature.

The energy equation through the mixing duct is

$$\dot{m}_F\left(H_{A7}+\frac{V_{A7}^2}{2}\right)+\dot{m}_{W7}\left(H_{f7}+\frac{V_{W7}^2}{2}\right) = \dot{m}_F\left(H_{A8}+\frac{V_{A8}^2}{2}\right)$$

$$+\left(\dot{m}_{W7}-X_8\dot{m}_F\right)\left(H_{f8}+\frac{V_{W8}^2}{2}\right)+X_8\dot{m}_F\left(H_{g8}+\frac{V_{A8}^2}{2}\right) \quad (26)$$

The analysis thus consisted of the equations (23), (25) and (26) with six unknowns: V_{W8}, V_{A8}, T_{W8}, T_{A8}, P_{A8} and X_8. A solution is found by specifying values for three ratios of unknowns:

$$TR8WA = T_{W8}/T_{A8} \quad (27)$$

$$VR8WA = V_{W8}/V_{A8} \quad (28)$$

$$PR87 = P_{A8}/P_{A7} \quad (29)$$

By varying these ratios, the effects of departure from thermal or dynamic equilibrium at the mixing duct exit and static pressure change through the duct can readily be examined. Although six equations with six unknowns exist, an explicit solution is not possible because equations (25) and (26) contain involved functions of T_{W8} through the enthalpy and partial pressure terms. However, it is possible to determine V_{A8} and V_{W8} using equations (23), (28) and (29). The remaining three equations, (25), (26) and (27), are then manipulated to obtain a function of T_{A8} only (called FUN). A Newton-Raphson iterative solution is then used in the form

$$T_{A8j} = T_{A8j-1} - FUN/DFUN \quad (30)$$

where subscript j indicates the j^{th} approximation, j-1 indicates the $(j-1)^{th}$ approximation, etc., and DFUN is the derivative of FUN with respect to T_{A8}, both functions being evaluated at T_{A8j-1}. The correct value of T_{A8} is obtained when the absolute value of FUN/DFUN becomes zero. It is then a simple matter, knowing T_{A8}, to determine X_8 and T_{W8} from equations (25) and (27).

9. Fan Nozzle Analysis

Following reasoning similar to that in the preceding section the specific humidity at the fan nozzle exit is

$$X_9 = \left(\frac{P_{PV9}}{P_{A9} - P_{PV9}}\right)\left(\frac{MW_V}{MW_A}\right)\left(\frac{T_{A9}}{T_{V9}}\right) \tag{31}$$

The constant area assumption made to allow solution of the momentum equation for the fan mixing duct analysis obviously does not apply through the nozzle. The approach taken (as in Ref. 2) is that the net change in entropy through the nozzle is zero.

$$(S_9 - S_8)_{AIR} + (S_9 - S_8)_{WATER} = 0 \tag{32}$$

Equation (32) when expanded gives

$$\dot{m}_F\left[C_{PC}\ln\left(\frac{T_{A9}}{T_{A8}}\right) - R\ln\left(\frac{P_{A9}}{P_{A8}}\right)\right] + \left[(\dot{m}_{W7} - X_9\dot{m}_F)S_{f9} + \dot{m}_F X_9 S_{g9}\right]$$

$$-\left[(\dot{m}_{W7} - X_8\dot{m}_F)S_{f8} + \dot{m}_F X_8 S_{g8}\right] = 0 \tag{33}$$

The exit pressure, P_{A9}, must equal atmospheric pressure, leaving two equations, (31) and (33), with unknowns T_{A9}, T_{W9} and X_9. By specifying

$$TR9WA = T_{W9}/T_{A9} \tag{34}$$

and solving equations (31) and (33) for a function of T_{A9}, a Newton-Raphson iteration again provides the solution for T_{A9}, T_{W9} and X_9.

The energy equation is

$$\dot{m}_F\left(H_{A8} + \frac{V_{A8}^2}{2}\right) + (\dot{m}_{W7} - X_8\dot{m}_F)\left(H_{f8} + \frac{V_{W8}^2}{2}\right) + \dot{m}_F X_8\left(H_{g8} + \frac{V_{A8}^2}{2}\right)$$

$$= \dot{m}_F\left(H_{A9} + \frac{V_{A9}^2}{2}\right) + (\dot{m}_{W7} - X_9\dot{m}_F)\left(H_{f9} + \frac{V_{W9}^2}{2}\right) + \dot{m}_F X_9\left(H_{g9} + \frac{V_{A9}^2}{2}\right) \tag{35}$$

The fan nozzle exit velocity, V_{A9}, is determined by specifying

$$VR9WA = V_{W9}/V_{A9} \tag{36}$$

and solving equation (35) for V_{A9} as shown on the following page.

$$V_{A9} = \left\{ \frac{C_{PC}(T_{A8} - T_{A9}) + X_8 H_{fg8} - X_9 H_{fg9} + MR(H_{f8} - H_{f9})}{\frac{1}{2}[1 + X_9 + (MR - X_9)(VR9WA)^2]} + \frac{V_{A8}^2 [1 + X_8 + (MR - X_8)(VR8WA)^2]}{[1 + X_9 + (MR - X_9)(VR9WA)^2]} \right\}^{1/2} \quad (37)$$

10. Specific Thrust and Propulsive Efficiency

The thrust of the water-augmented turbofan is determined from the momentum flux equation

$$TH = \dot{m}_T V_{A5} - \dot{m}_C V_0 + (\dot{m}_F + X_9 \dot{m}_F) V_{A9} - \dot{m}_F V_0 + (\dot{m}_{W7} - X_9 \dot{m}_F) V_{W9} - \dot{m}_{W7} V_{W0} + A_5 (P_{A5} - P_{A0}) \quad (38)$$

where the water velocity entering the inlet scoop, V_{WO}, is assumed equal to the craft velocity, V_0. The specific thrust is the thrust divided by total air mass flow through the engine.

$$ST = \frac{TH}{\dot{m}_C + \dot{m}_F} = \frac{1}{1 + BR} \Big[(1 + FAR) V_{A5} - V_0 + BR(1 + X_9) V_{A9} - BR(V_0) + (WGR - X_9 BR) V_{W9} - WGR(V_{W0}) + \frac{1 + FAR}{\rho_{A5} V_{A5}} (P_{A5} - P_{A0}) \Big] \quad (39)$$

The propulsive efficiency is a measure of how well the system converts the kinetic energy change of the working medium into thrust power and is is represented by the equation

$$\eta_{PR} = \frac{TH(V_0)}{TH(V_0) + \frac{1}{2}\dot{m}_T (V_{A5} - V_0)^2 + \frac{1}{2}(\dot{m}_F + X_9 \dot{m}_F)(V_{A9} - V_0)^2 + \frac{1}{2}(\dot{m}_{W7} - X_9 \dot{m}_F)(V_{W9} - V_{W0})^2} \quad (40)$$

C. OBJECTIVES OF THE PARAMETRIC STUDY

The major objective of the present analysis was to refine the computer procedure initiated by Knudson so that a more comprehensive parametric optimization could be carried out. The primary performance indicators were taken to be the specific thrust and propulsive efficiency. The specific thrust and propulsive efficiency of the water-augmented turbofan were compared to their counterparts for a "dry" turbofan which provided a thrust ratio and an efficiency ratio for the wet-to-dry case.

The system parameters described below were varied over ranges of practical values to determine effects on thrust and efficiency ratio.

1. Fan Total Pressure Ratio and Bypass Ratio

Perhaps the two most important parameters in the design of a turbofan engine are the fan total pressure ratio (FPR) and the bypass ratio (BR). Consequently it was expected that these parameters would also be of importance in the design criteria for a water-augmented turbofan engine and that information concerning the effect of bypass ratio and fan total pressure ratio related to various water-to-gas ratios and various water injection velocities could be very useful in optimizing the design of the fan section.

2. Water-to-Gas Ratio

The effect of water-to-gas ratio variation was expected to be important in optimizing the thrust and efficiency ratios since the basis of the entire concept is water-augmentation. The range of values of water volume fraction for mist flow in the fan duct was assumed from zero to about 15 percent at standard conditions which corresponds to a water-to-gas ratio range of zero to 500.

3. Water Injection Velocity

For a given water-to-gas ratio a wide range of possible water injection velocities (V_{INJ}) exists. The effect of losses caused by the mixing process in the fan mixing duct is directly related to the velocity ratio between the water and air in the injection plane making the water injection velocity a significant parameter. The forward velocity of a vehicle through the water provides only a certain maximum injection velocity without providing additional pump work. If water injection velocities are desired which are greater than the maximum ram velocity available, allowing for inlet duct losses, pump work must be added which necessarily reduces the efficiency and thrust of the gas generator. Only if the advantages of increased injection velocity outweigh the losses associated with the pump work required will the operation be worthwhile. Although the previous work by Knudson allowed variation of water injection velocity the pump work required was not considered. One of the objectives of the present analysis was to provide the capability for handling injection pump work as required by variations in water injection velocity.

4. Optimum Combinations of WGR and V_{INJ}

The efficient operation of a water-augmented turbofan propulsion system would require a knowledge of the optumum combinations of water-to-gas ratio and water injection velocity to provide maximum thrust at a given ship speed. With this in mind it was decided to provide information relating the optimum combinations required.

5. Mixing Duct and Nozzle Thermal and Dynamic Equilibrium

The water and air enter the mixing duct at different velocities and different temperatures, in general. During the mixing process the temperatures and velocities, respectively, tend to equalize so that different ratios of water temperature to air temperature and water velocity to air velocity can occur at the mixing duct exit. Similarly in the fan nozzle the accelerations and temperature changes undergone by the two phases can result in various temperature ratios and velocity ratios at the nozzle exit. It is of interest to determine how these ratios affect the thrust and efficiency of the propulsion system.

6. Fan Duct Pressure Drop

The change in static pressure of a flow in a duct is directly related to the wall shear force through the momentum equation. It is possible, therefore, to gain some understanding of the effects of wall shear friction losses in two-phase flow by looking at the effects caused by variation of the ratio of the static pressure at the fan mixing duct exit to the static pressure at the entrance to the fan mixing duct.

D. COMPUTER PROGRAM AND MODIFICATIONS

The computer program used in the present study is based upon a standard turbofan analysis which was modified by Knudson to consider the injection of water into the fan discharge duct. An explanation of various input and output parameters is given in Appendix I. A copy of the program itself and a sample of the computer output are presented in Appendix II.

Originally the computer program consisted of two separate parts: a "wet" turbofan program and a "dry" turbofan. A considerable amount of program revision was required to enable the combination of the two programs so that the ratios of water-augmented thrust and efficiency to dry thrust and efficiency, respectively, could be calculated directly. Of less importance, the output format was modified to present the important data in more compact form to allow wider ranges of the various parameters to be covered without excessive use of paper.

1. Total Entropy Determination at Burner Outlet

In the original program the calculation used in determining the total entropy at the burner outlet was based on the change in entropy from the burner entrance to the burner exit added to the reference entropy of the atmosphere. However, the use of the reference entropy of the atmosphere in Knudson's analysis was incorrect and the reference entropy was corrected to be the total entropy at the burner entrance.

2. Temperature Iterations

Several items in the iterations to determine the mixing duct air temperature and the fan nozzle air temperature were improved in accuracy or were added because of omissions in Knudson's program. Of these, the most important was the accuracy indicator used to determine the convergence of the Newton-Raphson iteration for air temperature at both the duct exit and the nozzle exit. Knudson examined only the numerator of the convergence term whereas the proper term to examine is the absolute value of the entire convergence term. This was corrected for the present analysis and repeatable results were obtained which in some cases differed significantly from those obtained by Knudson.

E. RESULTS AND DISCUSSION

The significant results of the computer study are presented in graphic form in Figs. 2 through 22. For all results shown the craft velocity was held at 50 knots although the computer program can handle any speed range. The constant velocity allowed more meaningful comparisons to be made among the results.

The following parameters were also held constant throughout the analysis, the values used being typical of presently available turbofan engines. The compressor total pressure ratio was maintained at 13.8 and the turbine inlet total temperature was fixed at 2500 degrees Rankine. The dry fan duct total pressure ratio was taken as unity since no separate fan duct exists on a dry turbofan engine. Except for the study of duct pressure ratio effects the wet fan duct static pressure ratio was arbitrarily fixed at 0.95 since the expected two-phase pressure drop was not known.

The maximum available velocity for water injection without injection pump work depends upon duct and piping losses in transferring the water from the inlet scoop to the injection nozzles. The velocity recovery factor chosen for the present analysis was 0.8. The mach number at the fan outlet (water injection plane) was assumed to be 0.2 The efficiencies assigned to the various components are listed below and are the same as those used in Refs. 2 and 4.

Diffuser	0.95
Compressor	0.90
Burner	1.00
Turbine	0.85
Nozzle	0.98
Fan Diffuser	0.95
Fan	0.90
Fan Nozzle	0.98
Water Injection Pump	0.90

1. Effects of Fan Pressure Ratio

It is of interest to determine the design criteria for maximizing thrust ratio with respect to fan pressure ratio and bypass ratio. The variation of thrust ratio with fan pressure ratio, while holding bypass ratio constant at 4.0, is presented for various water injection velocities in Fig. 2 and for various water-to-gas ratios in Fig. 3. The design envelope shown in both graphs is determined by the amount of turbine work required to drive the compressor, fan and water injection pump. The turbine work available is dependent on the maximum pressure drop allowable across the turbine. As the turbine work required exceeds the turbine work available the turbine exit pressure must go below atmospheric pressure. Since this is impossible, the design limit is reached when the turbine exit pressure equals atmospheric pressure.

It is observed from Fig. 2 that for a given water injection velocity or water-to-gas ratio the highest possible fan pressure ratio provides the maximum thrust ratio, except for an injection velocity of

100 knots, below a fan pressure ratio of 1.1. The increase in thrust ratio for low values of fan pressure ratio at high water injection velocities and high water-to-gas ratios is considered to be unrealistic because of the magnitudes of certain of the parameters. Specifically, a fan pressure ratio of 1.0 corresponds to a duct in the free stream into which water is injected with no losses occurring in the fan. Under this condition higher water injection velocities reduce the velocity differential between the water and the faster air thus possibly reducing mixing losses sufficiently to allow an increase in thrust ratio.

The optimum fan pressure ratio for duct and nozzle thermal and dynamic equilibrium, respectively, appears to be in the range 1.4 to 1.5 for a design speed of 50 knots. This range gives the maximum thrust ratio while still allowing the widest range for both water injection velocity and water-to-gas ratio. A fan pressure ratio of 1.5 was used for the remainder of the present analysis. The effect of variation of fan pressure ratio on efficiency ratio was also studied and exhibited trends generally similar to the corresponding thrust ratio curves.

2. <u>Effects of Bypass Ratio</u>

The selection of the optimum bypass ratio is also an important design criteria for the water-augmented turbofan engine. The variation of thrust ratio with bypass ratio, while holding fan pressure ratio constant at 1.5, is presented in Fig. 4 for various water injection velocities and Fig. 5 for various water-to-gas ratios. Again the design envelope reflects the maximum available turbine work limited by turbine exit pressure and atmospheric pressure.

Increases in both injection velocity and water-to-gas ratio provide increased thrust ratio within the design envelope. Increases in bypass ratio generally increase thrust ratio for a given injection velocity or water-to-gas ratio except for injection velocities above about 70 knots and water-to-gas ratios greater than 400. The decrease in thrust ratio with increasing bypass ratio for a given injection velocity above about 70 knots (see Fig. 4) may be attributed to the fact that the increase in pump work required to maintain the water-to gas ratio constant as bypass ratio increases detracts more from the thrust of the gas generator than the amount of thrust increase of the fan section. A similar explanation applies to the results of Fig. 5 regarding various water-to-gas ratios.

The optimum design bypass ratio for maximizing thrust ratio at a design speed of 50 knots appears to occur in the range of bypass ratios from 3.0 to 4.0. This range allows a wide selection of injection velocities and water-to-gas ratios while still remaining within the design envelope. The bypass ratio chosen for the remainder of the present analysis was 4.0. The effect of variation of bypass ratio on efficiency ratio followed trends generally similar to the corresponding thrust ratio curves.

3. Effects of Water-to-Gas Ratio

The variation of thrust ratio with water-to-gas ratio is presented in Fig. 6 for various values of water injection velocity. Figure 7 shows similar information with respect to efficiency ratio. It is apparent that both water-to-gas ratio and water injection velocity greatly affect the thrust ratio and the efficiency ratio. A maximum thrust ratio of slightly less than 4.0 is achieved for a water-to-gas ratio in the range 375 to 400 at a water injection velocity slightly higher than 60 knots and a craft velocity of 50 knots (see Fig. 6). However the efficiency ratio shown in Fig. 7 continues to increase for values of water-to-gas ratio exceeding 500. At a water-to-gas ratio of 500 the maximum efficiency ratio obtainable is about 6.2 for a water injection velocity slightly below 60 knots and a craft velocity of 50 knots. These results show that it is indeed advantageous to increase the injection velocity even at the expense of the pump work required.

The operating envelope shown in Figs. 6 and 7 indicates the maximum turbine work available for driving the compressor, fan and water injection pump and arises because the turbine exit pressure is lower than atmospheric pressure at the higher fan pressure ratios. The explanation given earlier in Section D.1 for design envelope applies to the operating envelope as well.

Each water injection velocity has an associated water-to-gas ratio at which thrust ratio is maximized and another water-to-gas ratio for which efficiency ratio is maximized. This may be explained by the consideration that for a fixed water injection velocity the initial velocity ratio between the water droplets and the air is constant. As the water-to-gas ratio increases the thrust from the fan nozzle is increased but the injection pump work increase required causes a decrease in the thrust of the gas generator. Initially the thrust increase from the fan section predominates but eventually the thrust decrease from the gas generator section becomes larger than the thrust gain and the net thrust begins to decrease.

4. Operating Curves

An important question concerns the optimization of water injection velocity and water-to-gas ratio to provide maximum thrust ratio at a given craft velocity. A suggested form for the presentation of such information is shown in Fig. 8. For a desired craft velocity and water injection velocity the water-to-gas ratio required to provide the maximum thrust ratio can be determined from the curve.

The curves do not, however, provide information concerning the optimum combination of both injection velocity and water-to-gas ratio required to provide the maximum possible thrust ratio at a given craft velocity. For example, at a water-to-gas ratio of 200 and craft velocity of 50 knots there exist two injection velocities, 41 knots and 79 knots, respectively, which will provide a maximum thrust ratio, but the greater of the two thrust ratios is not specified. However, comparison with Fig. 6 indicates that the higher thrust ratio coincides with the higher injection velocity. Figure 7 also shows this case to be the most efficient. This suggests that in cases where two possibilities exist for injection velocity the higher injection velocity should be used to provide the higher thrust and efficiency ratio.

The importance of the peaks at high water-to-gas ratios on the curves for craft velocities of 25 and 50 knots, respectively, lies in the fact that, for water-to-gas ratios above about 500, the fan duct contains such a high percentage of water that the water-jet principle is approached with its increased pumping requirements and consequently increased weight. At some point the weight increase will more than offset the performance advantage and the water-augmented turbofan loses its appeal. For this reason it is suggested that the water-to-gas ratios be kept as low as possible.

5. Fan Duct and Nozzle Equilibrium Parameters

One of the more important aspects of the present computer analysis has been the determination of the effect of fan duct and nozzle equilibrium parameters upon the thrust ratio and the efficiency ratio. The important equilibrium parameters are taken to be the fan duct exit velocity ratio, V_{W8}/V_{A8}, the fan duct exit temperature ratio, T_{W8}/T_{A8}, fan nozzle exit velocity ratio, V_{W9}/V_{A9}, and the fan nozzle exit temperature ratio, T_{W9}/T_{A9}; these ratios are referred to in the succeeding test as, respectively, duct velocity ratio, duct temperature ratio, nozzle velocity ratio and nozzle temperature ratio and are water-to-air ratios.

These parameters are important for several reasons. First, little is known about the nature of the mixing process; consequently, analysis must be made on an empirical basis. Second, Lockhart and Martinelli [Ref. 6] and Chenoweth and Martin [Ref. 7] indicate that mixing duct pressure losses are greater for the flow of a two-phase mixture than for either phase flowing separately. The extent of the increase and the factors which govern the increase are not very well known. Further discussion of this subject is presented in Section II of this paper.

a. Fan Duct Velocity Ratio

The variation of thrust ratio and efficiency ratio with duct velocity ratio is presented in Figs. 9 and 10, respectively, for various values of water injection velocity. Under the restriction that all other equilibrium parmeters have the value unity, the duct velocity ratio has only a very slight effect on thrust ratio and efficiency ratio. The duct velocity ratio, therefore, does not appear to be a significant parameter affecting thrust ratio and efficiency ratio.

b. Fan Duct Temperature Ratio

The effects of duct temperature ratio on thrust ratio and efficiency ratio are shown in Figs. 11 and 12, respectively, for various water injection velocities. The initial conclusion from Fig. 11 is that it would be highly desirable to maintain the duct temperature ratio as low as possible to attain the maximum thrust ratio. However, further consideration of the restrictions imposed, namely duct velocity equilibrium, nozzle velocity equilibrium and nozzle temperature equilibrium, create unrealistic, if not impossible, conditions for the flow to meet.

First, it is extremely unlikely that a low value of duct temperature ratio could, at the same time, produce equilibrium of the other three parameters. Second, the experimental results of Reese and Richard [Ref. 8] indicate that thermal equilibrium occurs in two-phase flows with contact times as low as the order of one millisecond. A typical expected contact time of the order of 20 milliseconds suggests thermal equilibrium at all times in the fan duct exit.

A further consideration is that for low values of duct temperature ratio the bulk of the mixing process must occur in the nozzle. Since the calculations through the nozzle include the assumption of no net entropy change, the thrust ratio resulting is larger than that which could realistically occur. These reasons suggest that the results given in Figs. 11 and 12 do not give an accurate indication of realistic effects.

c. Fan Nozzle Velocity Ratio

Figures 13 and 14, respectively, present the effect on thrust ratio and efficiency ratio of varying the ratio of water velocity to air velocity at the nozzle exit for various water injection velocities. For a given injection velocity neither thrust ratio nor efficiency ratio varies a great amount, however, the variation is greater than the similar case for variation of duct velocity ratio. For an injection velocity of 100 knots the thrust ratio increases from about 3.13 at a velocity ratio of 0.5 to about 3.22 at a velocity ratio of 1.0 and the efficiency ratio increases from about 3.77 to about 3.88. Both curves become nearly horizontal near a duct velocity ratio of 1.0.

It should be pointed out that the restriction of equilibrium conditions for the other parameters is not so unrealistic at the nozzle exit as it was at the duct exit. This is because the flow is accelerated through the nozzle and the air, because of its lower density, accelerates more quickly than the water causing a velocity difference at the nozzle exit regardless of the equilibrium state at the fan duct exit (nozzle entrance). As was the case with duct velocity ratio, the nozzle velocity ratio appears to have little significant effect upon thrust ratio and efficiency ratio.

d. Fan Nozzle Temperature Ratio

The variation of thrust ratio versus nozzle temperature ratio is presented for various water injection velocities in Fig. 15, and for various water-to-gas ratios in Fig. 16. In both cases the thrust ratio decreases smoothly with increasing nozzle temperature ratio indicating that the most desirable operating range is near thermal equilibrium where the curves are nearly flat. Again, based on the results of Reese and Richard, it is probable that the nozzle temperature ratio will be near unity in spite of the temperature changes of the air through the nozzle.

The variation of efficiency ratio with nozzle temperature ratio is shown in Figs. 17 and 18, respectively, for various water injection velocities and various water-to-gas ratios. The results tend to follow trends similar to those for the thrust ratio except for the higher values of water injection velocity and water-to-gas ratio. For a water injection velocity of about 80 knots in Fig. 17 the efficiency ratio is relatively unchanged over the range of nozzle temperature ratios. An injection velocity of 100 knots shows increasing efficiency ratio with increasing nozzle temperature ratio. Similarly a water-to-gas ratio of 400 or higher in Fig. 18 exhibits a similar trend of increasing efficiency ratio.

The information for temperature ratios significantly greater than unity is considered to be unrealistic in view of the predicted short contact times required to achieve thermal equilibrium. In addition the large pressure drop through the nozzle, which would be required for such a great air temperature change, is highly unlikely to occur.

6. Effects of Fan Duct Pressure Ratio

An important parmeter affecting the performance of the water-augmented turbofan engine is the pressure loss in the fan mixing duct. Since the wall shear force in two-phase flow is an unknown quantity which has not been treated analytically in this paper, a range of values for the ratio of static pressure at the mixing duct exit to the static pressure at the duct entrance has been used to determine the effect on thrust ratio and efficiency ratio. Figures 19 and 20 present thrust ratio versus duct pressure ratio for various water injection velocities and various water-to-gas ratios, respectively. Figures 21 and 22 present parallel results for efficiency ratio, respectively.

It is theoretically possible for the static pressure to increase in the direction of flow if large velocity variations exist over the injection plane and the wall shear stress is small. Thus, these plots have been extended to pressure ratios greater than one. It is easily seen that the most desirable range of operation to provide maximum thrust ratio is at the maximum duct pressure ratio. This is simply the expected result that minimum duct friction provides the best operating conditions. Also, as predicted by a momentum analysis, the highest water injection velocity provides the least sensitivity to duct pressure losses as well as providing the best thrust ratio.

The effect of duct pressure ratio on efficiency ratio is similar to the effect on thrust ratio; however, for a fixed water-to-gas ratio the efficiency ratio is virtually unchanged with varying duct pressure ratio. Again increasing water injection velocity decreases the effect on efficiency ratio of varying duct pressure ratio. As the water injection velocity increases to about 80 knots, the injection pump work required begins to predominate over the efficiency gain afforded by the high water injection velocity, causing the efficiency ratio to decrease with increasing duct pressure ratio (see Fig. 21).

F. CONCLUSIONS

The injection of water into the fan discharge duct of a turbofan engine provides a feasible propulsion system for high speed sea-borne vessels. Among the most important parameters affecting the thrust and propulsive efficiency of water-augmented turbofans are the water-to-gas ratio and the water injection velocity. Each water injection velocity has an associated water-to-gas ratio which maximizes thrust and another water-to-gas ratio which maximizes propulsive efficiency. Thrust ratios and efficiency ratios of the water-augmented turbofan to the dry turbofan of three or four are easily attainable. It should be noted that these figures do not account for the increased drag that would be caused by the water inlet scoop.

Velocity slip ratio in either the fan mixing duct or the fan nozzle has negligible effect upon the thrust ratio and efficiency ratio. The effect of temperature difference between water and air is somewhat greater than for the velocity ratio. However, the likelihood of non-equilibrium for either fan duct or fan nozzle temperature ratio is slight due to the short contact times required for thermal equilibrium.

Thrust ratio and efficiency ratio both increase with increasing fan duct pressure ratio. Fan duct pressure ratio can be related to fan duct wall friction forces through the momentum equation, indicating that minimum wall friction is desirable. Thrust ratio and efficiency ratio become less sensitive to fan duct pressure ratio with increasing water injection velocity and increasing water-to-gas ratio. Since little is known about two-phase pressure drop, experimental work should be done to increase the knowledge in the field. Section II of this paper describes the development of a test facility for wall shear force and pressure drop measurements in two-phase flow.

For a design speed of 50 knots, the ideal fan total pressure ratio falls within the range 1.4 to 1.5, if use of a wide range of water injection velocities and water-to-gas ratios is desired. At the same design speed, the optimum fan bypass ratio occurs in the range 3.0 to 4.0, to allow use of a wide range of water injection velocities and water-to-gas ratios.

For any given water injection velocity a set of curves may be constructed which provide the water-to-gas ratio required to achieve maximum thrust for a specified craft velocity. The present analysis has not considered the relationship between increasing the water injection velocity and the resulting weight increase due to pump requirements. As the water injection velocity and water-to-gas ratio increase the pure water-jet concept is approached and the performance advantages of the water-augmented turbofan concept, primarily the low system weight, are lost. A further study is thus required to determine the point at which weight and cost increases for water injection pumps begin to detract significantly from the overall system effectiveness.

II. DEVELOPMENT OF A TEST FACILITY FOR TWO-PHASE FLOW

A. TWO-PHASE PRESSURE DROP PREDICTION

The ability to predict the pressure drop occurring in a two-phase duct flow is vital to the accurate analysis of the water-augmented turbofan concept discussed in Section I. To the author's knowledge no complete, accurate, theoretical analysis of two-phase pressure drop has as yet been proposed. However, Dukler, Wicks and Cleveland [Ref. 9] and other available literature indicate that two empirical data correlations for the prediction of two-phase pressure drop have given consistently better results than other correlations. These correlations were developed, respectively, by Lockhart and Martinelli [Ref. 6] and Chenoweth and Martin [Ref. 7] . An explanation of each of the correlations and some of the special assumptions made in them is presented in the following text.

1. Lockhart-Martinelli Two-Phase Flow Correlation

The correlation of Lockhart and Martinelli is dependent upon which of four types of flow exists during the simultaneous flow of a liquid and a gas (or vapor). These flow regimes are:

1. Flow of both the liquid and the gas may be turbulent (turbulent-turbulent flow)
2. Flow of the liquid may be viscous and flow of the gas may be turbulent (viscous-turbulent flow)
3. Flow of the liquid may be turbulent and flow of the gas may be viscous (turbulent-viscous flow)
4. Flow of both the liquid and the gas may be viscous (viscous-viscous flow)

"Viscous" flow is the term used by Lockhart and Martinelli for what is more properly called laminar flow.

The assumptions made are that the "static pressure drop for the liquid phase must equal the static pressure drop for the gaseous phase regardless of the flow pattern, as long as an appreciable radial static pressure difference does not exist" and "the volume occupied by the liquid plus the volume occupied by the gas at any instant must equal the total volume of the pipe." It is further assumed that the transition from laminar to turbulent flow occurs in the range of Reynolds numbers between 1000 and 2000. The Reynolds number is calculated using the mass flow rate of the phase in question and the inside diameter of the pipe. For example, the liquid phase Reynolds number is determined from the equation

$$Re_L = \frac{4\dot{m}_L}{\pi D \mu_L} \tag{41}$$

where $\dot{m}_L$ is the liquid mass flow rate, in pounds-mass per second, D is the inside pipe diameter in feet and μ_L is the absolute viscosity of the liquid in pounds-mass per foot-second.

Having determined which of the flow regimes is appropriate from the Reynolds number calculation for each phase, the all-liquid and all-gas pressure drops, respectively, are calculated. The all-liquid pressure drop in a pipe L feet in length is based upon the liquid flowing at a rate $\dot{m}_L$ with a density ρ_L as in the equation

$$\Delta P_L = \rho_L f_L \frac{L}{D} \frac{V_L^2}{2} \tag{42}$$

where the liquid velocity, V_L, is determined from continuity, assuming that the liquid occupies the entire pipe, and f_L is the liquid friction factor based on Re_L. Similarly, an all-gas pressure drop is found from

$$\Delta P_G = \rho_G f_G \frac{L}{D} \frac{V_G^2}{2} \tag{43}$$

The ratio of the all-liquid pressure drop to the all-gas pressure drop is the square of the two-phase flow modulus, χ , or

$$\chi \equiv \left[\frac{\Delta P_L}{\Delta P_G}\right]^{1/2} \tag{44}$$

Figure 23 shows the relationship between χ and the correlation parameter Φ for each of the various flow regimes, as determined experimentally by Lockhart and Martinelli. If Φ_L is taken from the curve the two-phase pressure drop is

$$\Delta P_{TP} = \Phi_L^2 \Delta P_L \tag{45}$$

Similarly, if Φ_G is taken from the curve the two-phase pressure drop is

$$\Delta P_{TP} = \Phi_G^2 \Delta P_G \tag{46}$$

It should be noted that Lockhart and Martinelli state that more data are needed to establish the validity of their correlation at very high and very low values of the flow modulus χ (nearly all-liquid and nearly all-gas flow, respectively).

2. Chenoweth-Martin Two-Phase Flow Correlation

Chenoweth and Martin developed an "improved correlation for two-phase pressure drop in horizontal pipes" which is especially valid for pressures up to 100 psia. The correlations can be used for any two-phase mixture as long as the flow is turbulent and it predicts single-phase values when the flow is all liquid or all gas. The two input parameters for the use of the correlation are the liquid volume fraction (LVF) and the ratio of a fictitious all-gas pressure drop to a fictitious all-liquid pressure drop.

The liquid volume fraction is calculated from the flow rates and densities of the two-phases using the equation

$$\text{LVF} = \frac{\text{Volume flow rate of liquid}}{\text{Total volume flow rate}} = \frac{\dot{m}_L/\rho_L}{\dot{m}_L/\rho_L + \dot{m}_G/\rho_G} = \frac{1}{1 + \frac{\dot{m}_G \rho_L}{\dot{m}_L \rho_G}} \quad (47)$$

The ratio of the fictitious pressure drops is determined by computing the value of $\rho_L \Psi_G^* / \rho_G \Psi_L^*$

where

$$\Psi_{L*} \equiv f_{L*} \frac{L}{D} + \Sigma K \quad (48)$$

and

$$\Psi_{G*} \equiv f_{G*} \frac{L}{D} + \Sigma K \quad (49)$$

The subscripts L* and G* denote the fictitious all-liquid and all-gas states, respectively. The K's are loss coefficients for valves and fittings. The fictitious friction factor is determined in the normal manner using an artificial Reynolds number based on the total flow rate of liquid and gas and the physical properties of the phase in question. For example, f_{L*} is determined using the Reynolds number

$$Re_{L*} = \frac{4(\dot{m}_L + \dot{m}_G)}{\pi D \mu_L} \quad (50)$$

The fictitious all-liquid pressure drop is then computed as

$$\Delta P_{L*} = \rho_L f_{L*} \frac{L}{D} \frac{V_{L*}^2}{2} \quad (51)$$

where V_{L*} is a fictitious velocity determined from the equation

$$V_{L*} = \frac{\dot{m}_L + \dot{m}_G}{\rho_L A} \quad (52)$$

Figure 24 can now be used to predict the two-phase pressure drop, ΔP_{TP}.

In contrast to the Lockhart-Martinelli correlation, the Chenoweth-Martin correlation covers only all-turbulent two-phase mixtures but ties into single-phase values at either end. It is also valid over a wider range of pressures.

B. EQUIPMENT DESIGN OBJECTIVES AND DESCRIPTION

A test rig was developed for the experimental analysis of two-phase flows, in particular the mixing process which immediately follows injection of water into the air. Initially, fully established two-phase flows will be investigated by directly measuring the wall friction force and the overall pressure drop. Subsequent investigation will concentrate on determination of the pressure drop due to the mixing process in a developing flow. The direct measurement of the wall friction force will allow separation of the pressure drop due to mixing from the overall pressure drop. General views of the apparatus are shown in Figures 25 and 26. A flow diagram for the initial tests is shown in Figure 27.

Air enters the system through a 2-inch pipe from a plenum fed by a reciprocating compressor capable of supplying air at pressures up to 150 psig and flow rates up to 700 scfm. Water is supplied to the system through a 3-inch pipe from a centrifugal pump capable of supplying up to 500 gpm at 80 psig. The mass flow rates of the air and water are accurately determined using thin-plate orifice meters. The air and water flows are united by joining the two pipes into a 3-inch pipe. The two-phase mixture flows together for about 28 feet becoming fully established, then flows through a "floating" test section 10 feet long in which the wall shear force is measured. The downstream end of the test section exhausts to the atmosphere where the water is collected and returned to the water pump.

1. Flow Orifice Details

The flow measurement orifices shown in Fig. 28 were designed according to standard ASME specifications [Ref. 10] . Figures 29A and 29B give the dimensions of the orifices and the placement of the pressure taps with respect to the pipe. Each orifice plate was machined from type 304 stainless steel plate for which a coefficient of expansion curve is available in Ref. 10. Each of the flanges containing an orifice was machined with a circular groove centered with respect to the pipe axis to insure accurate alignment of the orifice with the pipe axis.

2. Initial Mixing of Air and Water

The mixing of the air and water is accomplished by merely joining the two pipes at a 45-degree angle (see Fig. 30). The mixing process occurs solely due to the turbulent nature of the flow; if the liquid volume fraction is sufficiently small a mist-flow will result. It is the mist-flow regime (liquid volume fractions below about 15 percent) which is directly applicable to the water-augmented turbofan engine described in Section I. However, the apparatus is designed to handle as wide a range of water-to-air mass flow ratios as permitted by the available water pump and air compressor capacities.

3. Test Section Details

The test section consists of a 10-foot long, 3.106-inch steel pipe which is supported two feet from each end. Each support has four, one-eighth inch diameter stainless steel rods, one vertically above, one vertically below, and one horizontally on each side as shown in Fig. 31. The rods are mounted on bearings which allow the test section to "float" longitudinally.

The wall shear force measurement is made through two cantilever flexures mounted horizontally, one on each side of the test section (see Fig. 32). Each flexure has four strain gages mounted to detect changes in bending moment caused by the force exerted by the test section. Figure 33 shows the wiring diagram for each flexure.

The labyrinth seal shown in Fig. 34 was designed to provide a pressure seal at the inlet to the test section which does not restrict longitudinal motion. The dimensional details of the labyrinth are given in Fig. 35. Experimental determination of the leakage rate is discussed in Section C below.

The pressure at the inlet to the test section is measured to allow the determination of the pressure drop through the test section. Additionally the test section inlet pressure is required in order to calculate the force on the labyrinth face at the test section inlet. This pressure force must be subtracted from the total force indicated on the flexures to obtain the true wall shear force.

C. CALIBRATION PROCEDURE

It is necessary to determine the amount of air leakage which occurs at the labyrinth seal over the range of expected internal to external pressure ratios. This was to have been accomplished by sealing the outlet of the test section, varying the internal pressure and measuring the mass flow rate of air leaving through the labyrinth seal. However, excessive leakage in the air supply line prevented the accurate measurement of the leakage rate through the labyrinth seal and insufficient time remained to complete the necessary repairs.

The flexures on which the strain gages are mounted require calibration before and after each series of test runs. The calibration procedure for the flexures involves placing a known force on the test section using a system of weights and a pulley as shown in Fig. 36. A typical calibration curve of force versus strain gage output is presented in Fig. 37.

D. DATA COLLECTION AND REDUCTION PROCEDURE

The important variables for the operation of the two-phase flow test rig are the mass flow rates of air and water, the force exerted on the test section due to wall friction and labyrinth pressure effects, and the pressure loss in the test section. To determine the mass flow rates it is necessary to record the static pressure upstream of the air orifice, the pressure drop across both orifices for both the flange taps and the D and half-D taps, respectively, the temperature of each fluid and the atmospheric temperature at each manometer.

The calculation of the two-phase pressure drop predictions of both Lockhart and Martinelli and Chenoweth and Martin require that the inlet static pressure in the test section and the temperature of the air-water mixture at the outlet of the test section be recorded. Atmospheric pressure must be recorded for use in mass flow rate calculations. The temperature is recorded at the outlet of the test section because the temperature probe will disturb the flow if it is installed at the inlet to the test section. It should be mentioned at this point that the temperature measured in a two-phase mixture can be subject to discussion because it is not known what effect the water droplets impinging on the probe have on the indicated temperature. The accuracy of the pressure drop predictions depends heavily upon an accurate temperature of the flow.

A computer program converts the raw experimental data into mass flow rates and two-phase pressure drop predictions. The input and output variables used for the computer program are defined in Appendix III and the computer program itself along with a sample output is presented in Appendix IV.

The pressure drop prediction of Chenoweth and Martin is not completely carried out by the computer program because of the difficulty in obtaining an analytical expression for the curves of the correlation in Fig. 24. The program does supply the variables necessary to enter Fig. 24. The value of $\Delta P_{TP}/\Delta P_{L*}$ thus found is multiplied by the fictitious all-liquid pressure drop, ΔP_{L*}, which is also computed in the program, to obtain the predicted two-phase pressure drop.

E. CURRENT STATUS AND SUGGESTIONS FOR FURTHER WORK

The work reported herein concerning the development of the two-phase flow test rig suffered several setbacks due to difficulty in obtaining parts. Because of these delays the installation of the water return system has not been completed.

Several suggestions for further work have become apparent during the course of the development of the two-phase flow test rig.

1. Labyrinth Air Leakage Determination

It will be necessary to determine the leakage rate of air through the labyrinth seal prior to taking experimental data. It should be noted that the possibility exists that the present metering system may not be adequate for measuring minimum flow rates of both air and water.

2. Labyrinth Water Leakage Determination

During operation with two-phase or all-liquid flow some water will probably leak out the labyrinth seal and provision must be made to measure this leakage.

3. Computerization of Friction Factor Curve

The friction factors used in calculating pressure drops in the computer program solutions for predicted two-phase pressure drop were assumed to be constant values. This is true only in the region of fully turbulent flow. The value of this friction factor used for high

Reynolds numbers should first be checked by simple pressure drop tests. The computer program must then be improved by the computerization of the friction factor curve so that the laminar flow and transition regions will be included.

4. Computerization of Chenoweth-Martin Correlation Curve

It would be helpful if an analytical expression could be found for the Chenoweth and Martin correlation curves of Fig. 24.

5. Evaluation of Predicted Pressure Drop

The knowledge gained from the continuation of the work reported herein should be used to evaluate the pressure drop correlations of Lockhart and Martinelli and Chenoweth and Martin. Also, a prediction for the two-phase wall shear has very recently been proposed by Muench and Ford [Ref. 11] and should be evaluated. The analysis of the two-phase flow calculations in the water-augmented turbofan should be re-examined in the light of experimental results.

6. Pressure Drop due to Two-Phase Mixing

The present test rig is set up to obtain fully developed two-phase flow in the test section. However if the water is injected immediately upstream from the test section it should be possible to separate the pressure drop into that caused by the mixing of the two phases and that caused by wall friction. This knowledge would be useful in further analysis of injection systems.

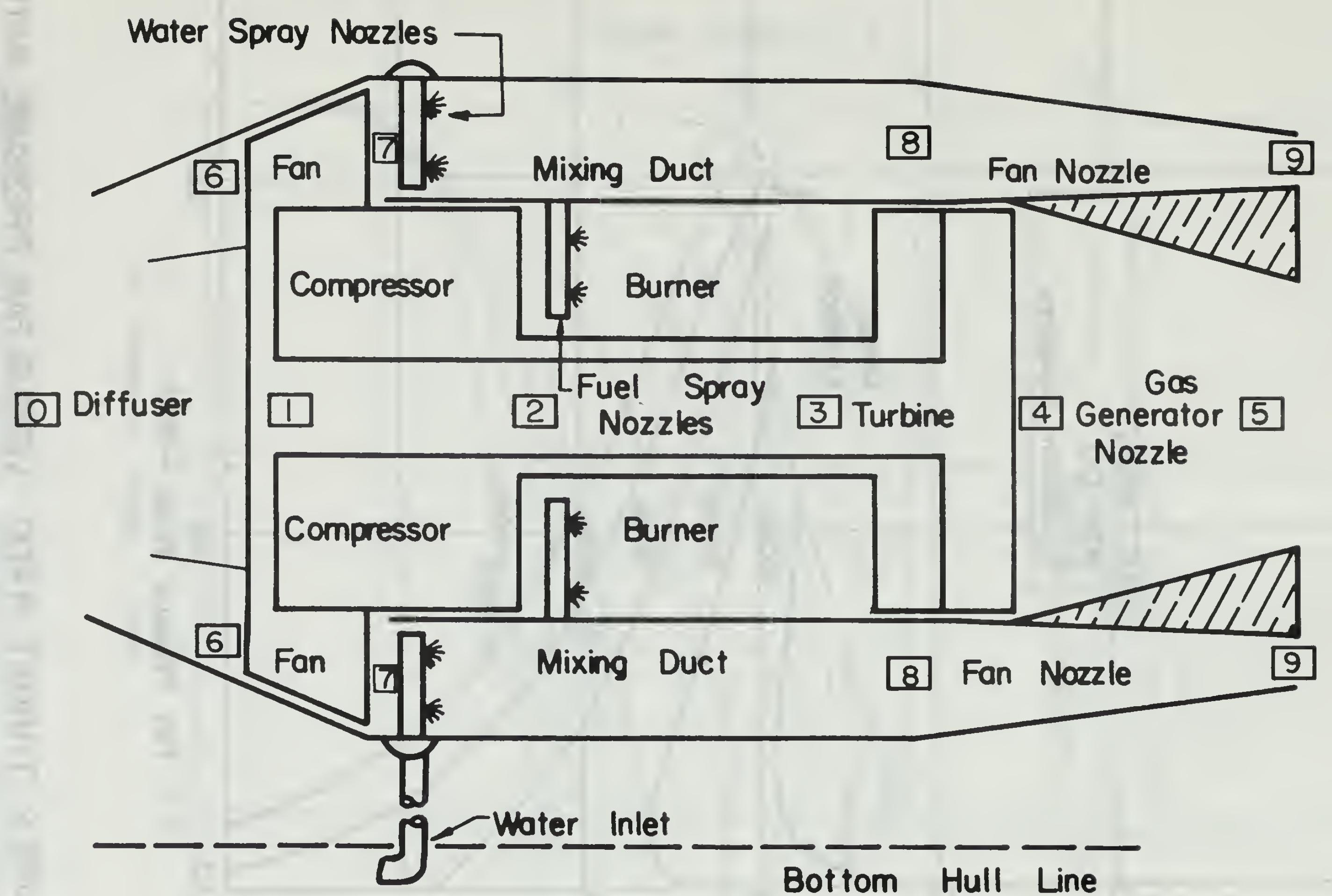

FIGURE 1

WATER-AUGMENTED TURBOFAN ENGINE

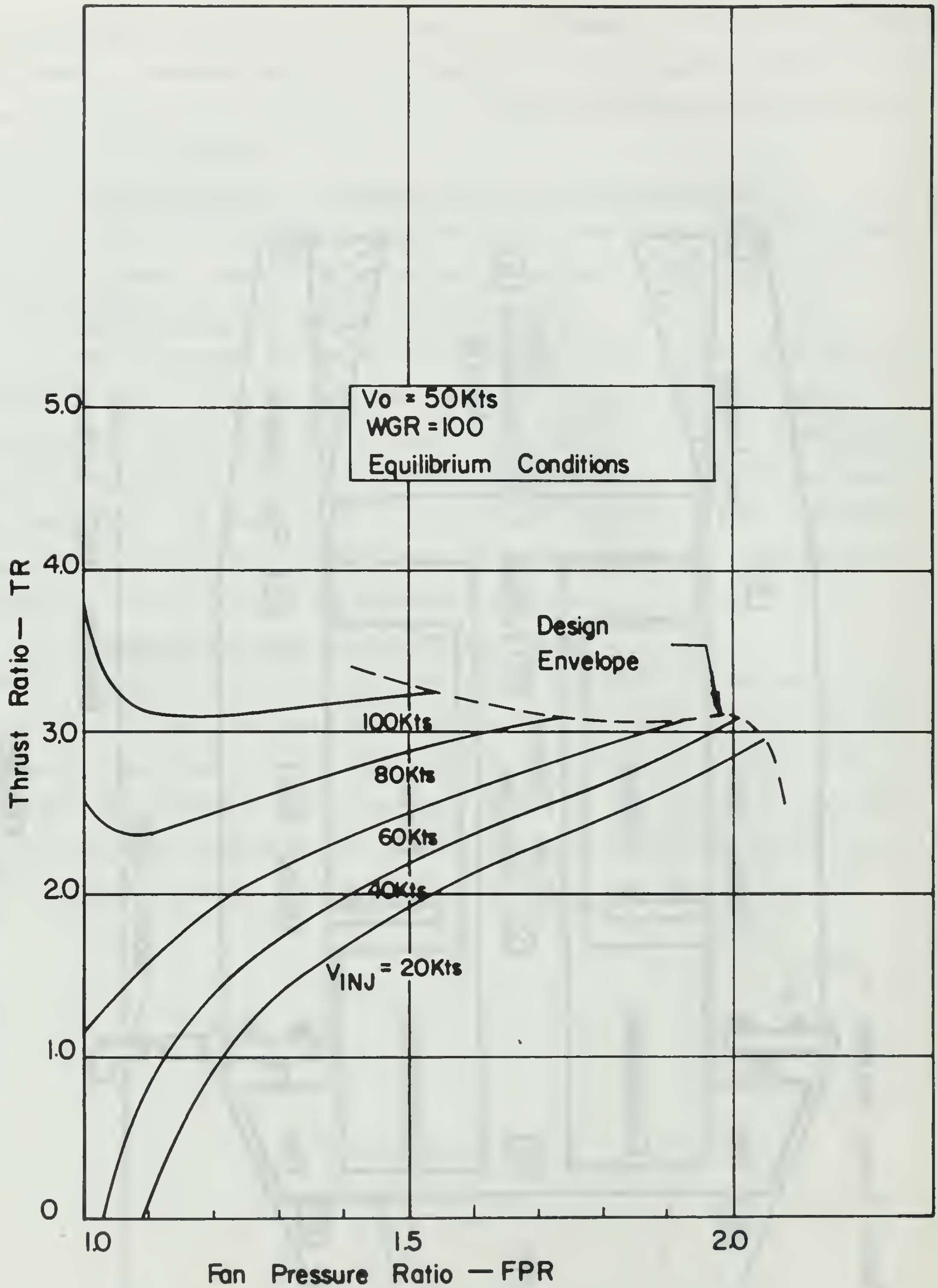

FIGURE 2 . THRUST RATIO VERSUS FAN PRESSURE RATIO FOR VARIOUS WATER INJECTION VELOCITIES

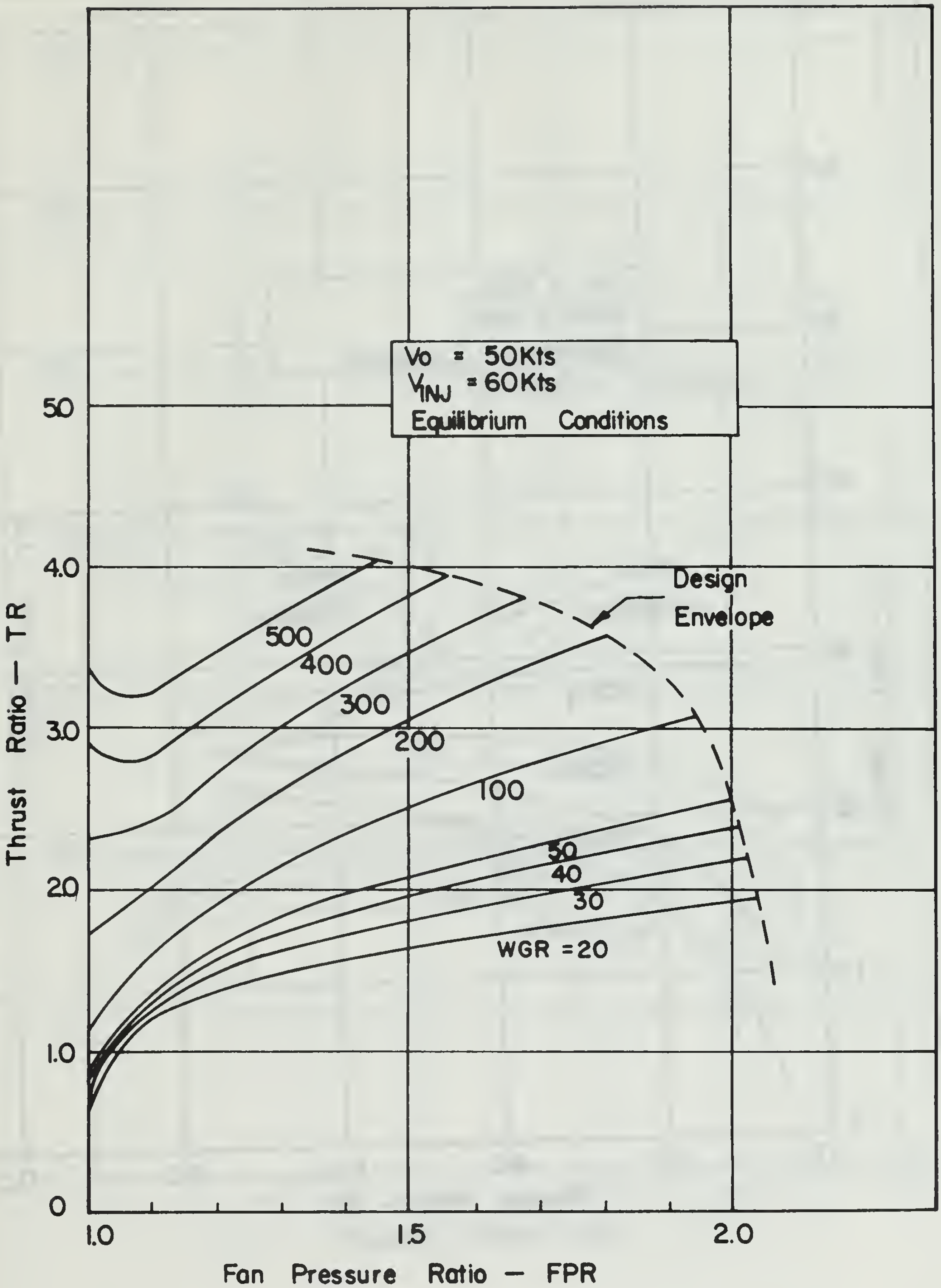

FIGURE 3 . THRUST RATIO VERSUS FAN PRESSURE RATIO FOR VARIOUS WATER-TO-GAS GENERATOR AIR RATIOS

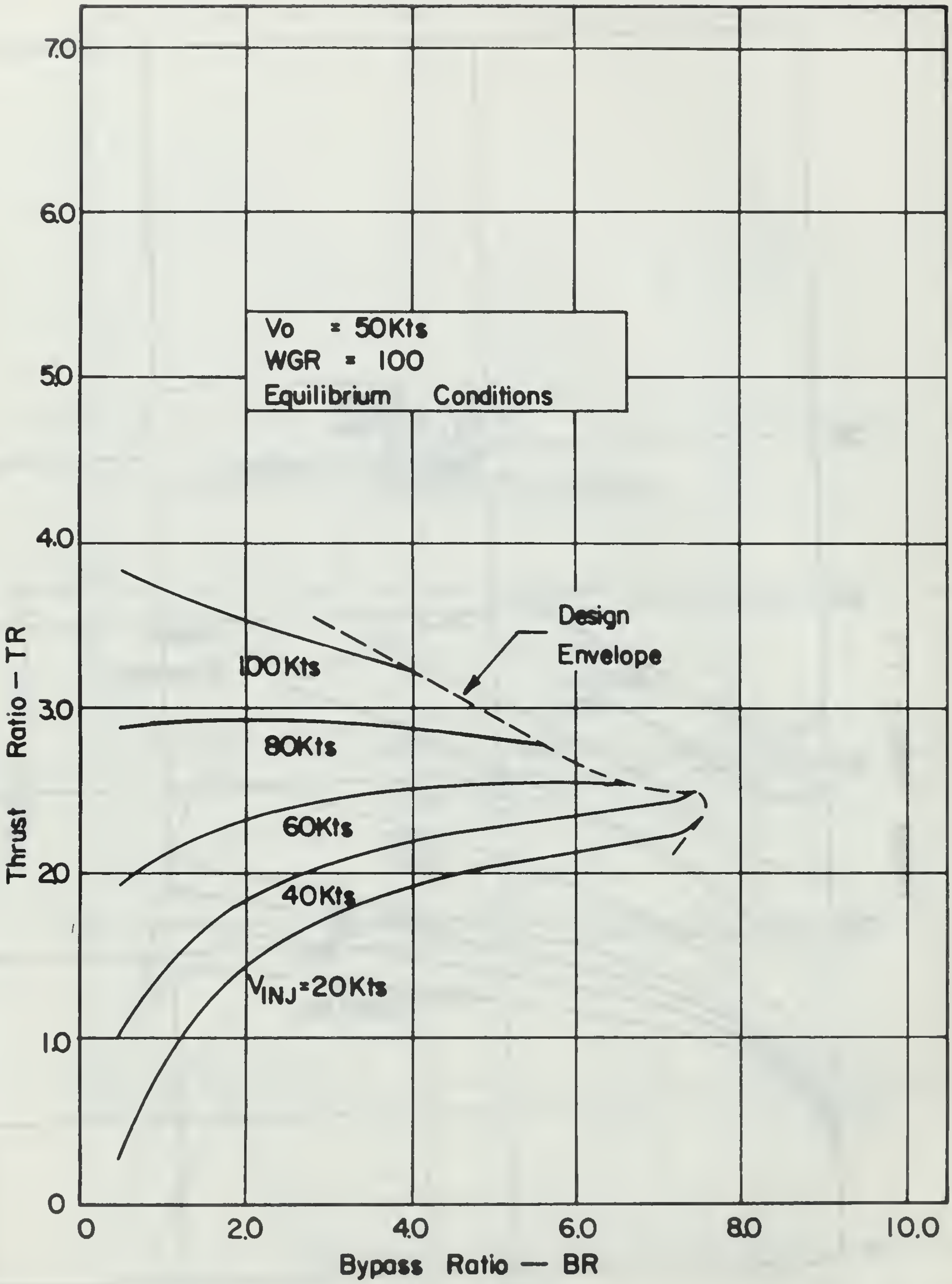

FIGURE 4 . THRUST RATIO VERSUS BYPASS RATIO FOR VARIOUS INJECTION VELOCITIES

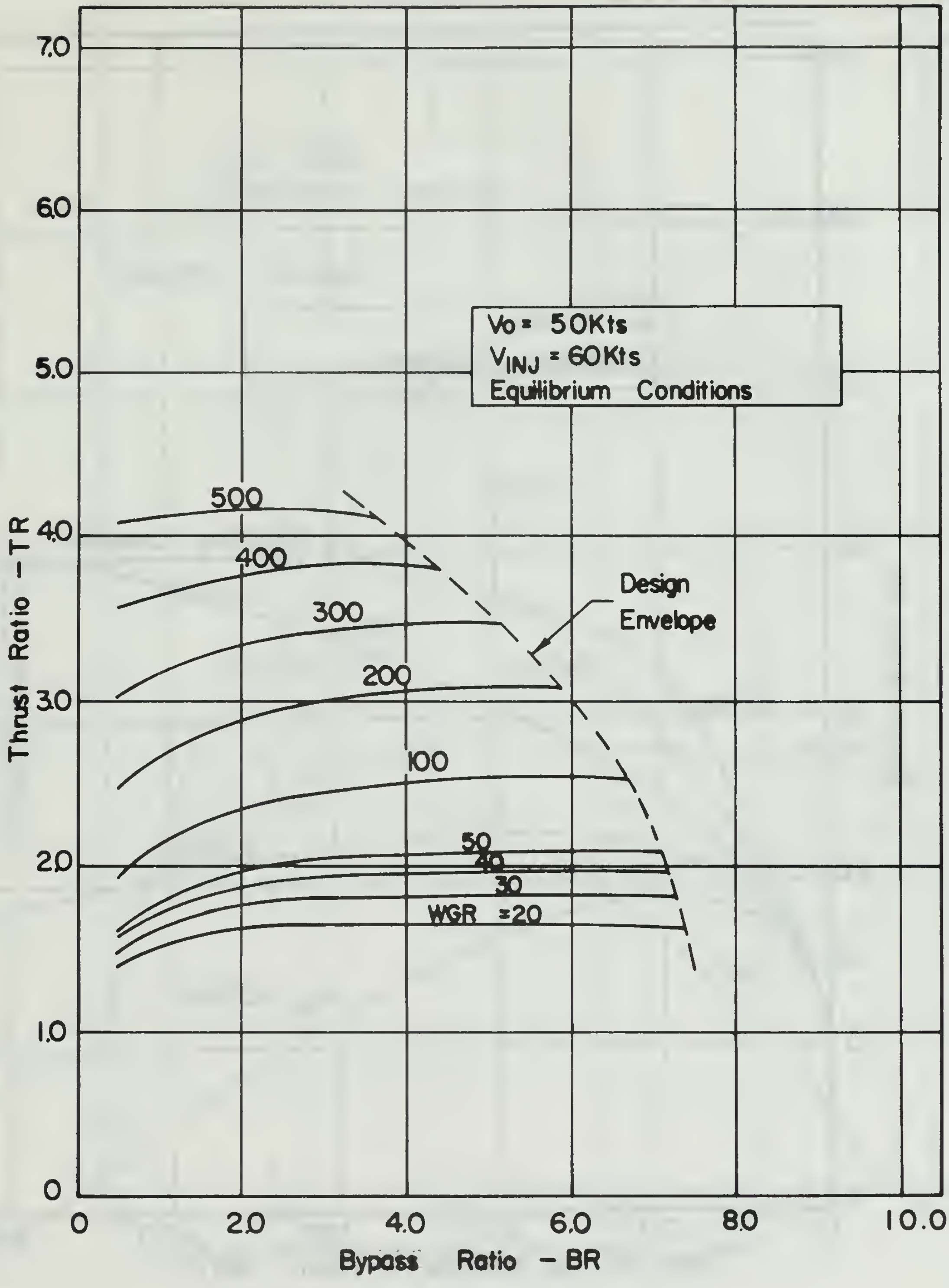

FIGURE 5 . THRUST RATIO VERSUS BYPASS RATIO FOR VARIOUS WATER-TO-GAS GENERATOR AIR RATIOS

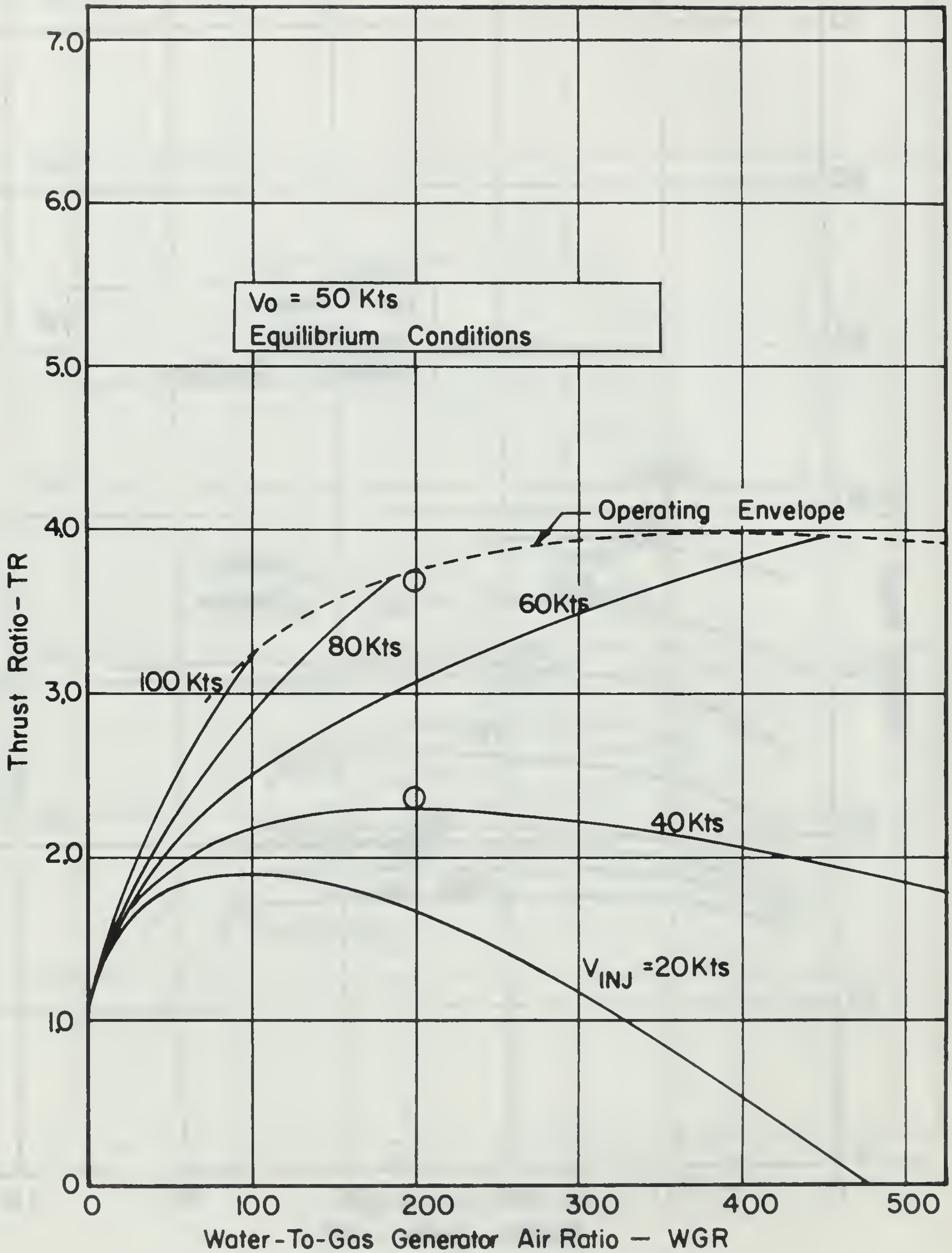

FIGURE 6 . THRUST RATIO VERSUS WATER-TO-GAS GENERATOR AIR RATIO FOR VARIOUS INJECTION VELOCITIES

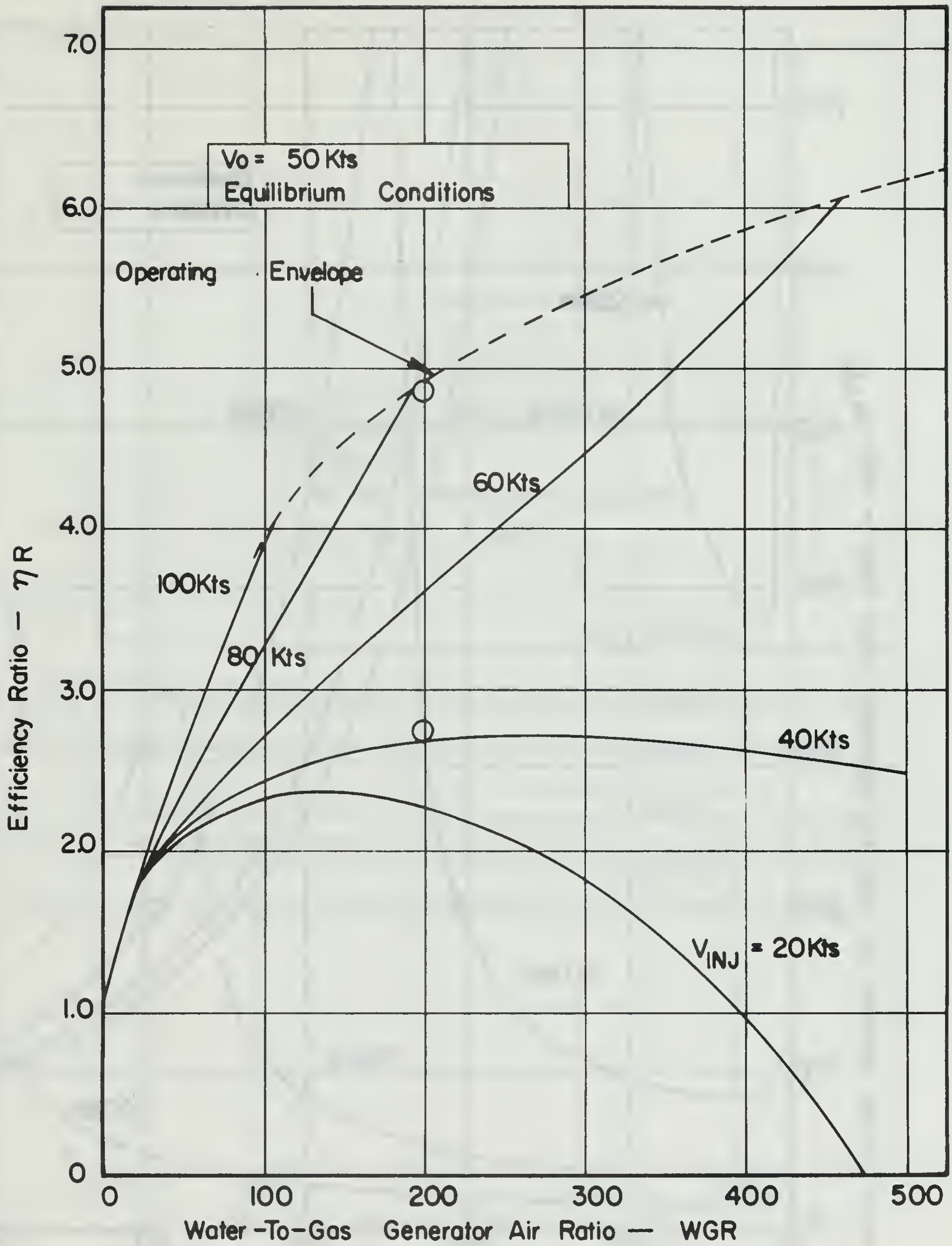

FIGURE 7. EFFICIENCY RATIO VERSUS WATER-TO-GAS GENERATOR AIR RATIO FOR VARIOUS INJECTION VELOCITIES

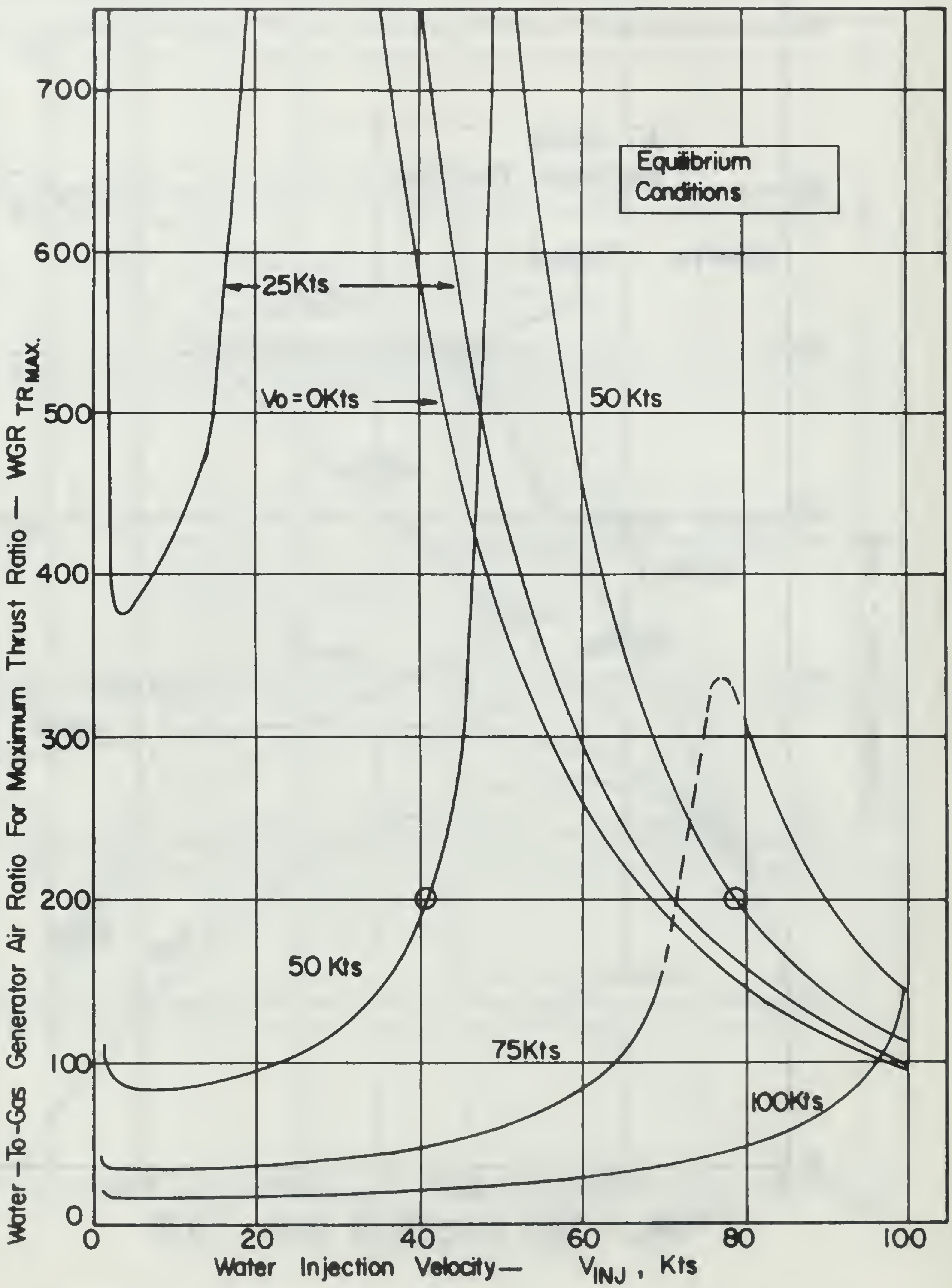

FIGURE 8. WATER–TO–GAS GENERATOR AIR RATIO FOR MAXIMUM THRUST RATIO VERSUS WATER INJECTION VELOCITY AT VARIOUS CRAFT VELOCITIES

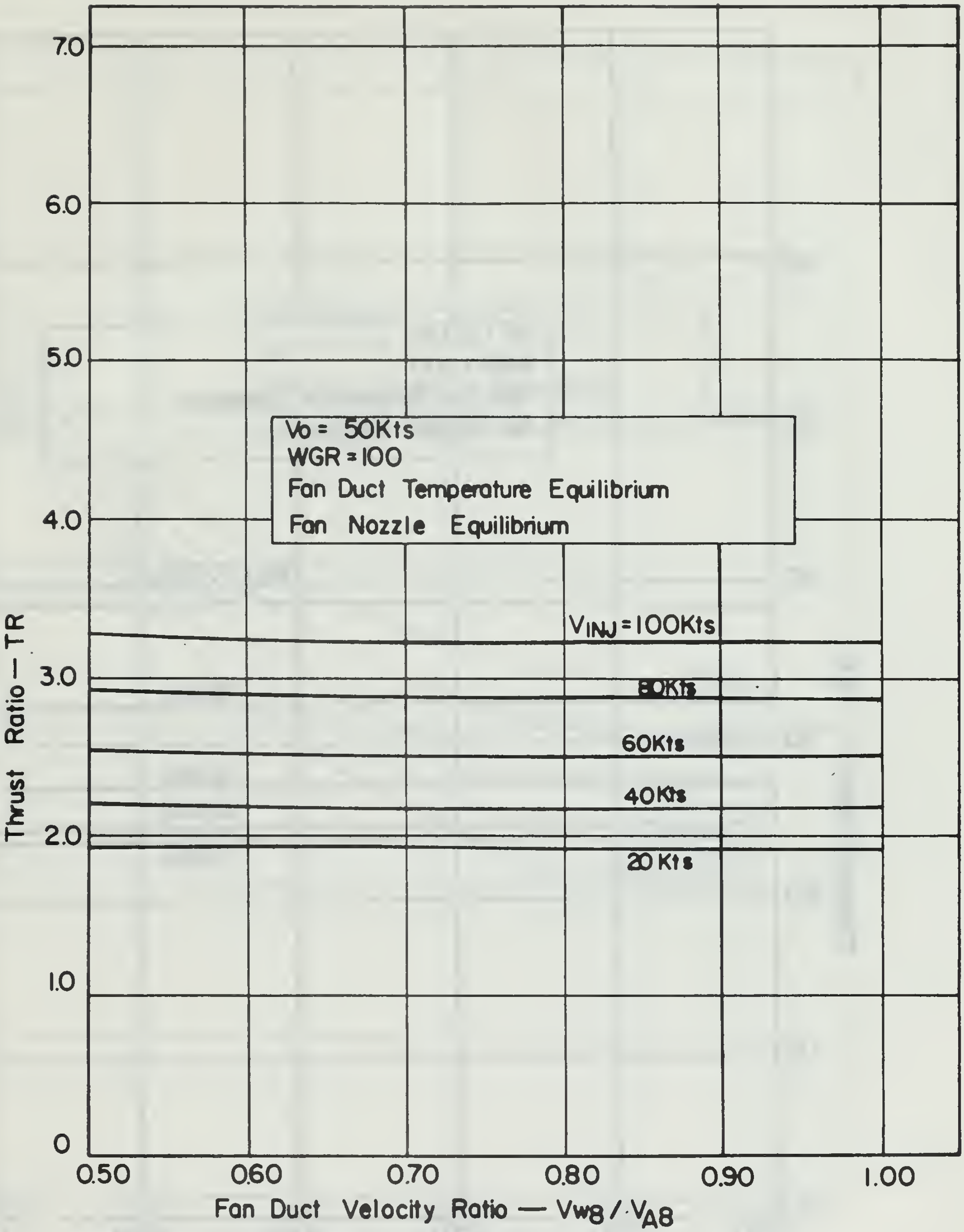

FIGURE 9 THRUST RATIO VERSUS FAN DUCT VELOCITY RATIO FOR VARIOUS WATER INJECTION VELOCITIES

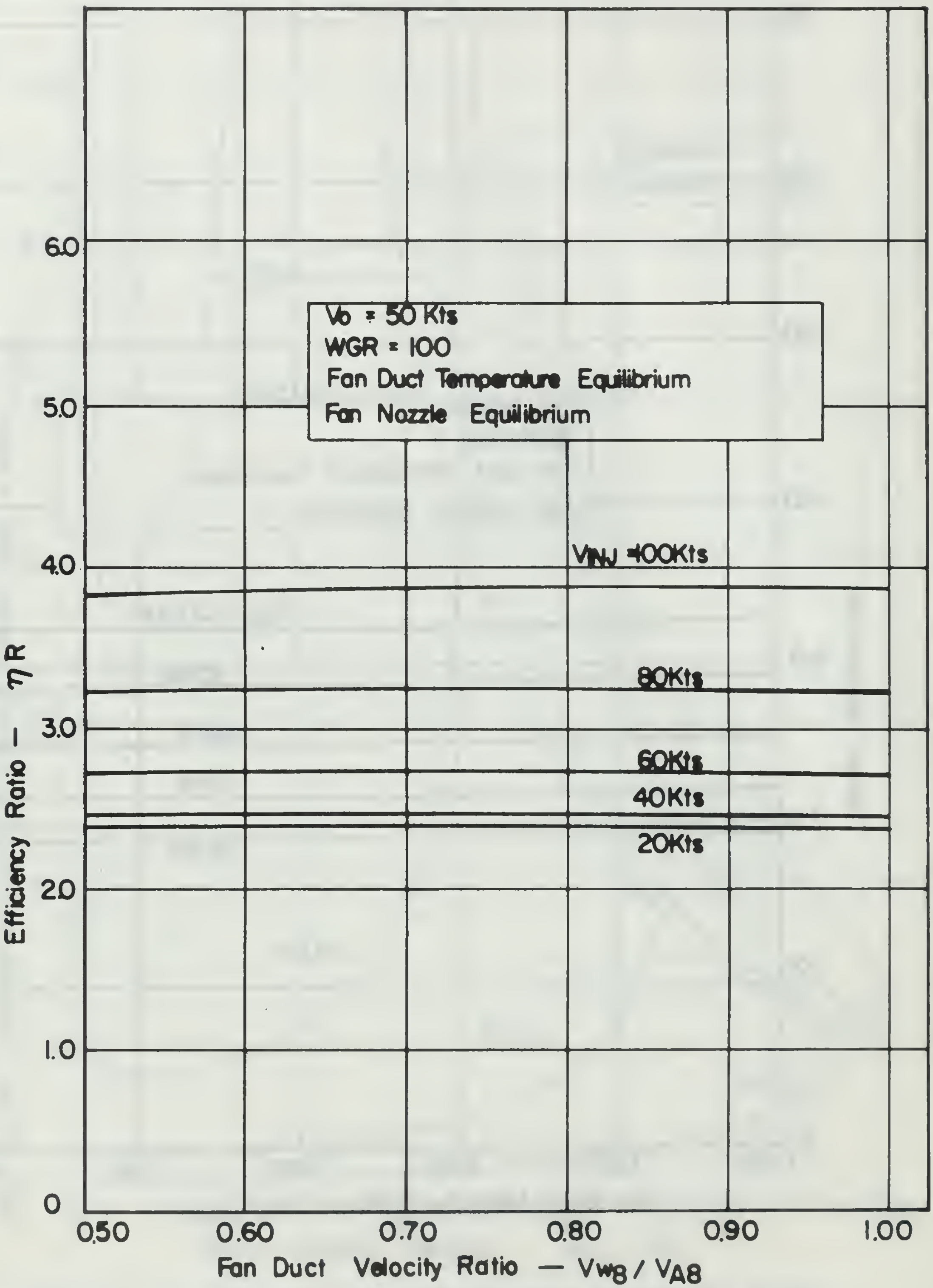

FIGURE 10. EFFICIENCY RATIO VERSUS FAN DUCT VELOCITY RATIO FOR VARIOUS WATER INJECTION VELOCITIES

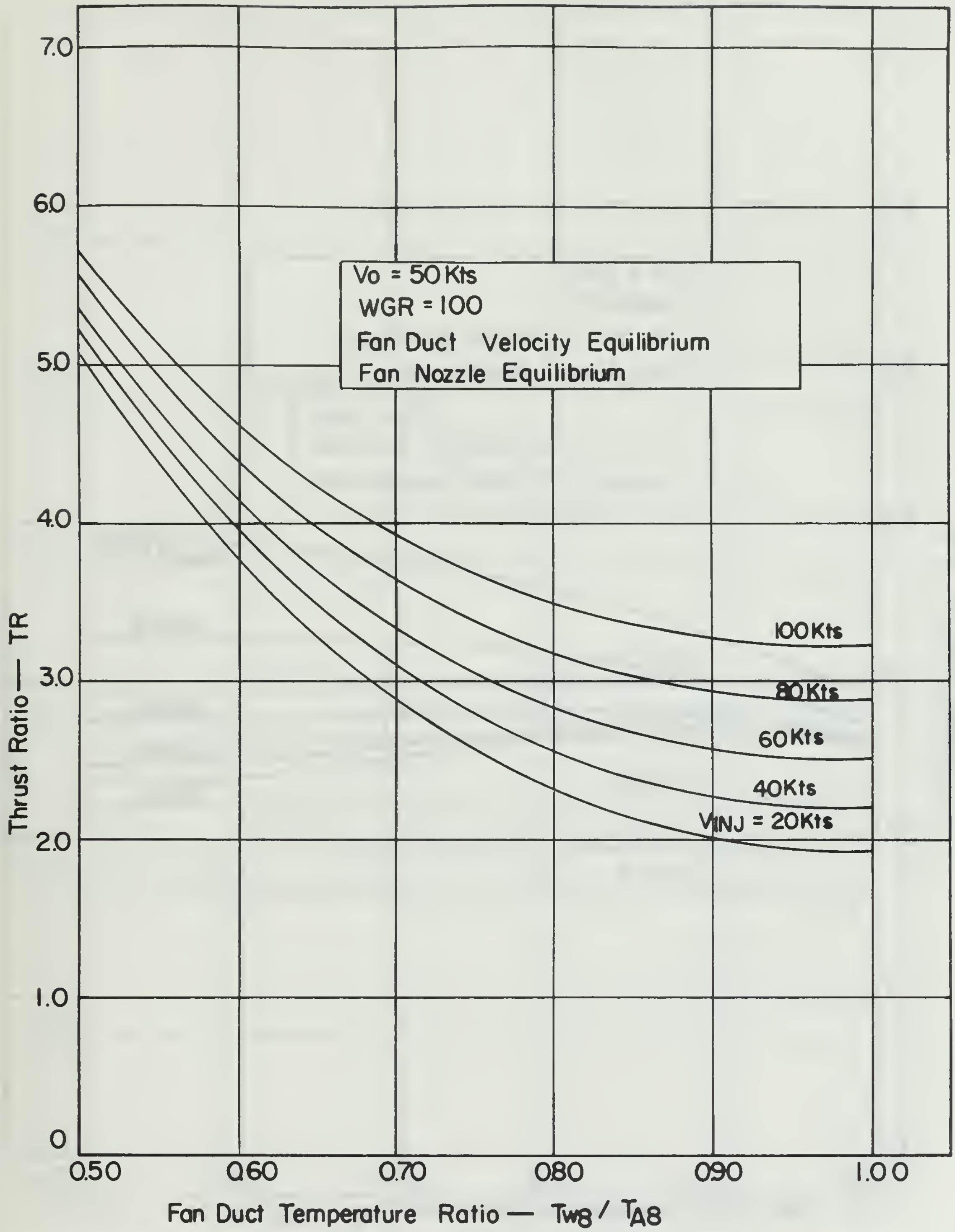

FIGURE 11. THRUST RATIO VERSUS FAN DUCT TEMPERATURE RATIO FOR VARIOUS WATER INJECTION VELOCITIES

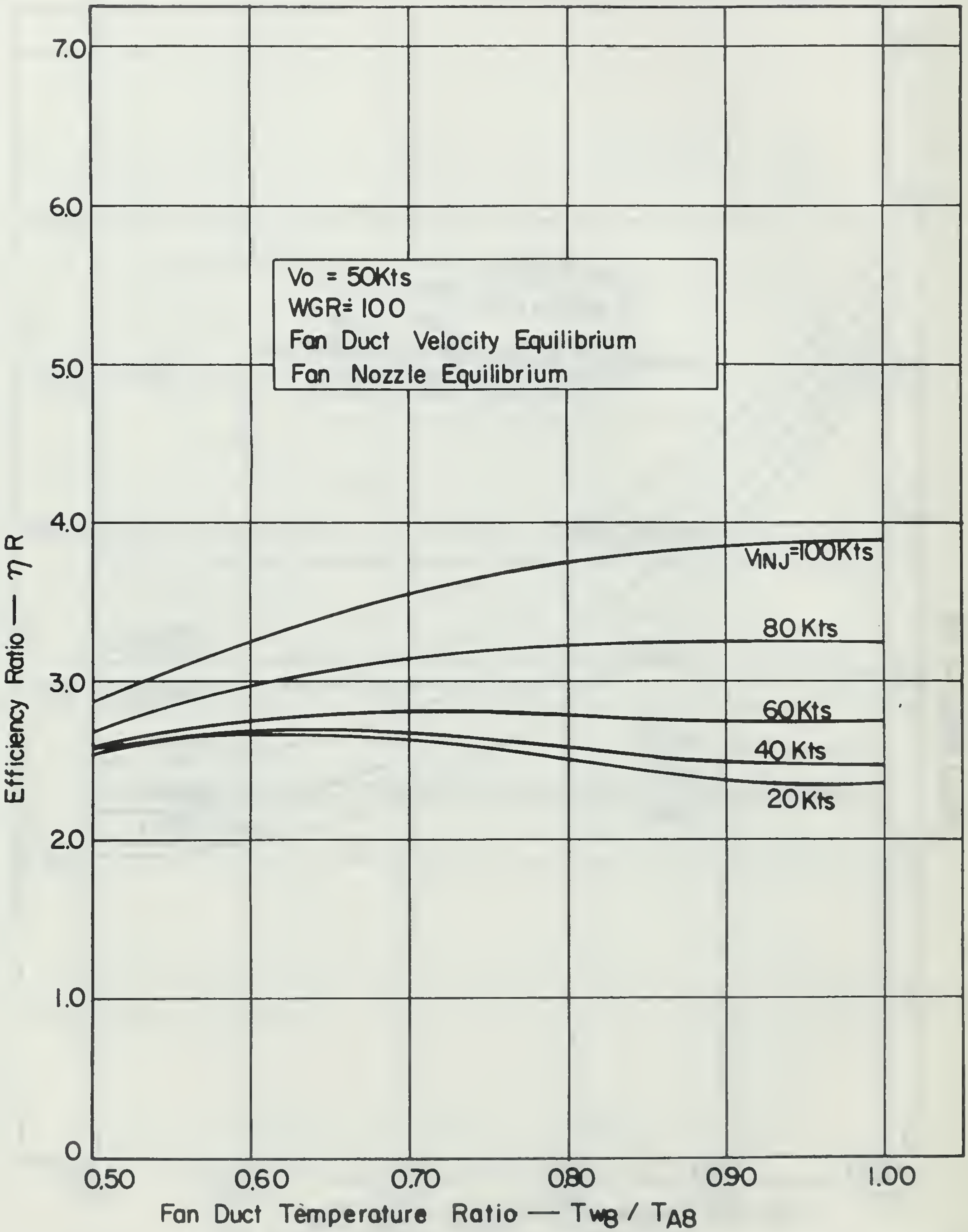

FIGURE 12. EFFICIENCY RATIO VERSUS FAN DUCT TEMPERATURE RATIO FOR VARIOUS WATER INJECTION VELOCITIES

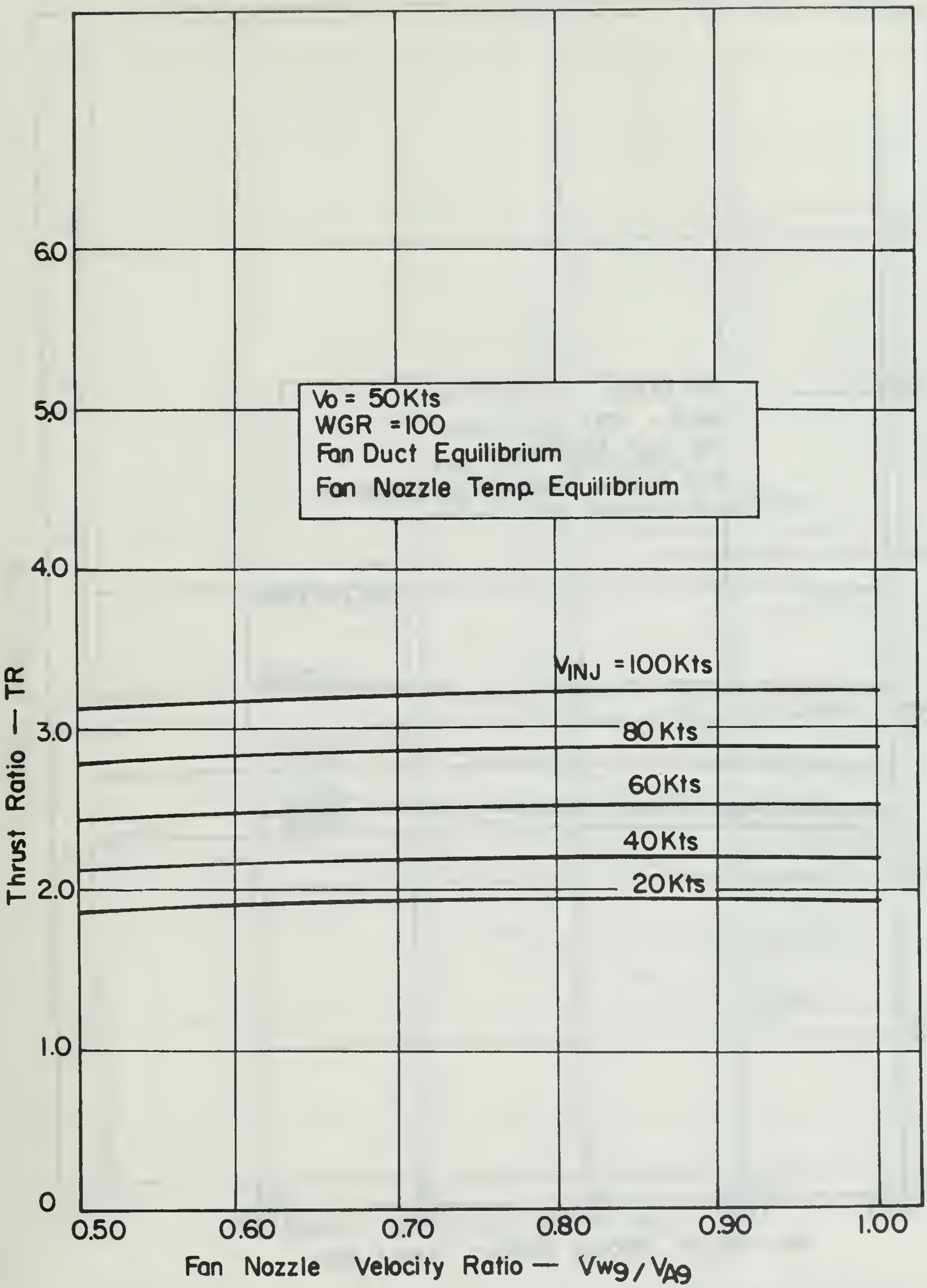

FIGURE 13. THRUST RATIO VERSUS FAN NOZZLE VELOCITY RATIO FOR VARIOUS WATER INJECTION VELOCITIES

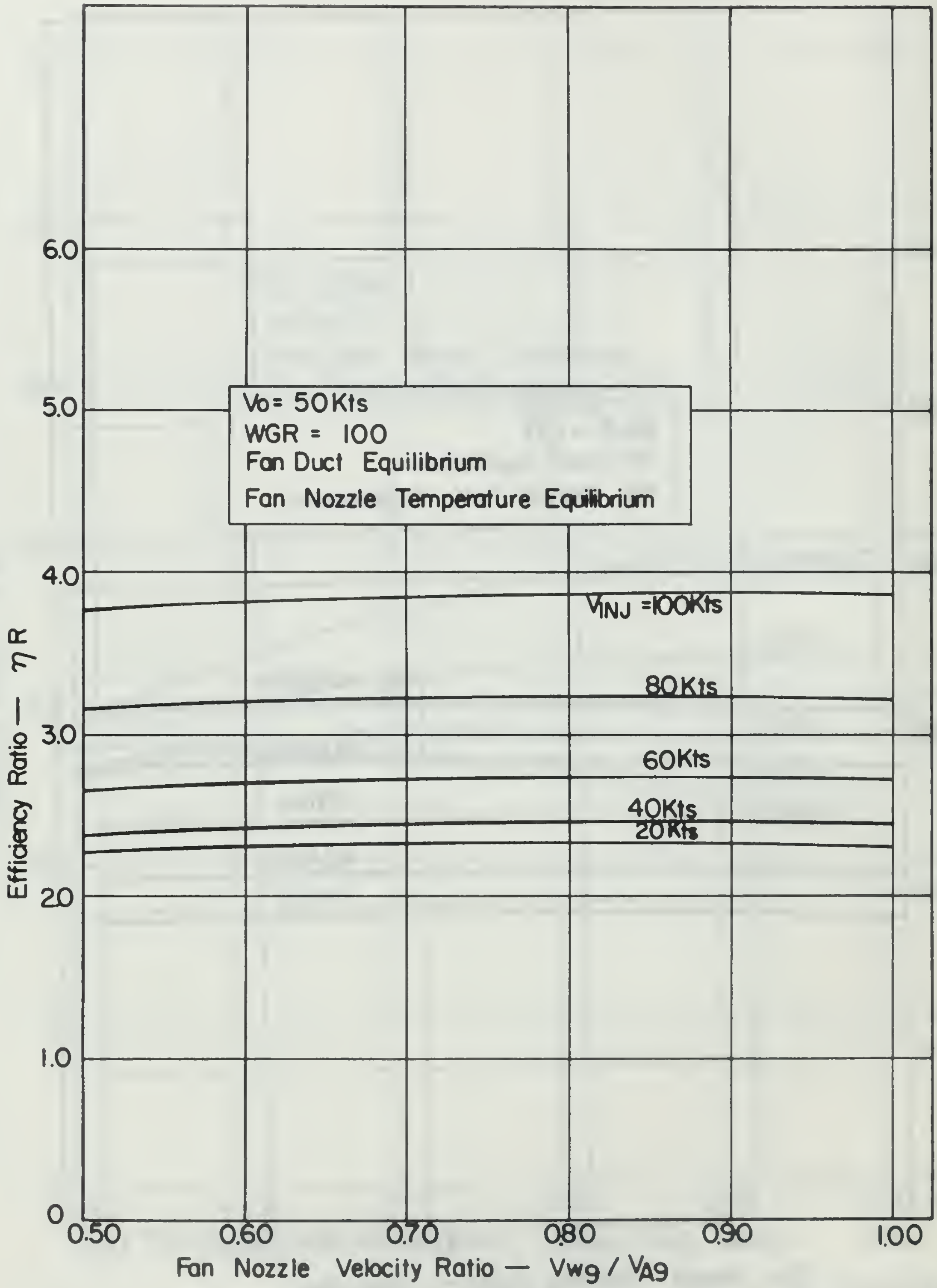

FIGURE 14. EFFICIENCY RATIO VERSUS FAN NOZZLE VELOCITY RATIO FOR VARIOUS WATER INJECTION VELOCITIES

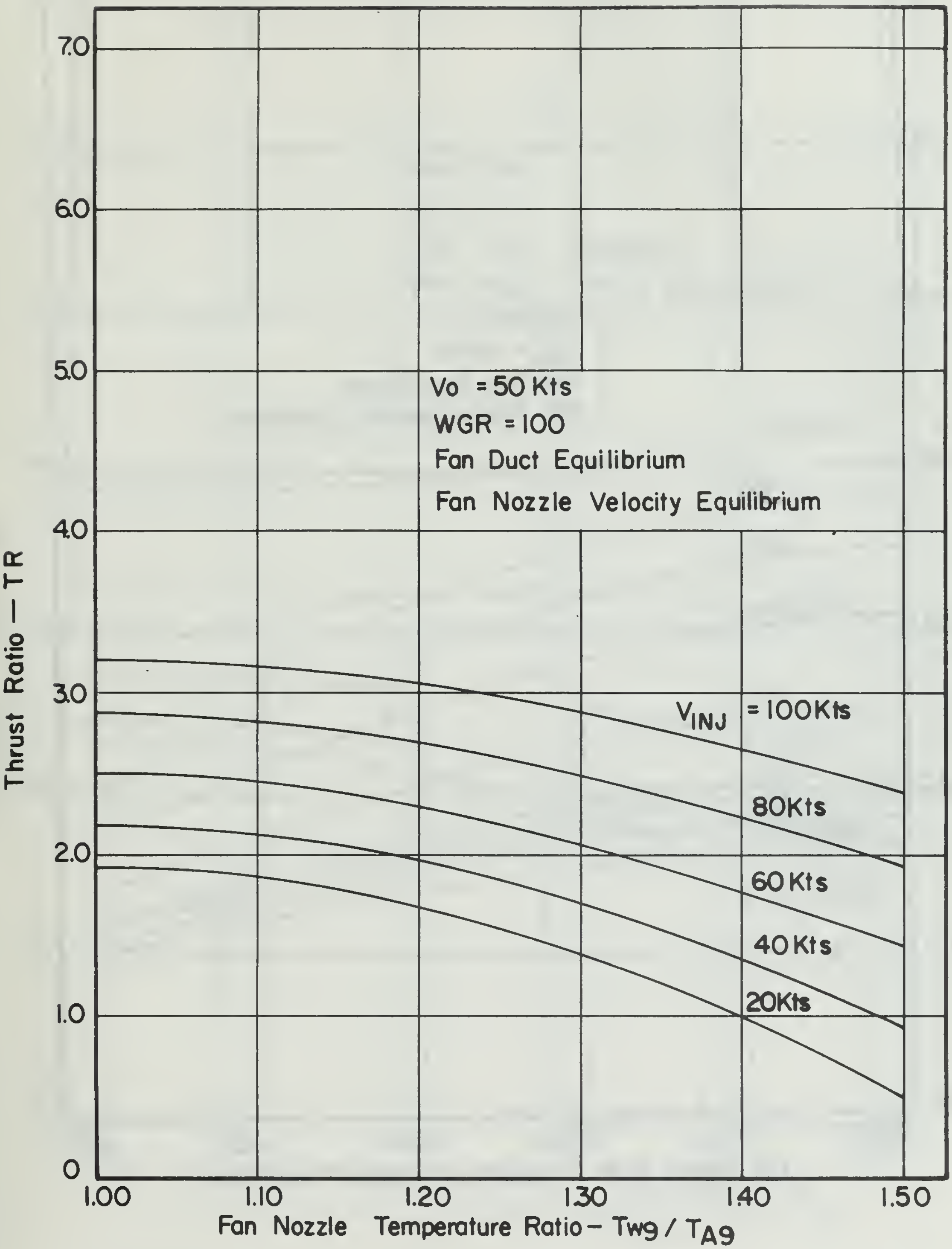

FIGURE 15. THRUST RATIO VERSUS FAN NOZZLE EXIT TEMPERATURE RATIO FOR VARIOUS WATER INJECTION VELOCITIES

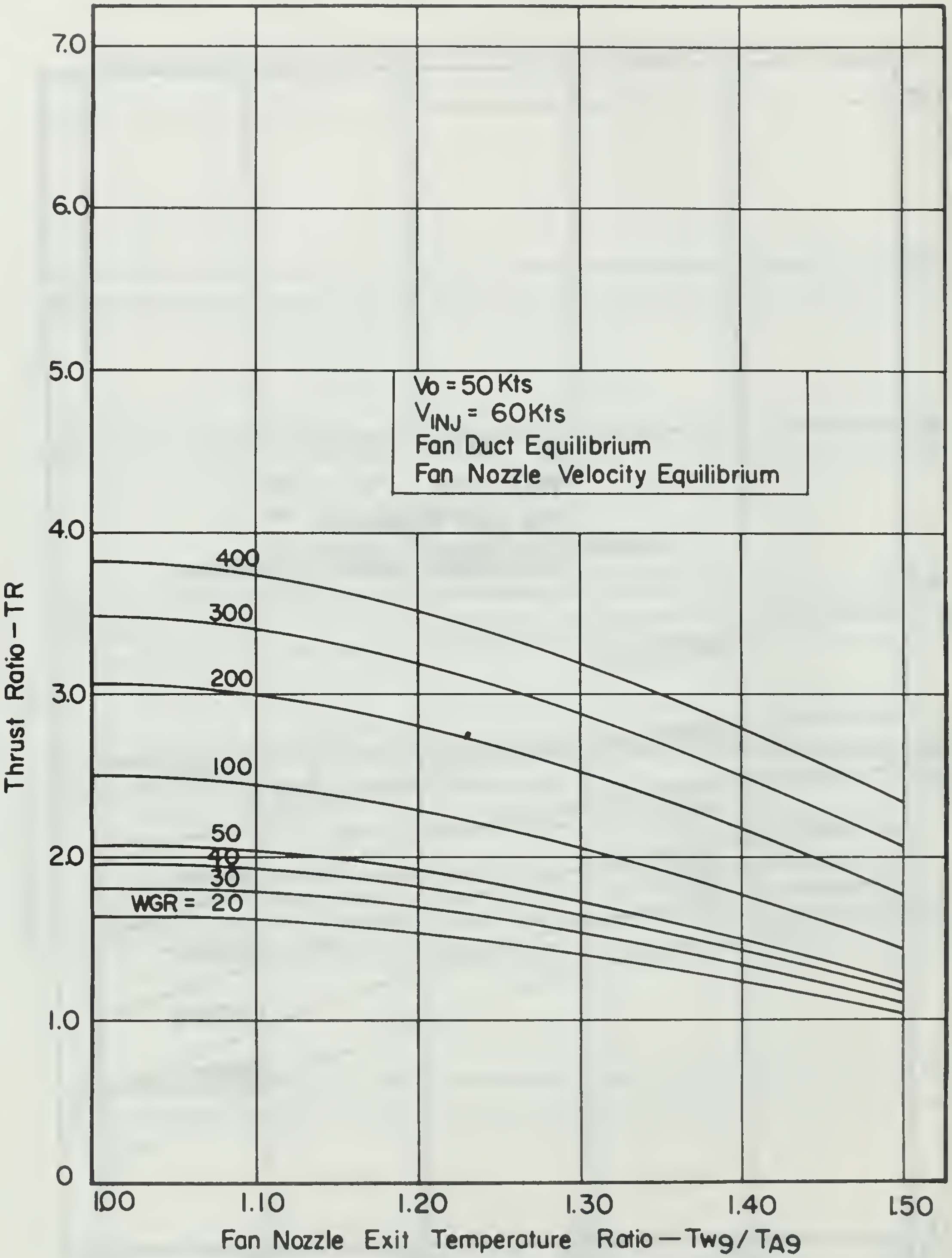

FIGURE 16. THRUST RATIO VERSUS FAN NOZZLE EXIT TEMPERATURE RATIO FOR VARIOUS WATER-TO-GAS GENERATOR AIR RATIOS

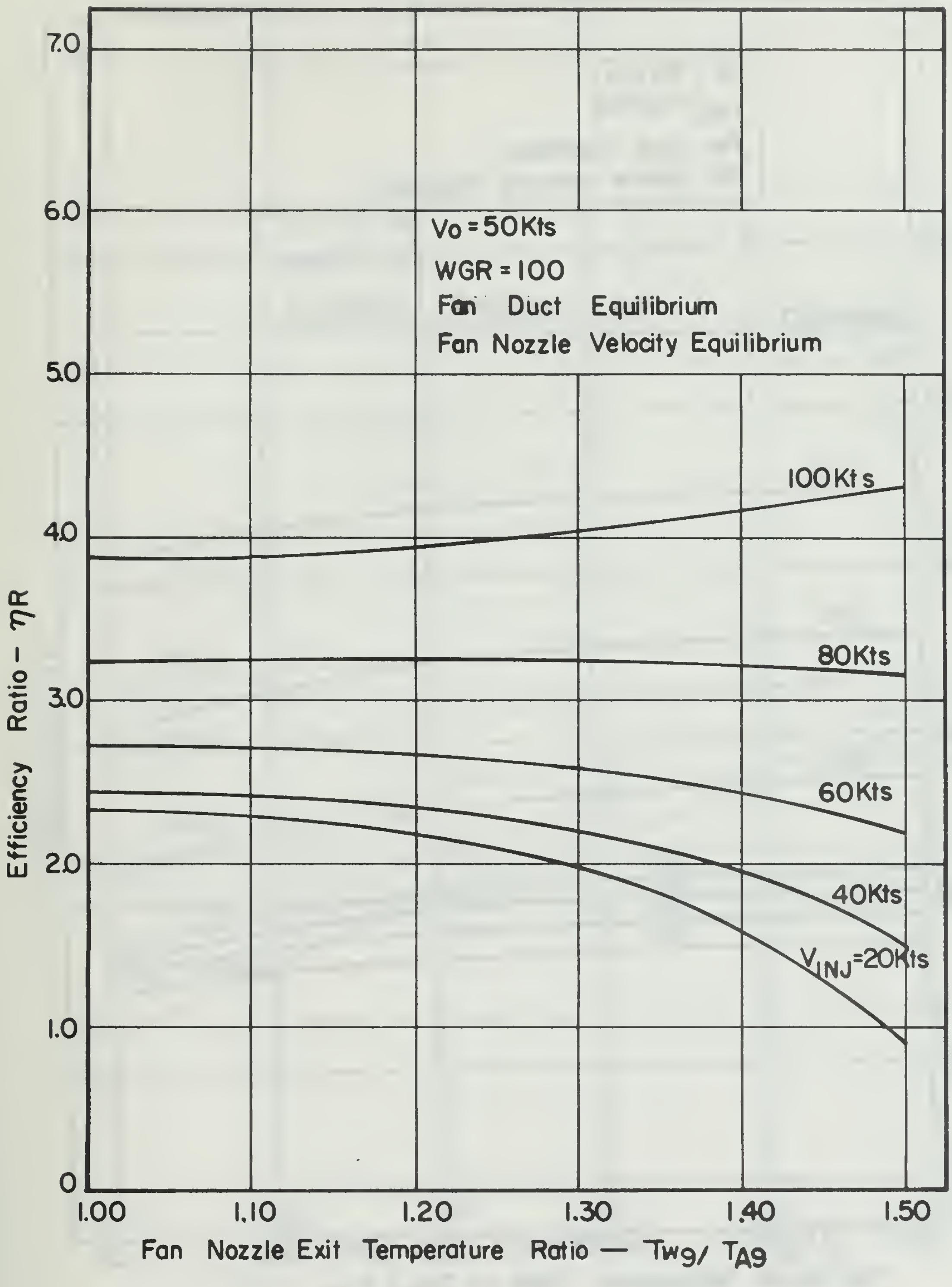

FIGURE 17. EFFICIENCY RATIO VERSUS FAN NOZZLE EXIT TEMPERATURE RATIO FOR VARIOUS WATER INJECTION VELOCITIES

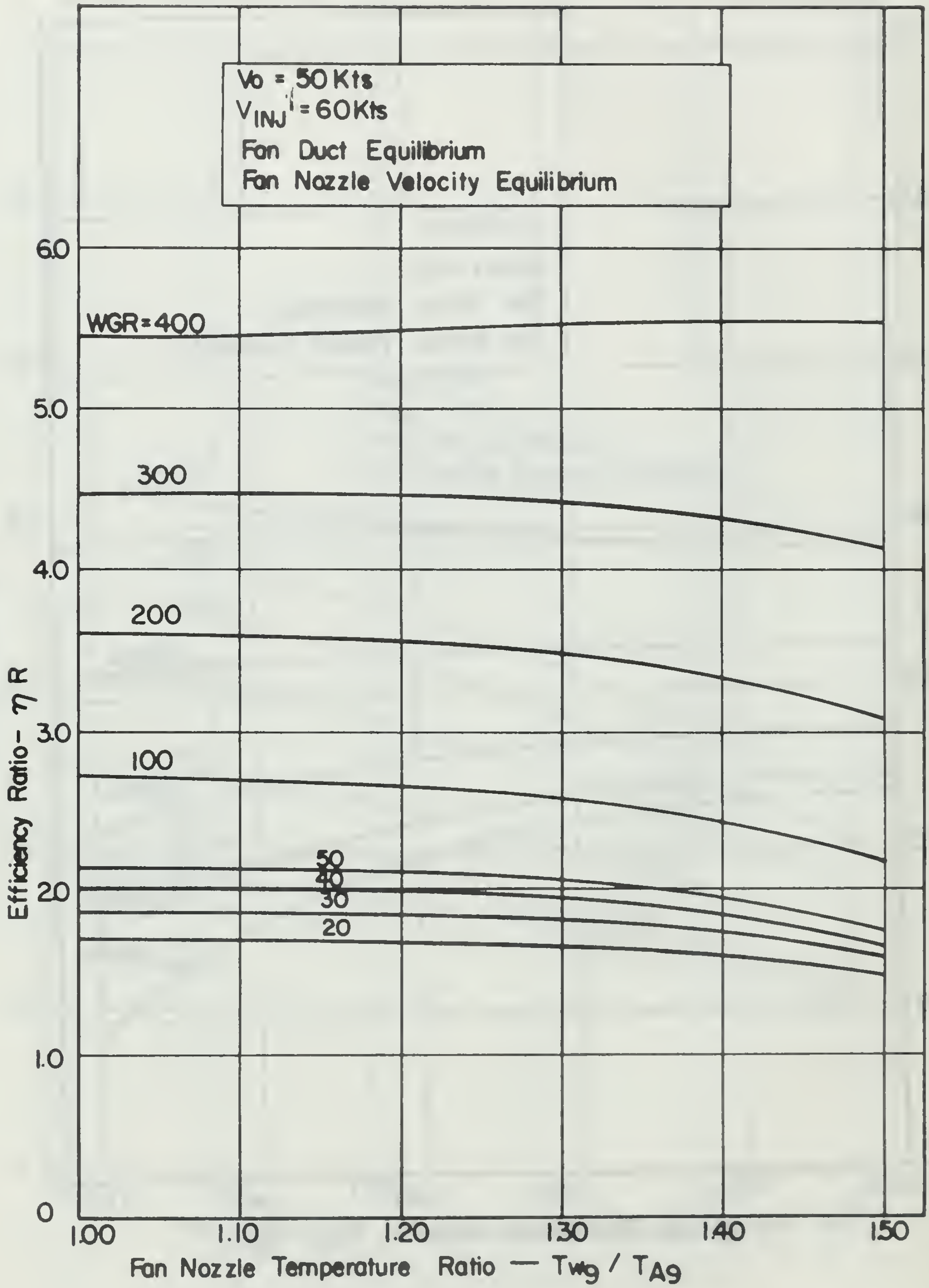

FIGURE 18. EFFICIENCY RATIO VERSUS FAN NOZZLE TEMP. RATIO FOR VARIOUS WATER-TO-GAS GENERATOR AIR RATIOS

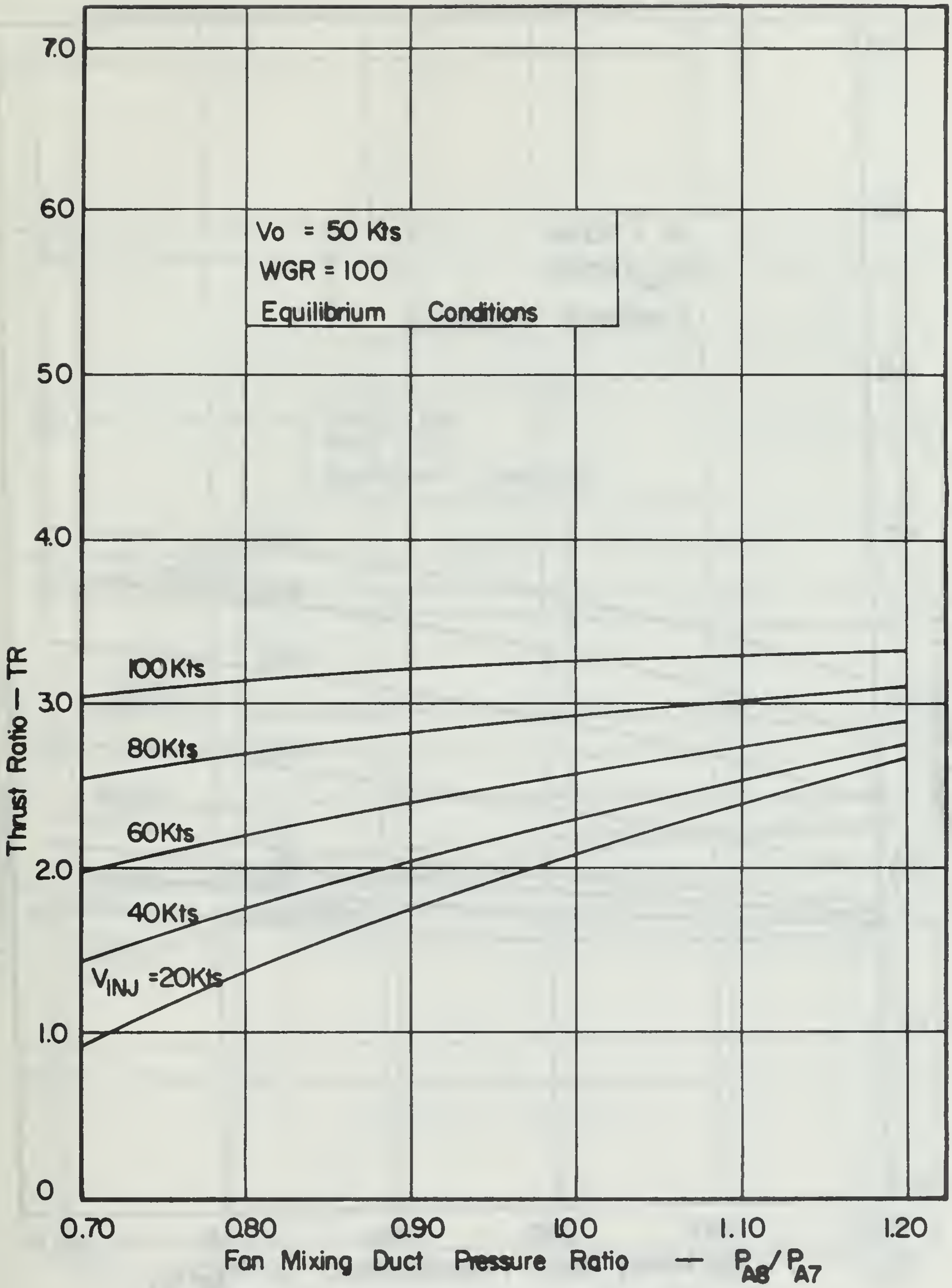

FIGURE 19 .THRUST RATIO VERSUS FAN MIXING DUCT PRESSURE RATIO FOR VARIOUS WATER INJECTION VELOCITIES

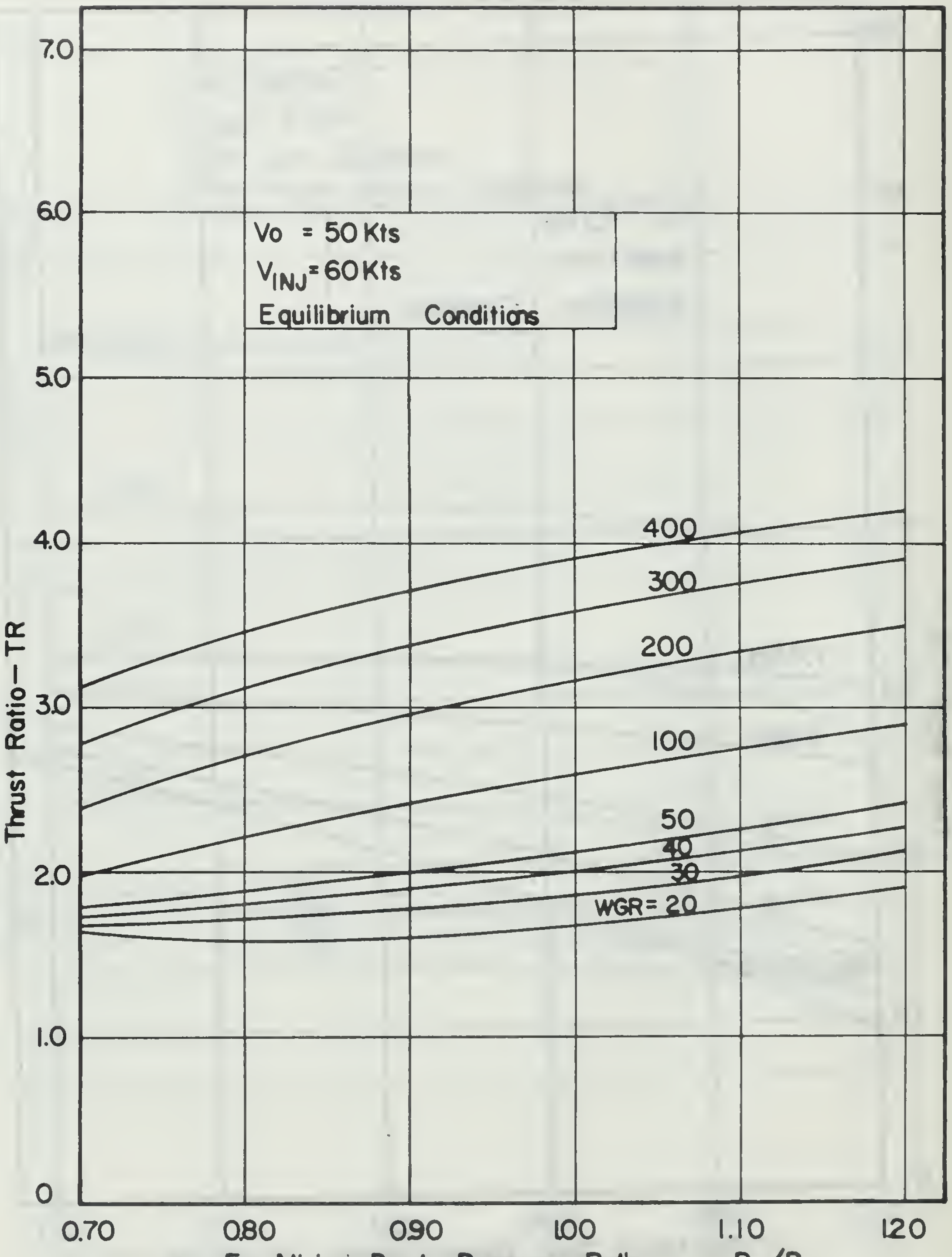

FIGURE 20. THRUST RATIO VERSUS FAN MIXING DUCT PRESSURE RATIO FOR VARIOUS WATER-TO-GAS GENERATOR AIR RATIOS

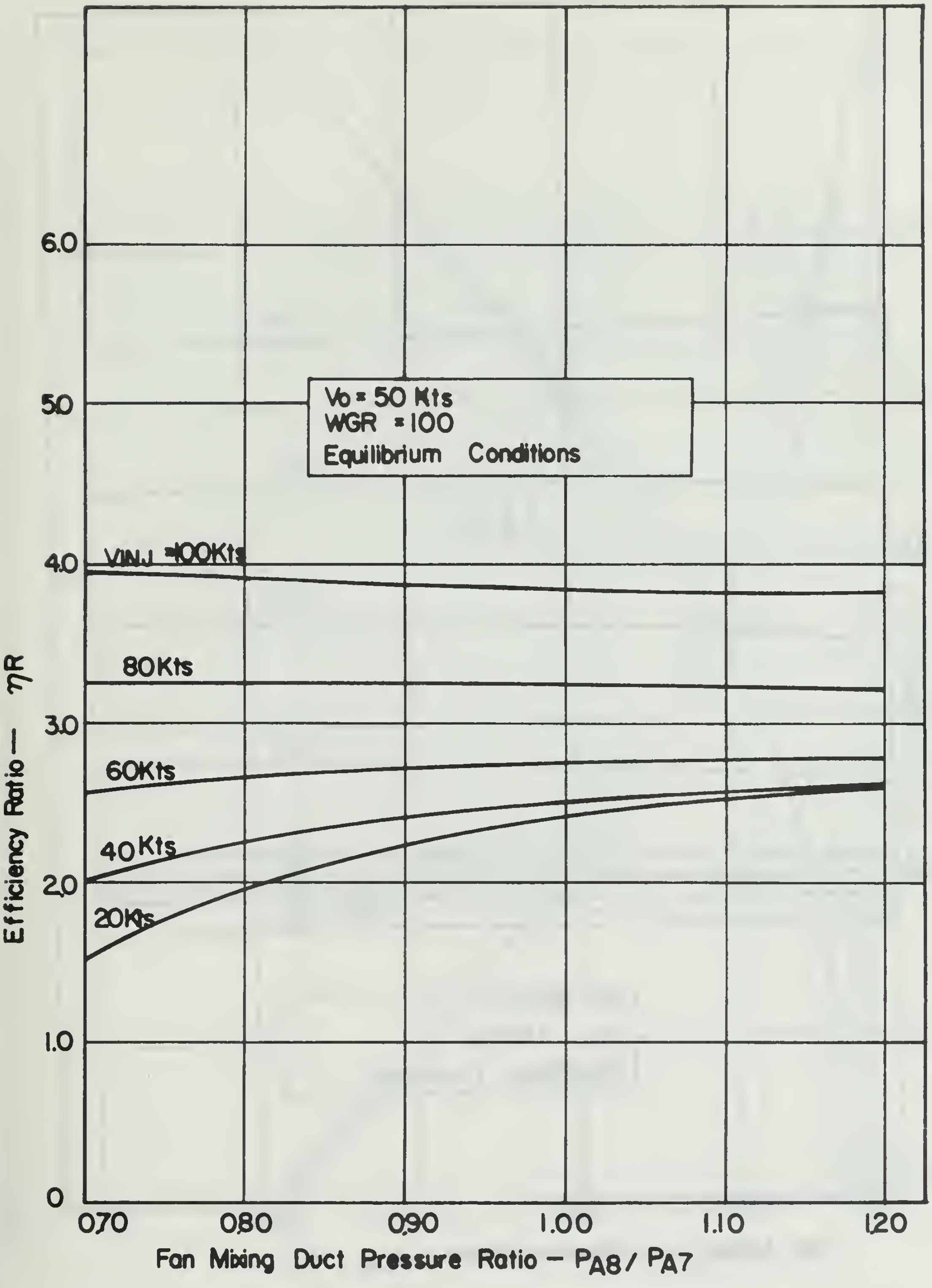

FIGURE 21. EFFICIENCY RATIO VERSUS FAN MIXING DUCT PRESSURE RATIO FOR VARIOUS WATER INJECTION VELOCITIES

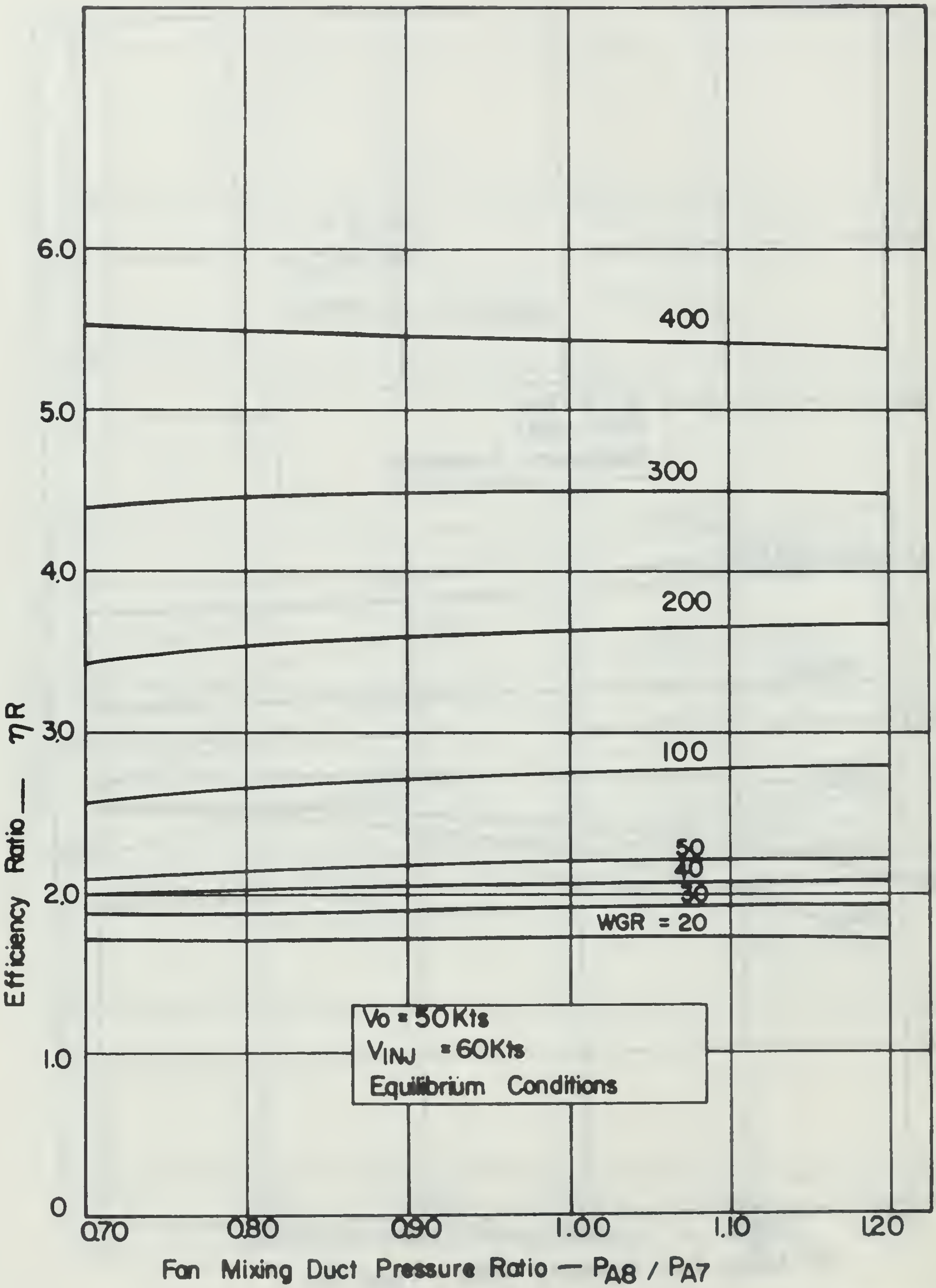

FIGURE 22. EFFCIENCY RATIO VERSUS FAN MIXING DUCT PRESSURE RATIO FOR VARIOUS WATER-TO-GAS GENERATOR AIR RATIOS

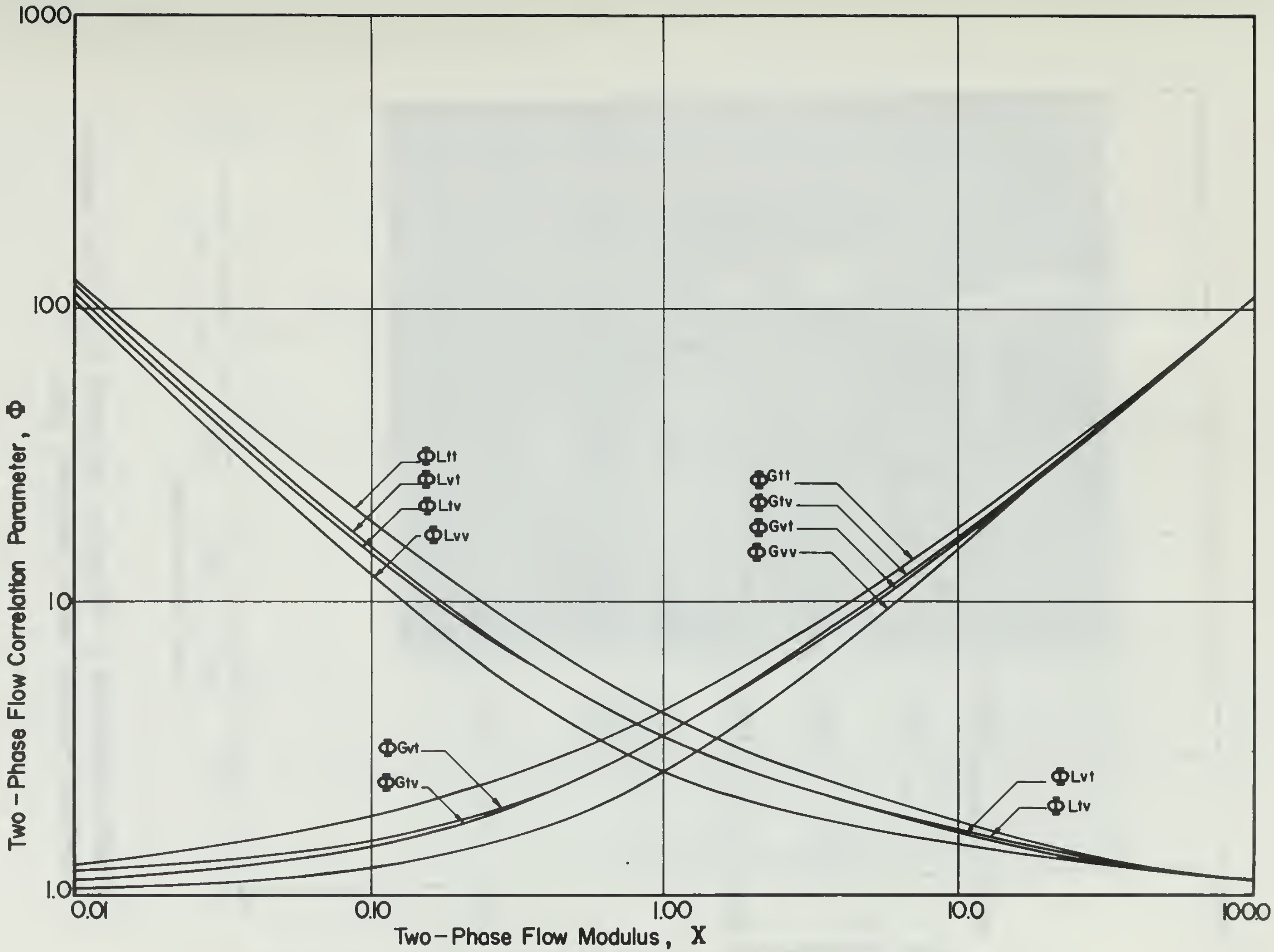

FIGURE 23. TWO PHASE FLOW CORRELATION OF LOCKHART–MARTINELLI [REF. 5]

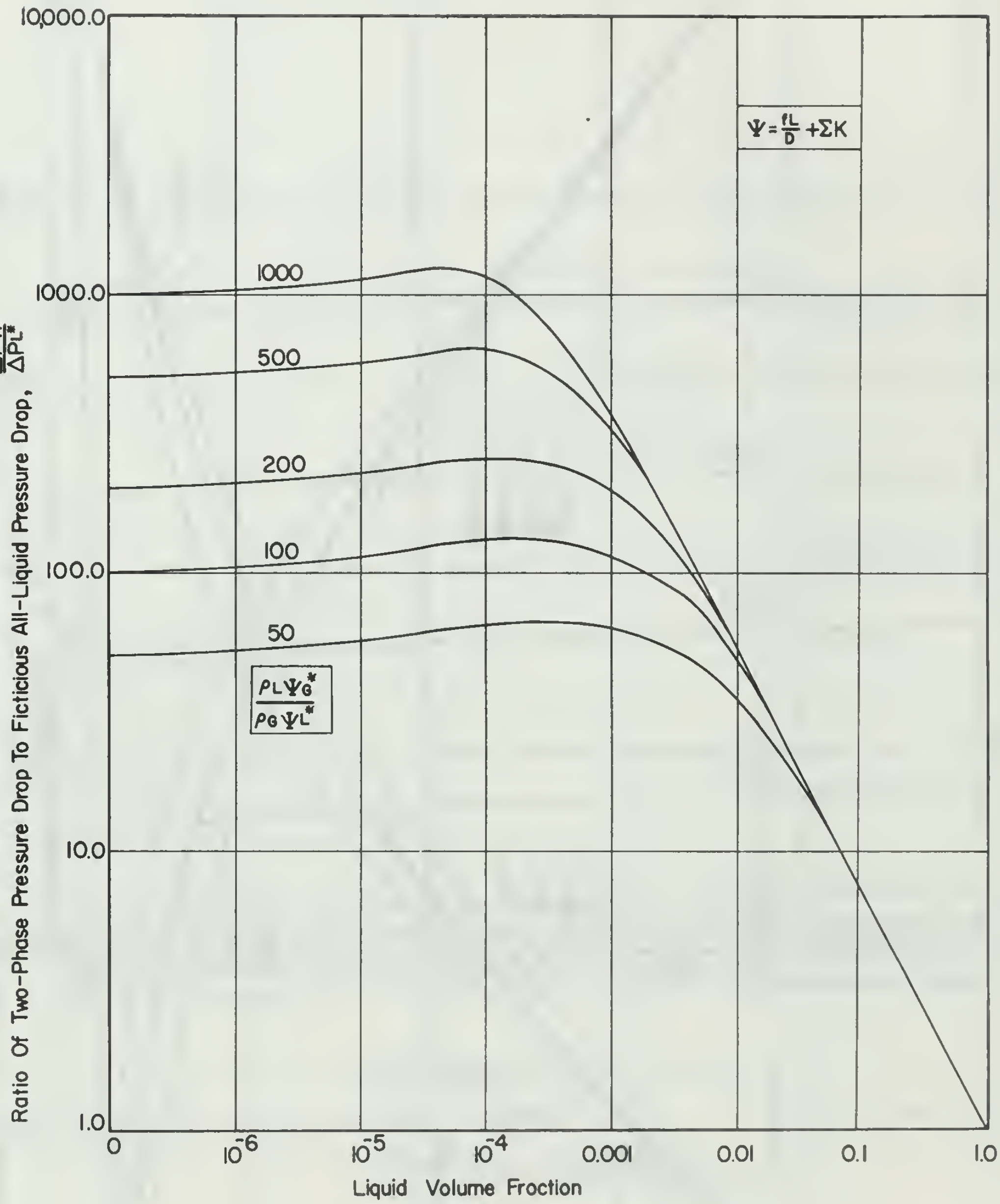

FIGURE 24. CORRELATION OF CHENOWETH AND MARTIN [REF 6] FOR TURBULENT TWO-PHASE PRESSURE DROP IN HORIZONTAL PIPES

FIGURE 25

TWO-PHASE FLOW TEST RIG

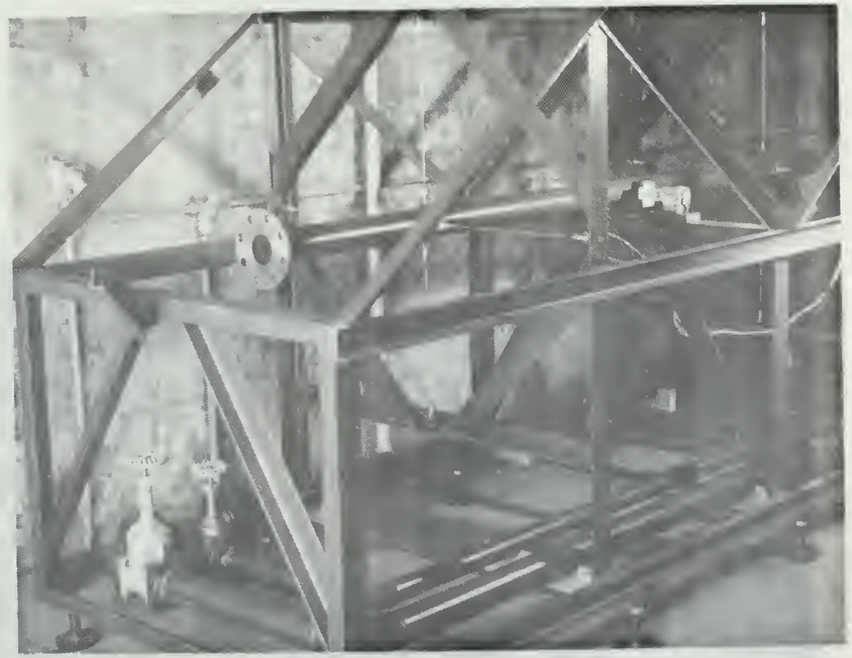

FIGURE 26

TWO-PHASE FLOW TEST RIG

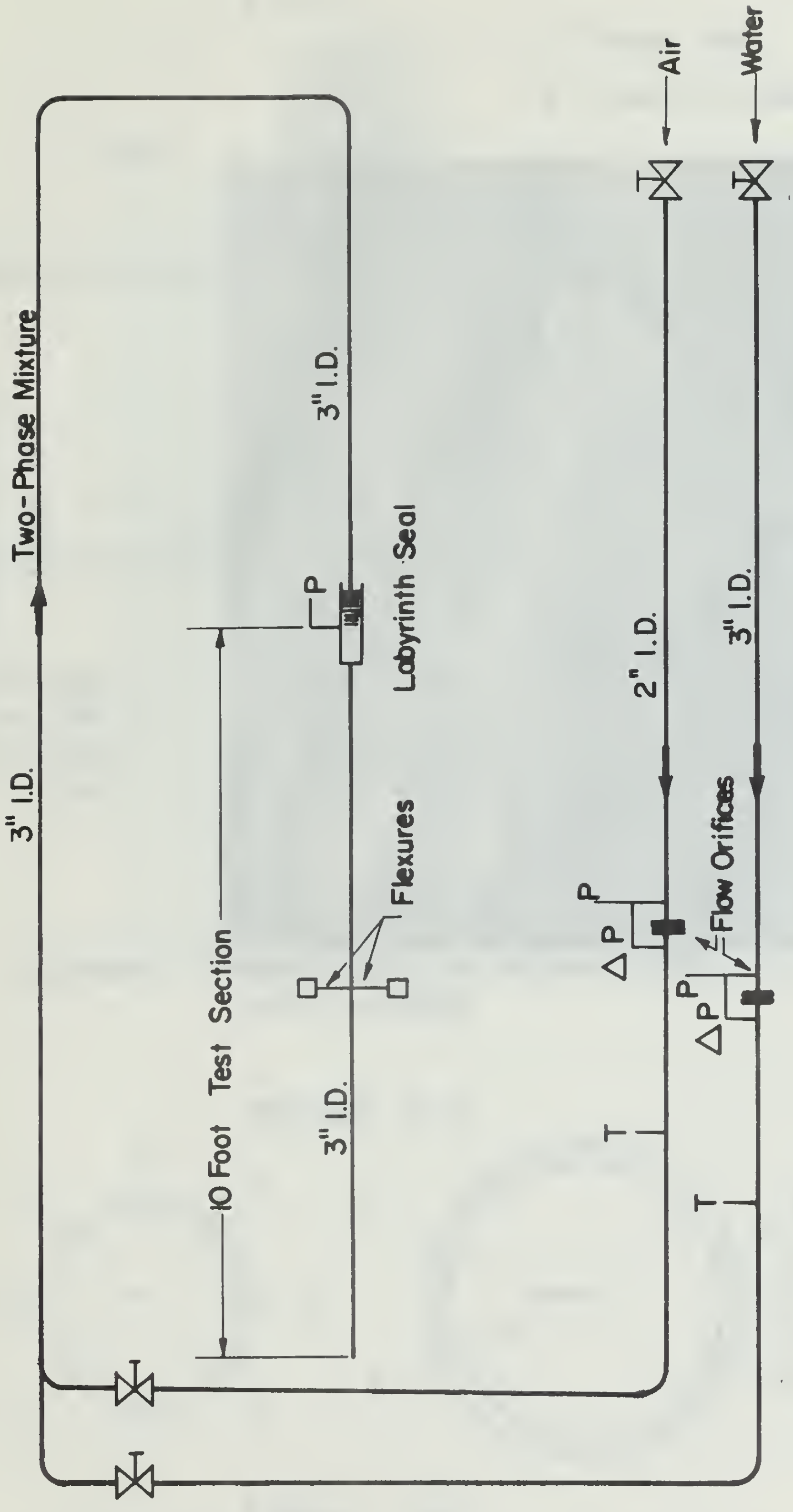

FIGURE 2.7

FLOW DIAGRAM OF TEST APPARATUS

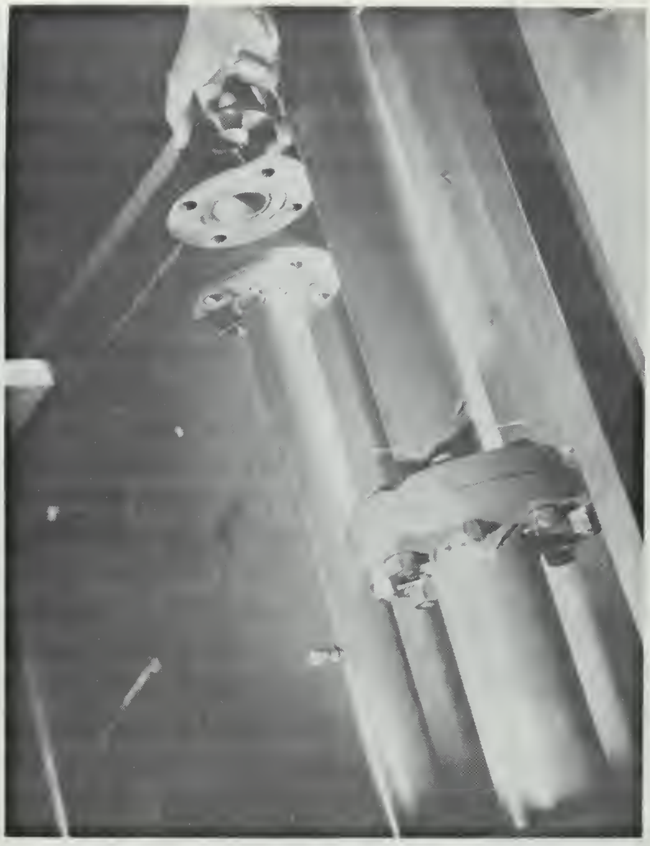

FIGURE 28

VIEW OF ORIFICES

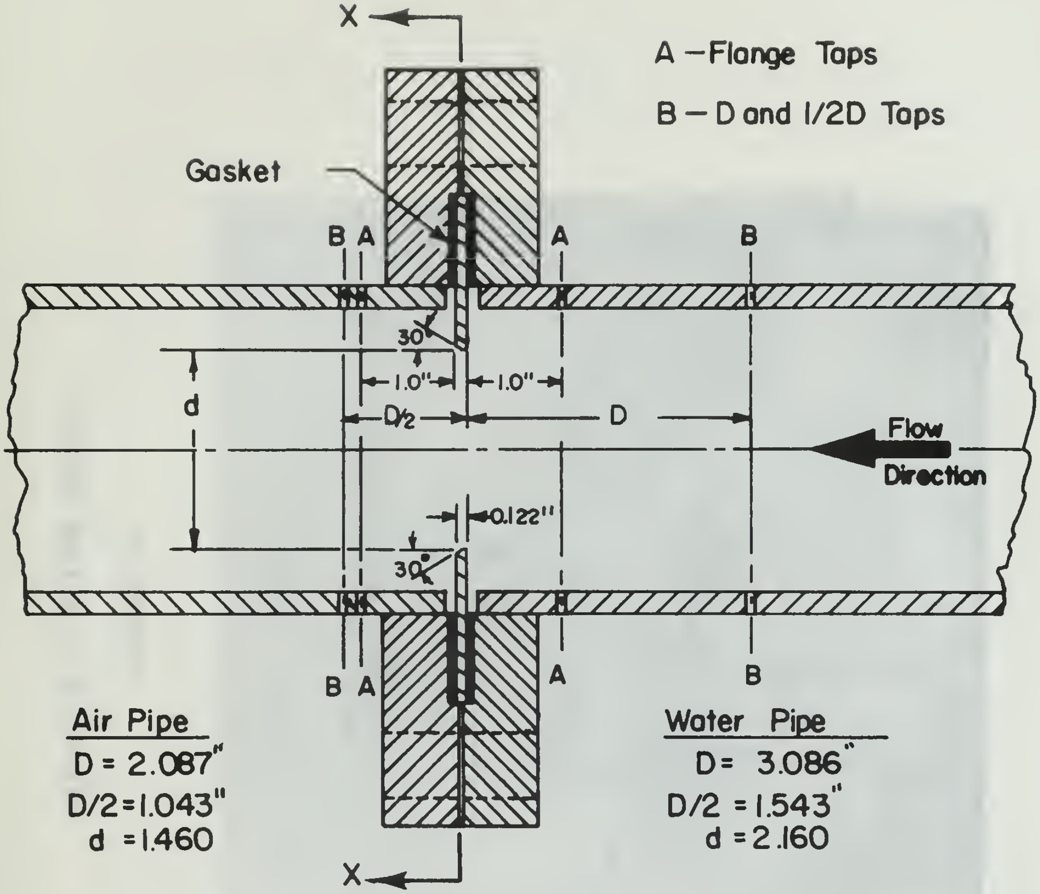

FIGURE 29 A.

GENERAL ARRANGEMENT OF FLOW ORIFICE INSTALLATIONS

SECTION X-X

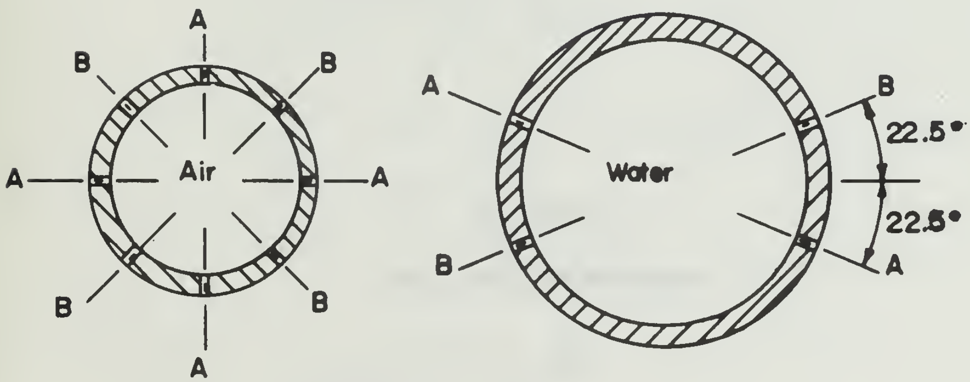

FIGURE 29B.

LOCATION OF ORIFICE PRESSURE TAPS AROUND PIPE

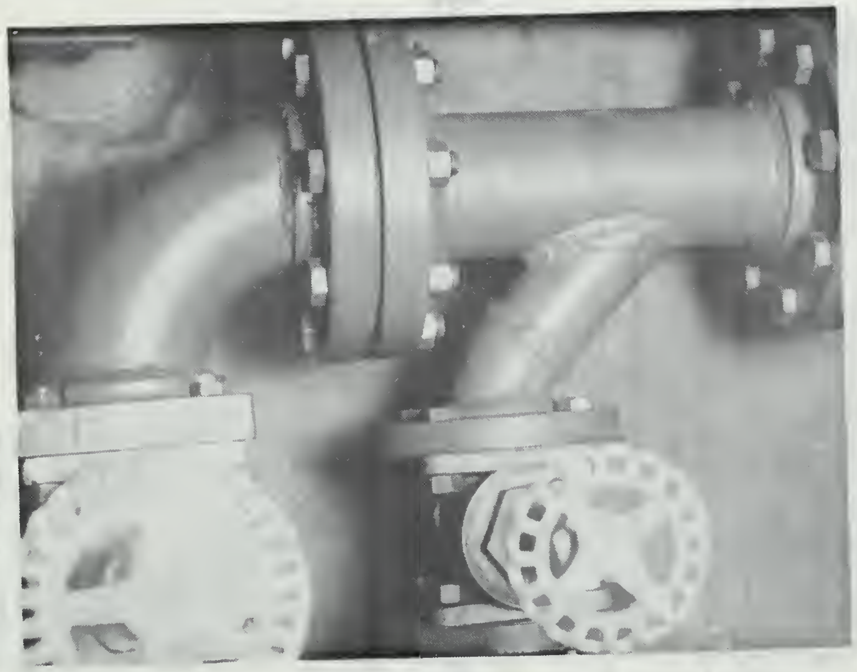

FIGURE 30

AIR-WATER INJECTION SECTION

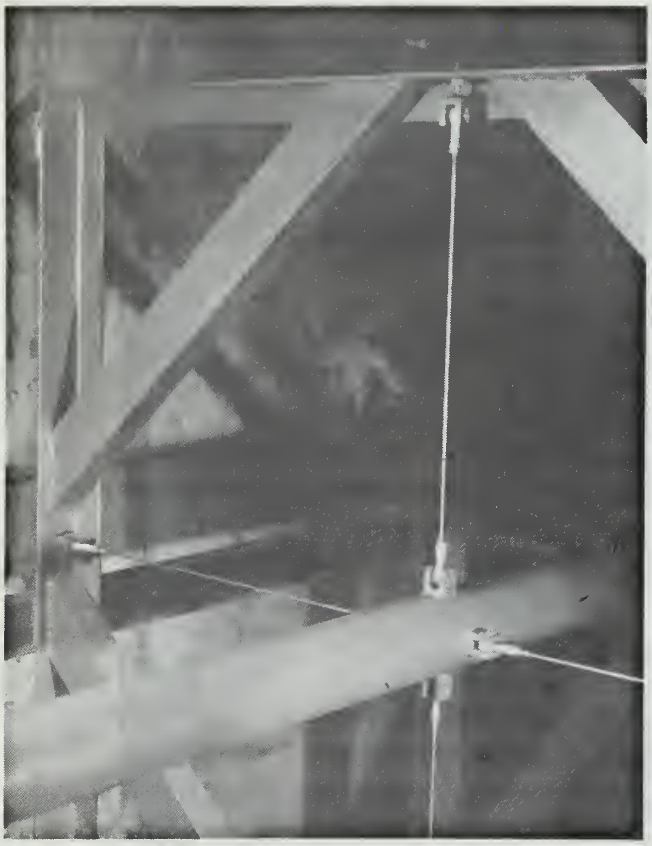

FIGURE 31

TEST SECTION SUPPORTS

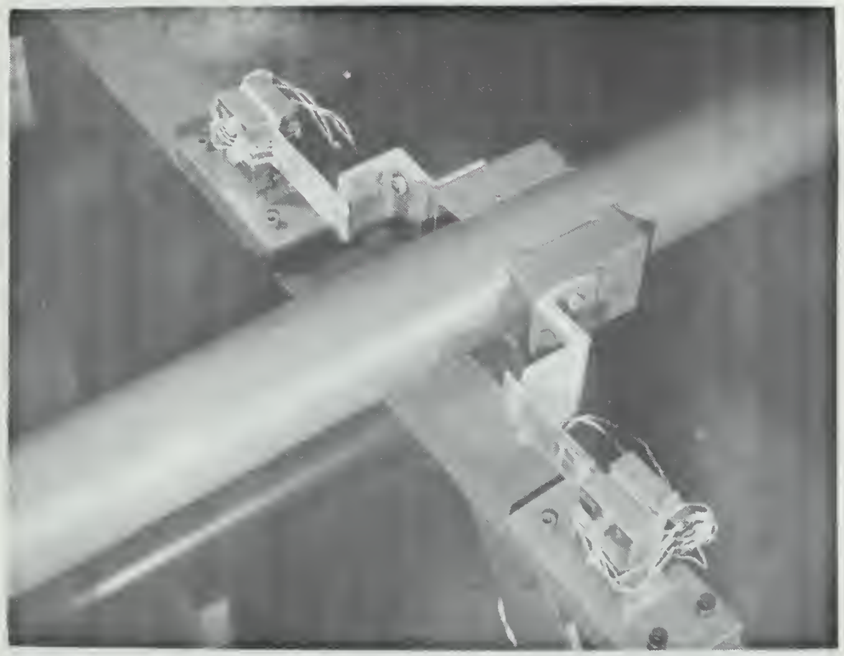

FIGURE 32

FLEXURES

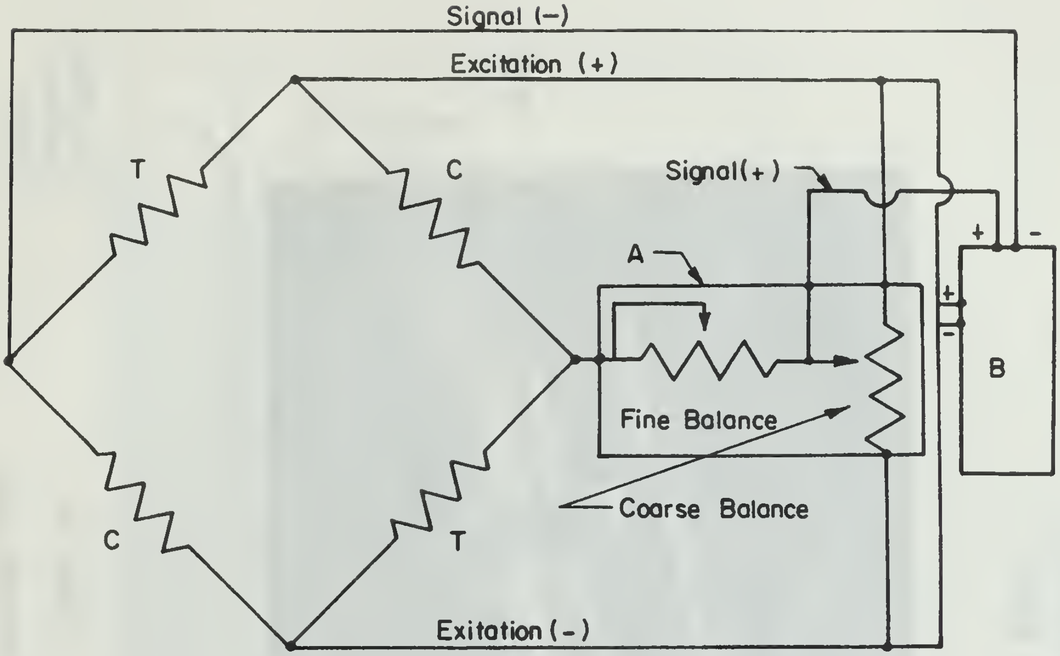

A. Switching And Balancing Unit

B. Daytronic Strain Gage Digital Indicator Model 700

C. Compression Strain Gages

T. Tension Strain Gages

Strain Gages: Budd 120 Ω Foil Gages

Bonding Agent: Eastman 910

Waterproofing: Dow Corning RTV

FIGURE 33

WIRING DIAGRAM FOR EACH FLEXURE

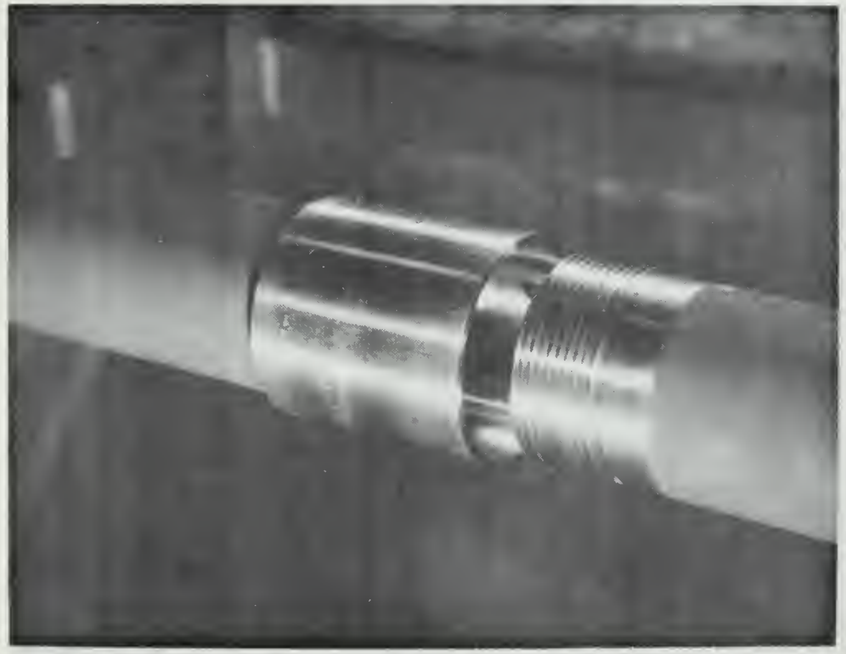

FIGURE 34

LABYRINTH SEAL

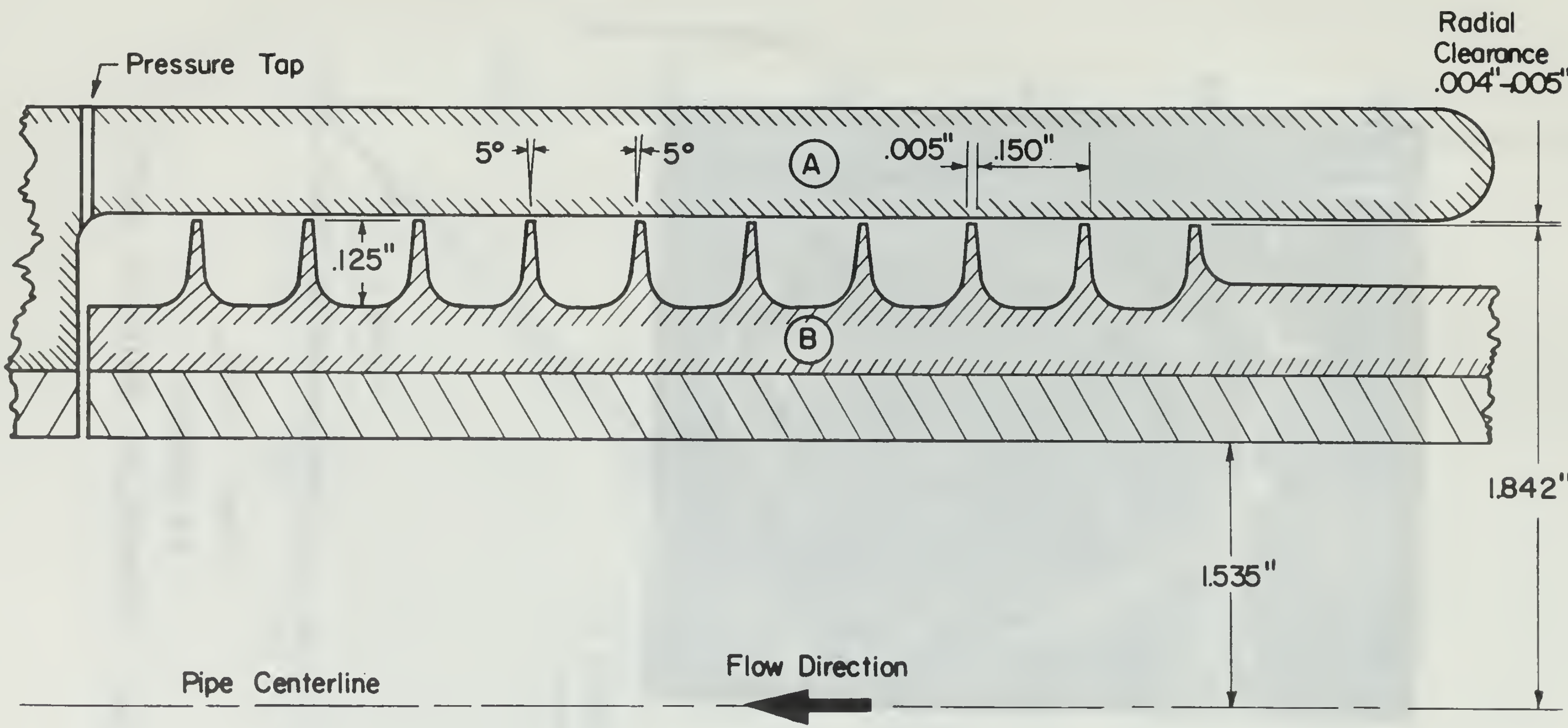

FIGURE 35

DETAILED VIEW OF LABYRINTH SEAL
(A) ATTACHED TO TEST SECTION (MOVABLE)
(B) ATTACHED TO INLET PIPE (STATIONARY)

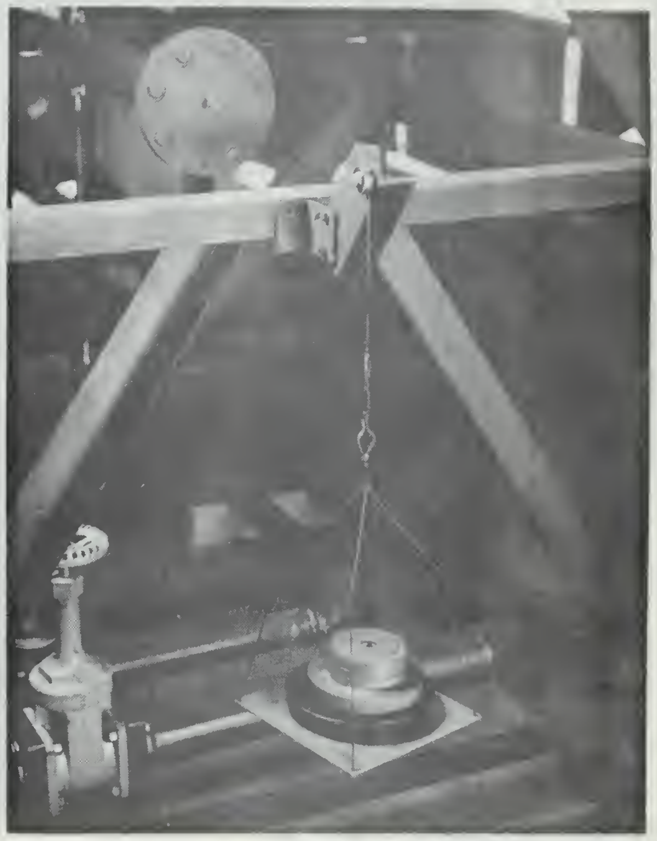

FIGURE 36

FLEXURE CALIBRATION SET-UP

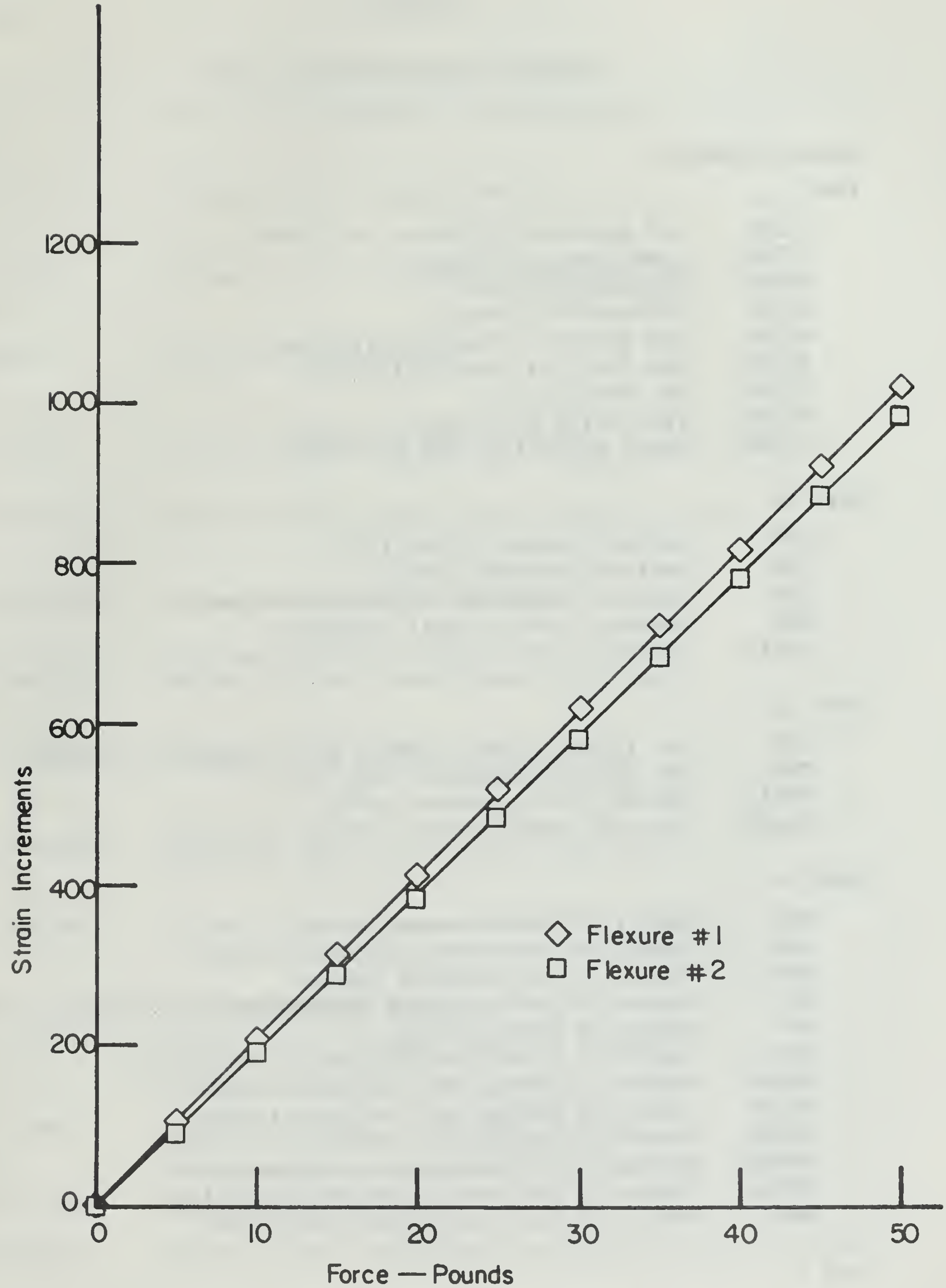

FIGURE 37

TYPICAL FLEXURE CALIBRATION CURVE

APPENDIX I

TURBOFAN PROGRAM NOMENCLATURE

Input Parameters

Card 1:

ETAD	Gas generator diffuser efficiency
ETAC	Compressor efficiency
ETAB	Burner efficiency
ETAT	Turbine efficiency
ETAN	Gas generator nozzle efficiency
ETAFD	Fan duct diffuser efficiency
ETAF	Fan efficiency
ETAFN	Fan nozzle efficiency
EPUMP	Water injection pump efficiency

Card 2:

DSO	Ambient density (slug/ft^3)
PSO	Ambient pressure (lb/ft^2)
TSO	Ambient temperature (degrees Rankine)
HVF	Heating value of fuel (BTU/lbm)
TREFA	Reference air temperature (492 deg. R)

Card 3:

AMN7	Air injection mach number (at fan duct entrance)
TWO	Sea water temperature (deg. R)
PTR32	Burner total pressure ratio
PTR87	Fan duct total pressure ratio (dry fan)

Card 4:

NVO	Number of vessel speeds
NCPR	Number of compressor pressure ratios
NFPR	Number of fan pressure ratios
NTT	Number of turbine inlet temperatures
NBR	Number of bypass ratios
NWGR	Number of water-to-gas generator air ratios
NMDPR	Number of mixing duct pressure ratios
NMDVR	Number of mixing duct velocity ratios
NMDTR	Number of mixing duct temperature ratios
NFNVR	Number of fan nozzle velocity ratios
NFNTR	Number of fan nozzle temperature ratios
NVPW	Number of water injection velocities

Card 5:

GC	Cool temperature specific heat ratio
GH	Hot temperature specific heat ratio

Card 6:

VO(I)	Values of vessel speed (knots)

Card 7:

PTR21(J)	Values of compressor pressure ratio

Card 8:

PTR76(M)	Values of fan pressure ratio

Card 9:

TT3(K)	Values of turbine inlet temperature (deg. R)

Card 10:

BR(L)	Values of bypass ratio

Card 11:

WGR(N)	Values of water-to-gas generator air ratio

Card 12:

PSR87(IJ)	Values of mixing duct static pressure ratio

Card 13:

VR8WA(IK)	Values of mixing duct velocity ratio

Card 14:

TSR8WA(IL)	Values of mixing duct temperature ratio

Card 15:

VR9WA(IM)	Values of fan nozzle velocity ratio

Card 16:

TSR9WA(IN)	Values of fan nozzle temperature ratio

Card 17:

VPW(NN)	Values of water injection velocity (knots)

OUTPUT PARAMETERS NOT PREVIOUSLY DEFINED

PWORK	Water injection pump work (ft-lb/slug)
DHT43	Turbine work (ft-lb/slug)
STHRUS	Specific thrust (lb thrust/lbm/sec)
TR	Ratio of water-augmented-to-dry specific thrust
ETAPRO	Propulsive efficiency
ERATIO	Ratio of water-augmented-to-dry propulsive efficiency

SFC	Specific fuel consumption (lb fuel/lb thrust-hr)
VA7	Air velocity at fan duct entrance (ft/sec)
TS8	Air static temperature at mixing duct exit (deg. R)
VA8	Air velocity at mixing duct exit (ft/sec)
TS9	Air static temperature at fan nozzle exit (deg. R)
VA9	Air velocity at fan nozzle exit (ft/sec)

```
C                              APPENDIX II

C                WATER-AUGMENTED TURBOFAN ENGINE PROGRAM
C                INCLUDING PUMP WORK REQUIRED TO INJECT
C                 WATER AT VELOCITIES GREATER THAN 0.8
C                       TIMES THE CRAFT VELOCITY

      REAL MR
      DIMENSION VO(5),PTR21(20),PTR76(20),TT3(5),BR(20),WGR(20),PSR87(20
     *),VR8WA(20),TSR8WA(20),VR9WA(20),TSR9WA(20),VPW(20)
C
C     STEAM TABLES FUNCTIONS AND DERIVATIVES
C
      HF(XX)= -522.44716 + 1.1719422*XX - .00031882153*XX*XX + .00000019
     *421466*XX**3
      HFG(XX)=1440.548 - 1.1017804*XX + .0010967588*XX*XX - .00000074163
     *358*XX**3
      SF(XX)=-1.6947235 + .0053250001*XX - .000004749752*XX*XX + .00000
     *00018892757*XX**3
      SFG(XX)=8.812883 - .024424801*XX + .000028390143*XX*XX - .00000001
     *2441932*XX**3
      DHF(XX)=1.1719422 - .00063764306*XX + .00000058264398*XX*XX
      DHFG(XX)=-1.1017804 + .0021935176*XX - .0000022249000074*XX*XX
      DSF(XX)=.0053250001 - .0000094999504*XX + .0000000056678271*XX*XX
      DSFG(XX)=-.024424801 + .000056780286*XX - .000000037325796*XX*XX
C
      READ(5,111)ETAD,ETAC,ETAB,ETAT,ETAN,ETAFD,ETAF,ETAFN,EPUMP
  111 FORMAT(9F5.2)
      READ(5,112)DSO,PSO,TSO,HVF,TREFA
  112 FORMAT(F10.6,4F10.1)
      READ(5,113)AMN7,TWO,PTR32,PTR87
  113 FORMAT(4F8.2)
      READ(5,114)NVO,NCPR,NFPR,NTT,NBR,NWGR,NMDPR,NMDVR,NMDTR,NFNVR,
     *NFNTR,NVPW
  114 FORMAT(12I3)
      READ(5,115)GC,GH
  115 FORMAT(2F9.6)
      READ(5,116)(VO(I),I=1,NVO)
```

```
      READ(5,116)(PTR21(J),J=1,NCPR)
      READ(5,116)(PTR76(M),M=1,NFPR)
      READ(5,116)(TT3(K),K=1,NTT)
      READ(5,116)(BR(L),L=1,NBR)
      READ(5,116)(WGR(N),N=1,NWGR)
      READ(5,116)(PSR87(IJ),IJ=1,NMDPR)
      READ(5,116)(VR8WA(IK),IK=1,NMDVR)
      READ(5,116)(TSR8WA(IL),IL=1,NMDTR)
      READ(5,116)(VR9WA(IM),IM=1,NFNVR)
      READ(5,116)(TSR9WA(IN),IN=1,NFNTR)
      READ(5,116)(VPW(NN),NN=1,NVPW)
  116 FORMAT(10F8.2)
      IPAGE = 1
      R=1717.61
      G=32.2
      CJ=778.26
      CPH=GH*R/(GH-1.0)
      CPC=GC*R/(GC-1.0)
      TW7=TWO
      HREFA= CPC*(TSO - TREFA)
      HREFW=HF(TWO)*CJ*G
      SREFA=0.0
      WRITE(6,50)
   50 FORMAT('1')
      WRITE(6,117)
  117 FORMAT(//////T35,'WATER-AUGMENTED TURBOFAN ENGINE PROGRAM')
      WRITE(6,118)
  118 FORMAT(//T44,'WITH WATER INJECTION')
      WRITE(6,119)
  119 FORMAT(//T48,'AT SEA LEVEL')
      WRITE(6,120)
  120 FORMAT(////T27,'AMBIENT PROPERTIES',T70,'EFFICIENCIES',//)
      WRITE(6,121)DSO,ETAD,PSO,ETAC,TSO,ETAB,TW7,ETAT,ETAN,ETAFD,ETAF,HR
     *EFA,ETAFN,HREFW,EPUMP,SREFA,AMN7
  121 FORMAT(T17,'AIR DENSITY         =',F9.6,T46,'SLUG/CU-FT',T63,'DIFFUS
     *ER(ETAD)        =',F5.2,/,T17,'AIR PRESSURE        =',F7.1,T46,'LB/SQ-
     *FT',T63,'COMPRESSOR(ETAC)     =',F5.2,/,T17,'AIR TEMPERATURE    =',F
     *6.1,T46,'DEG R.',T63,'BURNER(ETAB)          =',F5.2,/,T17,'WATER TEM
     *PERATURE =',F6.1,T46,'DEG R.',T63,'TURBINE(ETAT)        =',F5.2,/,T
     *63,'NOZZLE(ETAN)           =',F5.2,/,T26,'REFERENCE PROPERTIES', T63,
     *'FAN DIFFUSER(ETAFD) =',F5.2,/, T63,'FAN(ETAF)            =',F5.2,/
     *,T17,'AIR ENTHALPY    =',F9.1 ,T43,'FT-LB/SLUG',T63,'FAN NOZZLE(ETA
     *FN)    =',F5.2,/, T17,'WATER ENTHALPY =',F9.1,T43,'FT-LB/SLUG',T63,
     *'PUMP(EPUMP)            =', F5.2,/,T17,'AIR ENTROPY    =',F9.1,T43,'F
     *T-LB/SLUG-DEG R.',//,T17,'MACH NUMBER AT FAN OUTLET(AMN7) =',F6.2)
      WRITE(6,500)
  500 FORMAT(//T17,'ENERGY   RECOVERY FACTOR FOR WATER INTAKE SYSTEM = 0
     *.64',/,T17,'VELOCITY RECOVERY FACTOR FOR WATER INTAKE SYSTEM = SQR
```

```
     *T(0.64) = 0.80')
      DO 36 I=1,NVO
      OV=VO(I)*1.688944
      VWO=OV
      AO=SQRT(GC*R*TSO)
      AMNO=OV/AO
      VW7=0.8 * VWO
C
C     GAS GENERATOR DIFFUSER
C
      PTO  =   PSO*((1.0+((GC-1.0)/2.0)*AMNO*AMNO)**(GC/(GC-1.0)))
      PT1=ETAD *(PTO-PSO) + PSO
      TT1=TSO*(1.0+((GC-1.0)/2.0)*AMNO*AMNO)
      ST1=CPC*ALOG(TT1/TSO)-R*ALOG(PT1/PSO)+SREFA
      HT1=CPC*(TT1-TSO)+HREFA
C
C     FAN DIFFUSER
C
      PT6=ETAFD*(PTO-PSO) + PSO
      TT6=TSO*(1.0+((GC-1.0)/2.0)*AMNO*AMNO)
      ST6=CPC*ALOG(TT6/TSO)-R*ALOG(PT6/PSC)+SREFA
      HT6=CPC*(TT6-TSO)+HREFA
C
C     GAS GENERATOR COMPRESSOR
C
      DO 35 J=1,NCPR
      TT2I=TT1*PTR21(J)**((GC-1.0)/GC)
      DHT21I=CPC*(TT2I-TT1)
      HT2=DHT21I/ETAC + HT1
      TT2=(HT2-HREFA)/CPC + TSO
      PT2=PTR21(J)*PT1
      ST2=CPC*ALOG(TT2/TSO)-R*ALOG(PT2/PSO) + SREFA
C
C     GAS GENERATOR BURNER
C
      DO 34 K=1,NTT
      PT3=PTR32*PT2
      CPB=(CPH + CPC)/2.0
      HT3=CPB*(TT3(K)-TT2) + HT2
      ST3=CPB*ALOG(TT3(K)/TT2) - R*ALOG(PT3/PT2) + ST2
      FAR=1.0/((ETAB*HVF*G*CJ)/(CPH*(TT3(K)-TT2))-1.0)
C
C     FAN
C
      DO 33 M=1,NFPR
      TT7I=TT6*(PTR76(M)**((GC-1.0)/GC))
      DHT76I=CPC*(TT7I-TT6)
      HT7=DHT76I/ETAF + HT6
```

```
      TT7=(HT7-HREFA)/CPC + TSO
      PT7=PTR76(M)*PT6
      ST7=CPC*ALOG(TT7/TSO)-R*ALOG(PT7/PSO) + SREFA
C
C     GAS GENERATOR TURBINE
C
      DO 32 L=1,NBR
      WRITE(6,50)
      WRITE(6,13)TT3(K),PTR21(J),PTR76(M),PTR87,BR(L)
      WRITE(6,600)
      WRITE(6,990)
   13 FORMAT(  T6,'TURBINE INLET TEMPERATURE            (TT3) =',F8.2,T58
     *,'DEGREES R.',/,T6,'COMPRESSOR TOTAL PRESSURE RATIO   (PTR21) =',F
     *8.2,/,T6,'FAN TOTAL PRESSURE RATIO            (PTR76) =',F8.2,/,T6,'
     *DRY FAN DUCT TOTAL PRESSURE RATIO (PTR87) =',F8.2,/,T6,'BYPASS RAT
     *IO',T43,'(BR) =',F8.2)
  600 FORMAT(////,T1,' CRAFT  INJ.  WATER  TEMP  VEL   TEMP  VEL    INJ.
     *PUMP    TURBINE    SPEC  THRUST  PROP.   EFF.   SFC   TEMP   VEL
     *   TEMP   VEL',/,T2,' VEL    VEL   /GAS   RATIO RATIO RATIO RATIO
     * WORK        WORK      THRUST RATIO   EFF.   RATIO        AIR/8  A
     *IR/8   AIR/9  AIR/9',/,T2,' KTS    KTS    RATIO  8W/A  8W/A   9W/A   9
     *W/A  FT-LB/SLUG  FT-LB/SLUG',T105,'DEG R  FT/SEC  DEG R  FT/SEC')
  990 FORMAT(T1,' -------------------------------------------------------
     *------------------------------------------------------------------
     *-----------',/ )
      BY=BR(L)
      CMF=1.0
      FMF=BY
      TMF=CMF + CMF*FAR
C
C     THE REMAINING GAS GENERATOR TURBINE CALCULATIONS OCCUR LATER IN
C     THE PROGRAM
C
C     FAN MIXING DUCT
C
  123 DO 310 N=1,NWGR
    1 DO 3310 NN=1,NVPW
      IF(WGR(N).NE.0.0) GO TO 602
      IF(NN.LT.NVPW) GO TO 3310
      GO TO 603
C
C     WATER INJECTION PUMP CALCULATIONS
C
  602 VPW7 = VPW(NN)*1.688944
      PWORK = (VPW7**2-VW7**2)/(2*EPUMP)
      IF (PWORK.GE.0.0) GO TO 601
  603 PWORK = 0.0
C
```

```
C
C     GAS GENERATOR TURBINE CALCULATIONS RESUME HERE
C
  601 DHT43 = (CMF*(HT2-HT1)+FMF*(HT7-HT6)+WGR(N)*CMF*(PWORK))/TMF
      HT4=HT3-DHT43
      DHT43I=DHT43/ETAT
      HT4I=HT3-DHT43I
      TT4I=TT3(K)-(HT3-HT4I)/CPH
      TT4=TT3(K)-(HT3-HT4)/CPH
      PT4I=PT3*((TT4I/TT3(K))**(GH/(GH-1.0)))
      PT4=PT4I
      IF((PT4-PSO).GE.0.0) GO TO 400
      IF(WGR(N).GT.0.0) GO TO 24
      VPWNN = 0.0
      WRITE(6,25)VO(I),VPWNN,WGR(N)
      GO TO 3310
   24 WRITE(6,25)VO(I),VPW(NN),WGR(N)
   25 FORMAT(2F6.1,F7.1,T58,'TURBINE EXIT PRESSURE IS  LOWER   THAN    ATM
     *OSPHERIC')
      GO TO 3310
  400 ST4=CPH*ALOG(TT4/TT3(K))-R*ALOG(PT4/PT3) + ST3
C
C     GAS GENERATOR NOZZLE
C
      PS5=PSO
      PS5I=PSO
      TT5I=TT4*((PS5I/PT4)**((GH-1.0)/GH))
      TS5=TT4 - ETAN*(TT4-TT5I)
      TT5=TT4
      ST5=CPH*ALOG(TS5/TT3(K))-R*ALOG(PS5/PT3) + ST3
      VA5=SQRT(2.0*CPH*(TT5-TS5))
      A5=SQRT(GH*R*TS5)
      AMN5=VA5/A5
      STADD=0.0
      IF(AMN5.LE.1.0) GO TO 401
      AMN5=1.0
      VA5=SQRT((2.0*CPH*TT5)/(1.0+2.0*CPH/(GH*R)))
      A5=VA5
      TS5=A5*A5/(GH*R)
      TT5I=(ETAN*TT4-TT4+TS5)/ETAN
      PS5=PT4*(TT5I/TT4)**(GH/(GH-1.0))
      ST5=CPH*ALOG(TS5/TT3(K))-R*ALOG(PS5/PT3) + ST3
      DS5=PS5/(R*TS5)
      STADD=(1.0+FAR)/((1.0+BY)*DS5*VA5)*(PS5-PSO)
  401 IF(WGR(N).GT.0.0) GO TO 128
C
C
C
```

```
C     DRY TURBOFAN CALCULATION FOR NO WATER INJECTION
C
C     FAN MIXING DUCT--NO WATER INJECTION
C
      PT8=PTR87*PT7
      TT8=TT7
      ST8=CPC*ALOG(TT8/TSO)-R*ALOG(PT8/PSO) + SREFA
C
C     FAN NOZZLE--NO WATER INJECTION
C
      PS9=PSO
      PS9I=PSO
      TT9I=TT8*((PS9I/PT8)**((GC-1.0)/GC))
      TS9=TT8-ETAFN*(TT8-TT9I)
      TT9=TT8
      ST9=CPC*ALOG(TS9/TSO)-R*ALOG(PS9/PSO) + SREFA
      VA9=SQRT(2.0*CPC*(TT9-TS9))
      A9=SQRT(GC*R*TS9)
      AMN9=VA9/A9
C
C     SPECIFIC THRUST AND PROPULSIVE EFFICIENCY CALCULATIONS FOR DRY
C     TURBOFAN
C
      STHRUD=(((1.+FAR)/(1.0+BY))*VA5 - (1.0/(1.0+BY))*OV +
     *(BY/(1.0+BY))*(VA9-OV)  + STADD) / G
      THRUST=STHRUD*(CMF + FMF)* G
      TP=THRUST*OV
      ETAPRD=TP/(TP+TMF/2.0*(VA5-OV)**2 + FMF/2.0*(VA9-OV)**2)
      FUMF=(TMF - CMF)
      FUWF=FUMF*G
      SFCD = (FUWF/THRUST)*3600.0
      VPWNN = 0.0
      TR = 1.0
      ERATIO = 1.0
      VR8WAD = 0.0
      TR8WAD = 0.0
      VR9WAD = 0.0
      TR9WAD = 0.0
      WRITE(6,301)VO(I),VPWNN,WGR(N),VR8WAD,TR8WAD,VR9WAD,TR9WAD,PWORK,D
     *HT43,STHRUD,TR,ETAPRD,ERATIO,SFCD,TT8,VPWNN,TS9,VA9
      GO TO 3310
C
C
C
C
C
C
C
```

```
C     CALCULATIONS FOR WET TURBOFAN RESUME HERE
C
  128 MR=WGR(N)/BY
      WV7=0.8*VO(I)
  129 WMF=WGR(N)*CMF
      TS7=TT7/(1.0+(GC-1.0)/2.0*AMN7*AMN7)
      HS7=(TS7-TSC)*CPC + HREFA
      A7=SQRT(GC*R*TS7)
      VA7=AMN7*A7
      VM7=(VA7+MR*VPW7    )/(1.0+MR)
      PS7=PT7/(1.0+(GC-1.0)/2.0*AMN7*AMN7)**(GC/(GC-1.0))
      DA7=PS7/(R*TS7)
C
C         MIXING DUCT TEMPERATURE ITERATION
C
      DO 300 IJ=1,NMDPR
      PS8=PSR87(IJ)*PS7
C
C     DENSITY OF WATER = 1.9378 SLUG/CU-FT
C
      DW7=1.9378
      VM8=VM7 + (PS7-PS8)*(1./(1.+MR))*(1./(DA7*VA7)+MR/(DW7*VPW7))
      DO 28 IL=1,NMDTR
      DO 29 IK=1,NMDVR
      VA8=VM8/((1.+MR*VR8WA(IK))/(1.+MR))
      VW8=VR8WA(IK)*VA8
      TS8=530.
      ZA= 3.2437814
      ZB= .00586826
      ZC= .000000011702379
      ZD= .0021878462
      JAKE = 1
  124 TW8=TSR8WA(IL)*TS8
      ZE= CPC*(TT7-TS8) + MR*(HF(TW7)-HF(TW8))*CJ*G + MR*VPW7    **2/2.
     * - MR*VW8*VW8/2. - VA8*VA8/2.
      X=(374.11 - (TSR8WA(IL)*TS8 - 492.)*5./9.)
      TK=(273.16 + (TSR8WA(IL)*TS8 - 492.)*5./9.)
      PPV8=  10.**(ALOG10(218.167) - X/TK*((ZA+ZB*X+ZC*X**3)/(1.0+ZD*X))
     *)*14.6959*144.
      Z =PPV8/(PS8-PPV8)*0.6218847/TSR8WA(IL)
      PFUN8=ZE/(HFG(TW8)*CJ*G +0.5*(VA8**2 - VW8**2)) - Z
      DZE=-CPC - MR*DHF(TW8)*CJ*G*TSR8WA(IL)
      DT=5./9.*TSR8WA(IL)
      DX=-5./9.*TSR8WA(IL)
      ZM=((1. +ZD*X)*(ZB*DX + 3.*ZC*DX*X**2) - (ZA +ZB*X+ZC*X**3)*(ZD*DX
     *))/(1.+ZD*X)**2
      ZN=(TK*DX - X*DT)/TK**2
      DPPV8= PPV8*(X/TK*ZM + (ZA+ZB*X+ZC*X**3)/(1.+ZD*X)*ZN)*ALOG(10.C)
```

```
      DZ=((PS8-PPV8)*DPPV8 + PPV8*DPPV8)/(PS8-PPV8)**2*0.6218847/TSR8WA(
     *IL)
      DPFUN8=(HFG(TW8)*CJ*G*DZE-ZE*DHFG(TW8)*CJ*G*TSR8WA(IL))/(HFG(TW8)*
     *CJ*G)**2 - DZ
      TS8=TS8 - PFUN8/DPFUN8
      PDP8 = ABS(PFUN8/DPFUN8)
      IF(JAKE.GE.100) GO TO 66
      JAKE = JAKE + 1
      GO TO 68
   66 WRITE(6,67)
   67 FORMAT(T12,'TOO MANY DUCT TEMPERATURE ITERATIONS--COMPUTATIONS PRO
     *CEEDING WITH LAST VALUE FOUND')
      GO TO 125
   68 IF(PDP8.LE.0.5E-03) GC TO 125
      GO TO 124
  125 TW8=TSR8WA(IL)*TS8
      X=(374.11 - (TSR8WA(IL)*TS8 - 492.)*5./9.)
      TK=(273.16 + (TSR8WA(IL)*TS8 - 492.)*5./9.)
      PPV8=  10.**(ALOG10(218.167) - X/TK*((ZA+ZB*X+ZC*X**3)/(1.0+ZD*X))
     *)*14.6959*144.
      X8=PPV8/(PS8-PPV8)*0.6218847/TSR8WA(IL)
C
C     FAN NOZZLE
C
      PS9=PSO
      TS9=520.
      DO 27 IN=1,NFNTR
      JUNK = 1
  126 TW9=TSR9WA(IN)*TS9
      ZQ=(CPC*ALOG(TS8/TS9) - R*ALOG(PS8/PS9) + X8*SFG(TW8)*CJ*G + MR*
     *  (SF(TW8)-SF(TW9))*CJ*G)
      X=(374.11 - (TSR9WA(IN)*TS9 - 492.)*5./9.)
      TK=(273.16 + (TSR9WA(IN)*TS9 - 492.)*5./9.)
      PPV9=  10.**(ALOG10(218.167) - X/TK*((ZA+ZB*X+ZC*X**3)/(1.0+ZD*X))
     *)*14.6959*144.
      ZR=PPV9/(PS9-PPV9)*.6218847/TSR9WA(IN)
      PFUN9=ZQ/(SFG(TW9)*CJ*G) - ZR
      DZQ=-CPC/TS9 - MR*DSF(TW9)*CJ*G*TSR9WA(IN)
      DT=5./9.*TSR9WA(IN)
      DX=-5./9.*TSR9WA(IN)
      ZM=((1. +ZD*X)*(ZB*DX + 3.*ZC*DX*X**2) - (ZA +ZB*X+ZC*X**3)*(ZD*DX
     *))/(1.+ZD*X)**2
      ZN=(TK*DX - X*DT)/TK**2
      DPPV9= PPV9*(X/TK*ZM + (ZA+ZB*X+ZC*X**3)/(1.+ZD*X)*ZN)*ALOG(10.0)
      DZ=((PS9-PPV9)*DPPV9 + PPV9*DPPV9)/(PS9-PPV9)**2*0.6218847/TSR9WA(
     *IN)
      DPFUN9=((SFG(TW9)*DZQ-ZQ*DSFG(TW9)*TSR9WA(IN))*CJ*G)/(SFG(TW9)*CJ*
     *G)**2 - DZ
```

```
      TS9=TS9 - PFUN9/DPFUN9
      PDP9 = ABS(PFUN9/DPFUN9)
   55 FORMAT( 4E20.6)
      IF(JUNK.GE.100) GO TO 56
      JUNK = JUNK + 1
      GO TO 58
   56 WRITE(6,57)
   57 FORMAT(T12,'TOO MANY FAN NOZZLE TEMPERATURE ITERATIONS--COMPUTATIO
     *NS PROCEEDING WITH LAST VALUE FOUND')
      GO TO 127
   58 IF(PDP9.LE.0.5E-03) GO TO 127
      GO TO 126
  127 TW9=TSR9WA(IN)*TS9
      X=(374.11 - (TSR9WA(IN)*TS9 - 492.)*5./9.)
      TK=(273.16 + (TSR9WA(IN)*TS9 - 492.)*5./9.)
      PPV9= 10.**(ALOG10(218.167) - X/TK*((ZA+ZB*X+ZC*X**3)/(1.0+ZD*X))
     *)*14.6959*144.
      X9=PPV9/(PS9-PPV9)*.6218847/TSR9WA(IN)
      DO 26 IM=1,NFNVR
      VA9VA9=((CPC*(TS8-TS9) + X8*HFG(TW8)*CJ*G + MR*HF(TW8)*CJ*G - X9*
     * HFG(TW9)*CJ*G - MR*HF(TW9)*CJ*G +VA8*VA8/2.*(1.+X8+(MR-X8)*VR8WA(
     *IK)**2))*2./(1. + X9 + (MR-X9)*VR9WA(IM)**2))
      IF(VA9VA9.GE.0.0) GO TO 171
      WRITE(6,170)VO(I),VPW(NN),WGR(N),TSR8WA(IL),VR8WA(IK),TSR9WA(IN),
     *VR9WA(IM)
  170 FORMAT(2F6.1,F7.1,4F6.2,T115,'VA9   IS   IMAGINARY')
      GO TO 26
  171 VA9=SQRT(VA9VA9)
      VW9=VR9WA(IM)*VA9
      A9=SQRT(GC*R*TS9)
      AMN9=VA9/A9
C
C     SPECIFIC THRUST AND PROPULSIVE EFFICIENCY CALCULATIONS
C
      STHRUS=(((1.+FAR)/(1.0+BY))*VA5 - (1.0/(1.0+BY))*OV +
     *(BY+BY*X9)/(1.+BY)*VA9 - (BY/(1.+BY))*OV + (WGR(N)-BY*X9)/(1.+BY)*
     * VW9 - (WGR(N)/(1.+BY))*VWO + STADD) /G
      THRUST=STHRUS*(CMF + FMF) * G
      TP=THRUST*OV
      ETAPRO=TP/(TP+TMF/2.0*(VA5-OV)**2 + (FMF+X9*FMF)/2.*(VA9-OV)**2 +
     * (WMF-FMF*X9)/2.*(VW9-VWO)**2)
      FUMF=(TMF - CMF)
      FUWF=FUMF*G
      SFC=(FUWF/THRUST)*3600.0
      TR = STHRUS/STHRUD
      IF(ETAPRD.EQ.0.0) GO TO 230
      ERATIO = ETAPRO/ETAPRD
      GO TO 240
```

```
230 ERATIO = 1.0
240 WRITE(6,301)VO(I),VPW(NN),WGR(N),TSR8WA(IL),VR8WA(IK),TSR9WA(IN),V
   *R9WA(IM),PWORK,DHT43,STHRUS,TR,ETAPRO,ERATIO,SFC,TS8,VA8,TS9,VA9
301 FORMAT(2F6.1,F7.1,4F6.2,1P2E12.4,0PF7.2,4F7.3,F7.1,F8.1,F7.1,F8.1)
 26 CONTINUE
 27 CONTINUE
 29 CONTINUE
 28 CONTINUE
300 CONTINUE
3310 CONTINUE
310 CONTINUE
 32 CONTINUE
 33 CONTINUE
 34 CONTINUE
 35 CONTINUE
  2 WRITE(6,302)PSR87(1)
302 FORMAT(////T6,'WET FAN DUCT STATIC PRESSURE RATIO (PSR87) =',F8.2)
    WRITE(6,303) VA7
303 FORMAT(     T6,'AIR VELOCITY AT FAN OUTLET (VA7), FT/SEC   =',F8.2)
    WRITE(6,51) IPAGE
 51 FORMAT(     T120,'PAGE',I6)
    IPAGE = IPAGE + 1
 36 CONTINUE
    RETURN
    END
```

TURBINE INLET TEMPERATURE (TT3) = 2500.00 DEGREES R.
COMPRESSOR TOTAL PRESSURE RATIO (PTR21) = 13.90
FAN TOTAL PRESSURE RATIO (PTR76) = 1.50
DRY FAN DUCT TOTAL PRESSURE RATIO (PTR87) = 1.00
BYPASS RATIO (BR) = 4.00

CRAFT VEL KTS	INJ. VEL KTS	WATER /GAS RATIO	TEMP RATIO 8W/A	VEL RATIO 8W/A	TEMP RATIO 9W/A	VEL RATIO 9W/A	INJ. PUMP WORK FT-LB/SLUG	TURBINE WORK FT-LB/SLUG	SPEC THRUST	THRUST RATIO	PROP. EFF.	EFF. RATIO	SFC	TEMP AIR/8 DEG R	VEL AIR/8 FT/SEC	TEMP AIR/9 DEG R	VEL AIR/9 FT/SEC
50.0	0.0	0.0	0.0	0.0	0.0	0.0	0.0	5.4837E 06	31.28	1.000	0.132	1.000	0.454	551.6	0.0	527.7	877.1
50.0	20.0	20.0	1.00	1.00	1.00	1.00	0.0	5.4837E 06	48.40	1.548	0.224	1.701	0.293	521.4	105.1	518.7	331.4
50.0	40.0	20.0	1.00	1.00	1.00	1.00	-0.0	5.4837E 06	49.82	1.593	0.225	1.706	0.285	521.3	132.2	518.6	341.0
50.0	60.0	20.0	1.00	1.00	1.00	1.00	3.1695E 03	5.5459E 06	51.31	1.641	0.225	1.709	0.277	521.2	160.1	518.5	352.7
50.0	80.0	20.0	1.00	1.00	1.00	1.00	7.6068E 03	5.6329E 06	52.96	1.693	0.225	1.713	0.268	521.2	188.0	518.4	366.2
50.0	100.0	20.0	1.00	1.00	1.00	1.00	1.3312E 04	5.7448E 06	54.73	1.750	0.233	1.772	0.259	521.1	216.1	518.4	381.4
50.0	20.0	30.0	1.00	1.00	1.00	1.00	0.0	5.4837E 06	52.29	1.672	0.246	1.868	0.272	521.0	84.8	519.1	277.2
50.0	40.0	30.0	1.00	1.00	1.00	1.00	-0.0	5.4837E 06	54.43	1.740	0.248	1.881	0.261	520.9	113.6	519.0	287.3
50.0	60.0	30.0	1.00	1.00	1.00	1.00	3.1695E 03	5.5770E 06	56.75	1.814	0.249	1.892	0.250	520.9	143.0	519.0	300.2
50.0	80.0	30.0	1.00	1.00	1.00	1.00	7.6068E 03	5.7075E 06	59.39	1.899	0.257	1.950	0.239	520.8	172.7	518.9	315.3
50.0	100.0	30.0	1.00	1.00	1.00	1.00	1.3312E 04	5.8754E 06	62.25	1.990	0.271	2.058	0.228	520.8	202.4	518.9	332.5
50.0	20.0	40.0	1.00	1.00	1.00	1.00	0.0	5.4837E 06	55.02	1.759	0.262	1.992	0.258	520.7	73.7	519.3	243.4
50.0	40.0	40.0	1.00	1.00	1.00	1.00	-0.0	5.4837E 06	57.89	1.851	0.265	2.015	0.245	520.7	103.4	519.3	253.9
50.0	60.0	40.0	1.00	1.00	1.00	1.00	3.1695E 03	5.6081E 06	61.14	1.955	0.268	2.036	0.232	520.7	133.7	519.2	267.7
50.0	80.0	40.0	1.00	1.00	1.00	1.00	7.6068E 03	5.7821E 06	64.88	2.075	0.284	2.159	0.219	520.6	164.3	519.2	284.2
50.0	100.0	40.0	1.00	1.00	1.00	1.00	1.3312E 04	6.0059E 06	68.92	2.204	0.306	2.324	0.206	520.6	194.9	519.2	302.9
50.0	20.0	50.0	1.00	1.00	1.00	1.00	0.0	5.4837E 06	56.95	1.821	0.275	2.088	0.249	520.6	66.8	519.4	219.7
50.0	40.0	50.0	1.00	1.00	1.00	1.00	-0.0	5.4837E 06	60.62	1.938	0.279	2.123	0.234	520.6	97.0	519.4	230.7
50.0	60.0	50.0	1.00	1.00	1.00	1.00	3.1695E 03	5.6392E 06	64.87	2.074	0.285	2.166	0.219	520.5	127.9	519.4	245.3
50.0	80.0	50.0	1.00	1.00	1.00	1.00	7.6068E 03	5.8567E 06	69.78	2.231	0.310	2.353	0.204	520.5	159.0	519.3	262.8
50.0	100.0	50.0	1.00	1.00	1.00	1.00	1.3312E 04	6.1365E 06	75.04	2.399	0.340	2.582	0.189	520.5	190.1	519.3	282.8
50.0	20.0	100.0	1.00	1.00	1.00	1.00	0.0	5.4837E 06	60.05	1.920	0.307	2.334	0.236	520.3	52.1	519.7	159.5
50.0	40.0	100.0	1.00	1.00	1.00	1.00	-0.0	5.4837E 06	68.33	2.185	0.323	2.451	0.208	520.3	83.4	519.7	172.3
50.0	60.0	100.0	1.00	1.00	1.00	1.00	3.1695E 03	5.7946E 06	78.36	2.505	0.358	2.723	0.181	520.3	115.5	519.7	189.9
50.0	80.0	100.0	1.00	1.00	1.00	1.00	7.6068E 03	6.2297E 06	89.81	2.872	0.426	3.240	0.158	520.3	147.8	519.7	211.1
50.0	100.0	100.0	1.00	1.00	1.00	1.00	1.3312E 04	6.7892E 06	100.57	3.216	0.509	3.865	0.141	520.2	180.2	519.7	234.9
50.0	20.0	200.0	1.00	1.00	1.00	1.00	0.0	5.4837E 06	52.06	1.665	0.300	2.278	0.273	520.2	44.3	519.9	116.4
50.0	40.0	200.0	1.00	1.00	1.00	1.00	-0.0	5.4837E 06	71.66	2.291	0.354	2.689	0.198	520.1	76.2	519.8	131.9
50.0	60.0	200.0	1.00	1.00	1.00	1.00	3.1695E 03	6.1054E 06	95.71	3.060	0.475	3.609	0.148	520.1	108.9	519.8	153.1
50.0	80.0	200.0						TURBINE	EXIT	PRESSURE IS	LOWER	THAN	ATMOSPHERIC				
50.0	100.0	200.0						TURBINE	EXIT	PRESSURE IS	LOWER	THAN	ATMOSPHERIC				
50.0	20.0	300.0	1.00	1.00	1.00	1.00	0.0	5.4837E 06	36.21	1.158	0.238	1.809	0.392	520.1	41.6	519.9	97.5
50.0	40.0	300.0	1.00	1.00	1.00	1.00	-0.0	5.4837E 06	69.19	2.212	0.357	2.716	0.205	520.1	73.8	519.9	115.0
50.0	60.0	300.0	1.00	1.00	1.00	1.00	3.1695E 03	6.4162E 06	108.70	3.476	0.590	4.482	0.131	520.1	106.7	519.9	138.4
50.0	80.0	300.0						TURBINE	EXIT	PRESSURE IS	LOWER	THAN	ATMOSPHERIC				
50.0	100.0	300.0						TURBINE	EXIT	PRESSURE IS	LOWER	THAN	ATMOSPHERIC				
50.0	20.0	400.0	1.00	1.00	1.00	1.00	0.0	5.4837E 06	16.56	0.529	0.127	0.964	0.858	520.1	40.2	519.9	86.4
50.0	40.0	400.0	1.00	1.00	1.00	1.00	-0.0	5.4837E 06	64.17	2.052	0.347	2.641	0.221	520.1	72.5	519.9	105.4
50.0	60.0	400.0	1.00	1.00	1.00	1.00	3.1695E 03	6.7270E 06	119.36	3.816	0.717	5.447	0.119	520.1	105.6	519.9	130.4
50.0	80.0	400.0						TURBINE	EXIT	PRESSURE IS	LOWER	THAN	ATMOSPHERIC				
50.0	100.0	400.0						TURBINE	EXIT	PRESSURE IS	LOWER	THAN	ATMOSPHERIC				
50.0	20.0	500.0	1.00	1.00	1.00	1.00	0.0	5.4837E 06	-5.44	-0.174	-0.050	-0.379	-2.609	520.1	39.4	519.9	79.0
50.0	40.0	500.0	1.00	1.00	1.00	1.00	-0.0	5.4837E 06	57.71	1.845	0.328	2.496	0.246	520.1	71.8	519.9	99.2
50.0	60.0	500.0						TURBINE	EXIT	PRESSURE IS	LOWER	THAN	ATMOSPHERIC				
50.0	80.0	500.0						TURBINE	EXIT	PRESSURE IS	LOWER	THAN	ATMOSPHERIC				
50.0	100.0	500.0						TURBINE	EXIT	PRESSURE IS	LOWER	THAN	ATMOSPHERIC				

WET FAN DUCT STATIC PRESSURE RATIO (PSR87) = 0.95
AIR VELOCITY AT FAN OUTLET (VA7), FT/SEC = 237.60

APPENDIX III

DATA REDUCTION PROGRAM NOMENCLATURE

INPUT PARAMETERS

M_ _ Number of interpolation pairs for subroutine SPLIN1

R_ _ (I) Reynolds number values

K_ _ (I) Discharge coefficient values corresponding to R_ _ (I)

Subscripts for M_ _, R_ _ (I), K_ _(I):

- FA Flange pressure taps, air
- DA D and ½ D pressure taps, air
- FW Flange pressure taps, water
- DW D and ½ D pressure taps, water

Example: RDA(I) Reynolds number for D and ½ D taps for air flow

M_ Number of interpolation pairs for subroutine SPLIN1

X_ (I) Lockhart-Martinelli two-phase flow modulus values, χ

F_ _ _ (I) Lockhart-Martinelli correlation parameter values, Φ

Subscripts for M_, X_(I), F_ _ _ (I):

- G Lockhart-Martinelli gas correlation
- L Lockhart-Martinelli liquid correlation
- TT Turbulent-turbulent flow
- TV Turbulent-viscous flow
- VT Viscous-turbulent flow
- VV Viscous-viscous flow

Example: FGTV(I) Correlation parameter, Φ_G, for gas-phase turbulent-viscous flow

D1A Inside diameter of air pipe at orifice (in)

D2A Diameter of air orifice (in)

D1W Inside diameter of water pipe (in)

D2W Diameter of water orifice (in)

HMFA Manometer fluid differential, flange taps, air (in H_2O)

HMDA Manometer fluid differential, D and ½ D taps, air (in H_2O)

HMFW Manometer fluid differential, flange taps, water (in Hg)

HMDW Manometer fluid differential, D and ½ D taps, water (in Hg)

T1FA	Air flow temperature at orifice (deg. F)
T1FW	Water flow temperature at orifice (deg. F)
TAFA	Air temperature at air orifice manometer (deg. F)
TAFW	Air temperature at water orifice manometer (deg. F)
P1	Air static pressure upstream of orifice (lb/in^2)
PT	Static pressure at test section inlet (lb/in^2)
TTFA	Air temperature at test section outlet (deg. F)
TTFW	Water temperature at test section outlet (deg. F)
DT	Inside diameter of test section (in)
LT	Length of test section (ft)

OUTPUT PARAMETERS NOT PREVIOUSLY DEFINED

BETAA	Ratio of orifice-to-pipe inside diameter, air pipe
BETAW	Ratio of orifice-to-pipe inside diameter, water pipe
RFAI	Air Reynolds number based on flange taps
RDAI	Air Reynolds number based on D and ½ D taps
RFWI	Water Reynolds number based on flange taps
RDWI	Water Reynolds number based on D and ½ D taps
KFAI	Air discharge coefficient based on flange taps
KDAI	Air discharge coefficient based on D and ½ D taps
KFWI	Water discharge coefficient based on flange taps
KDWI	Water discharge coefficient based on D and ½ D taps
FRFA	Air mass flow rate based on flange taps (lbm/sec)
FRDA	Air mass flow rate based on D and ½ D taps (lbm/sec)
FRFW	Water mass flow rate based on flange taps (lbm/sec)
FRDW	Water mass flow rate based on D and ½ D taps (lbm/sec)
D	Inside diameter of test section (ft)
RHOWT	Water density in test section (lbm/ft^3)
RHOAT	Air density in test section (lbm/ft^3)
RLM	Liquid Reynolds number (Lockhart-Martinelli)
RGM	Gas Reynolds number (Lockhart-Martinelli)
VL	Liquid velocity (ft/sec)
VG	Gas velocity (ft/sec)
PDROPL	Fictitious liquid pressure drop (lb/ft^2/10ft)
PDROPG	Fictitious gas pressure drop (lb/ft^2/10ft)
TPPDi	Lockhart-Martinelli two-phase pressure drop prediction (lb/in^2/10ft)

RLC	Liquid Reynolds number (Chenoweth-Martin)
RGC	Gas Reynolds number (Chenoweth-Martin)
PDLC	Dimensionless group, ψ_L (all-liquid flow)
PDGC	Dimensionless group, ψ_G (all-gas flow)
CORPAR	Chenoweth-Martin correlation parameter
VFR	Volumetric flow ratio (liquid-to-gas)
PDRLC	Fictitious all-liquid pressure drop ($lb/ft^2/10ft$)
LVOLFR	Liquid volume fraction

DATA INPUT CARD ORDER

Card 1: MFA, MDA, MFW, MDW

Card 2: RFA(I), I = 1, MFA

Card 3: KFA(I), = 1, MFA

Card 4: RDA(I), I = 1, MDA

Card 5: KDA(I), I = 1, MDA

Card 6: RFW(I), I = 1, MFW

Card 7: KFW(I), I = 1, MFW

Card 8: RDW(I), I = 1, MDW

Card 9: KDW(I), I = 1, MDW

Card 10: D1A, D2A, D1W, D2W

Card 11: HMFA, HMDA, T1FA, TAFA, P1

Card 12: HMFW, HMDW, T1FW, TAFW

Card 13: PT, TTFW, TTFA

Card 14: DT, LT

Card 15: MG, ML

Card 16: XG(I), I = 1, MG

Card 17: XL(I), I = 1, ML

Card 18: FGTT(I), I = 1, MG

Card 19: FGTV(I), I = 1, MG

Card 20: FGVT(I), I = 1, MG

Card 21: FGVV(I), I = 1, MG

Card 22: FLTT(I), I = 1, ML

Card 23: FLTV(I), I = 1, ML

Card 24: FLVT(I), I = 1, ML

Card 25: FLVV(I), I = 1, ML

```
C                            APPENDIX IV
C
C             WATER AND AIR MASS FLOW RATE DETERMINATION
C
C     SQUARE EDGE CONCENTRIC ORIFICE WITH FLANGE TAPS AND D&HALF-D TAPS
C                     STANDARD ASME METHODS USED
C             ORIFICE MATERIAL --- TYPE 304 STAINLESS STEEL
C
C                               AND
C
C         CALCULATION OF LOCKHART-MARTINELLI AND CHENOWETH-MARTIN
C                  TWO-PHASE PRESSURE DROP PREDICTION
C
      REAL LT, LVCLFR
      REAL*8 RFA(17) ,KFA(17) ,RFAI,KFAI,RDA(22) ,KDA(22) ,RDAI,KDAI,
     *RFW(23) ,KFW(23) ,RFWI,KFWI,RDW(23) ,KDW(23) ,RDWI,KDWI,
     *       XG(17) ,XL(53) ,XI,FGTT(17) ,FGTV(17) ,FGVT(17) ,FGVV(17),
     *FGTTI,FGTVI,FGVTI,FGVVI,  FLTT(53) ,FLTV(53) ,FLVT(53) ,FLVV(53) ,
     *FLTTI,FLTVI,FLVTI,FLVVI
C
C     VISCOSITY OF AIR AT TEMPERATURE XX (DEG F) (0<XX<500)
      VISCOA(XX) = 1.089790E-05 + 1.917221E-08*XX - 7.086247E-12*XX**2
C
C     VISCOSITY OF WATER AT TEMPERATURE XX (DEG F) (32<XX<120)
      VISCOW(XX) = 2.546764E-03 - 6.985562E-05*XX + 1.207512E-06*XX**2 -
     *1.285602E-08*XX**3 + 7.467161E-11*XX**4 - 1.788613E-13*XX**5
C
C     SPECIFIC GRAVITY OF WATER AT TEMPERATURE XX (DEG F) (39.2<XX<104)
      SPGRW(XX) = 0.99837633 + 1.060576E-04*XX - 1.593186E-06*XX**2
C
C     SPECIFIC GRAVITY OF MERCURY AT TEMPERATURE XX (DEG F) (32<XX<113)
      SPGRHG(XX) = 13.63905 - .0013630303 * XX
C
C     CONVERSION FACTOR -- INCHES OF WATER TO PSI AT TEMPERATURE XX (DEG F)
      CFH2O(XX) = 62.42732 * SPGRW(XX)/1728.0
C
C     CONVERSION FACTOR -- INCHES OF MERCURY TO PSI AT TEMPERATURE XX (DEG F)
      CFHG(XX) = 0.4891585 * SPGRHG(XX)/13.54
```

```
C
C     AREA EXPANSION FACTOR AT TEMPERATURE XX (DEG F)
      AREAEX(XX) = 1.0 + (XX - 68.0) * 1.85185E-05
C
      READ (5,100) MFA,MDA,MFW,MDW
  100 FORMAT(4I3)
      READ (5,210) (RFA(I),I = 1,MFA)
      READ (5,210) (KFA(I),I = 1,MFA)
      READ (5,210) (RDA(I),I = 1,MDA)
      READ (5,210) (KDA(I),I = 1,MDA)
      READ (5,210) (RFW(I),I = 1,MFW)
      READ (5,210) (KFW(I),I = 1,MFW)
      READ (5,210) (RDW(I),I = 1,MDW)
      READ (5,210) (KDW(I),I = 1,MDW)
      READ (5,210) D1A,D2A,D1W,D2W
      READ (5,210) HMFA,HMDA,T1FA,TAFA,P1
      READ (5,210) HMFW,HMDW,T1FW,TAFW
      READ (5,210) PT,TTFW,TTFA
      READ (5,210) DT, LT
  210 FORMAT(8F10.0)
      READ (5,150) MG,ML
  150 FORMAT (2I3)
      READ (5,200) (XG(I),I = 1,MG)
      READ (5,200) (XL(I),I = 1,ML)
      READ (5,200) (FGTT(I),I = 1,MG)
      READ (5,200) (FGTV(I),I = 1,MG)
      READ (5,200) (FGVT(I),I = 1,MG)
      READ (5,200) (FGVV(I),I = 1,MG)
      READ (5,200) (FLTT(I),I = 1,ML)
      READ (5,200) (FLTV(I),I = 1,ML)
      READ (5,200) (FLVT(I),I = 1,ML)
      READ (5,200) (FLVV(I),I = 1,ML)
  200 FORMAT (10F8.0)
      WRITE (6,390)
  390 FORMAT('1')
      WRITE (6,391)
  391 FORMAT(////////////)
      BETAA = D2A/D1A
      BETAW = D2W/D1W
      WRITE(6,340)
  340 FORMAT( T58,'TWO-PHASE FLOW TEST RIG',//  ,T57,'NAVAL POSTGRADUATE
     * SCHOOL',//  ,T65,'JUNE 1969',//)
      WRITE (6,341)
  341 FORMAT( T25,'-------------------------------------------------------
     *-----------------------------------'//)
      WRITE (6,342)
  342 FORMAT( T56,'MASS FLOW RATE DETERMINATION',//, T55,'SQUARE-EDGE CO
     *NCENTRIC ORIFICE',//,  T63,'ASME STANDARD'///, T80,'AIR',T89,'WATE
```

```
     *R'/)
      WRITE(6,400) D1A,D1W,D2A,D2W,BETAA,BETAW,T1FA,T1FW,TAFA,TAFW
  400 FORMAT( T44,'PIPE DIAMETER (IN.)',  T75,2F1C.4,/, T44,'ORIFICE DIA
     *METER (IN.)',  T75,2F10.4,/,  T44,'BETA (D2/D1)', T75,2F10.4,/,
     *T44,  'TEMPERATURE IN PIPE (DEG.F.)',T75,2F10.4,/,   T44,'TEMPERAT
     *URE OF ATM. (DEG.F.)',  T75,2F10.4)
      WRITE(6,401) P1
  401 FORMAT( T44,'PRESSURE IN PIPE (PSIA)',T75,F10.4////)
      GAMMA = 1.4
      R = 53.3448
      T1A = T1FA + 459.69
C
C     GMU = 32.174 * MU (CCEFFICIENT OF VISCOSITY)
      GMUW = VISCCW(T1FW)
      GMUA = VISCCA(T1FA)
C
C     SPECIFIC GRAVITY OF WATER IN PIPE
      GH2O1 = SPGRW(T1FW)
C
C     DENSITY OF WATER IN PIPE
      RHOW1 = 62.42732 * GH2O1
C
C     SPECIFIC GRAVITY OF WATER IN AIR FLCW MEASUREMENT MANOMETER
      GH2OA = SPGRW(TAFA)
C
C     SPECIFIC GRAVITY OF WATER IN WATER FLOW MEASUREMENT MANOMETER
      GH2OW = SPGRW(TAFW)
C
C     SPECIFIC GRAVITY OF MERCURY IN WATER FLOW MEASUREMENT MANOMETER
      GHGW = SPGRHG(TAFW)
      GHGA  = SPGRHG(TAFA)
      RHOWA = GH2CA * 62.42732
      RHOWW = GH2OW * 62.42732
      RHOHGA = GHGW * RHOWW
      RHOAIR = 144.0 * P1/(R * T1A)
      HWFA = HMFA * (RHOWA - RHOAIR)/62.317
      HWDA = HMDA * (RHOWA - RHOAIR)/62.317
      HWFW = HMFW * (RHOHGA - RHOWW)/62.317
      HWDW = HMDW * (RHOHGA - RHOWW)/62.317
      DELPF = HWFA * CFH2C(68.0)
      DELPD = HWDA * CFH2C(68.0)
      YF = EXPFAC(BETAA,DELPF,P1,GAMMA)
      YD = EXPFAC(BETAA,DELPD,P1,GAMMA)
      FAA = AREAEX(T1FA)
      FAW = AREAEX(T1FW)
      FRFA = 0.35
      J = 0
  250 FRA1 = FRFA
```

```
      RFAI = 15.2784 * FRFA/(D1A * GMUA)
      IF (RFAI.LE.1.0E 06) GO TO 230
      KFAI = KFA(MFA)
      GO TO 260
  230 IF(J.GT.0) GO TO 240
      CALL SPLIN1(RFA,KFA,MFA,RFAI,KFAI)
      GO TO 260
  240 CALL SPLINN(RFA,KFA,MFA,RFAI,KFAI)
  260 FRFA = 0.16384266 * KFAI* D2A**2 * FAA * YF * SQRT(P1 * HWFA/T1A)
      J = J + 1
      IF(J.GT.100) GO TO 750
      EPS2 = ABS(FRFA - FRA1)
      IF (EPS2 .GT. 1.0E-06) GO TO 250
      GO TO 345
  750 WRITE(6,800)
  800 FORMAT(T25,'MORE THAN 100 ITERATIONS FOR AIR FLANGE TAPS -- LATEST
     * VALUES PRINTED'/)
  345 FRDA = FRFA
      K = 0
  350 FRA2 = FRDA
      RDAI = 15.2784 * FRDA/(D1A * GMUA)
      IF (RDAI.LE.1.0E 06) GO TO 360
      KDAI = KDA(MDA)
      GO TO 380
  360 IF(K.GT.0) GO TO 370
      CALL SPLIN1(RDA,KDA,MDA,RDAI,KDAI)
      GO TO 380
  370 CALL SPLINN(RDA,KDA,MDA,RDAI,KDAI)
  380 FRDA = 0.16384266 * KDAI* D2A**2 * FAA * YD * SQRT(P1 * HWFA/T1A)
      K = K + 1
      IF(K.GT.100) GO TO 850
      EPS3 = ABS(FRDA - FRA2)
      IF (EPS3 .GT. 1.0E-06) GO TO 350
      GO TO 498
  850 WRITE(6,900)
  900 FORMAT(T25,'MORE THAN 100 ITERATIONS FOR AIR    D    TAPS -- LATEST
     * VALUES PRINTED'/)
  498 L = 0
      FRFW = 35.0
  205 FRW1 = FRFW
      RFWI = 15.2784 * FRFW/(D1W * GMUW)
      IF (RFWI.LE.1.0E 06) GO TO 23
      KFWI = KFW(MFW)
      GO TO 26
   23 IF(L.GT.0) GO TO 24
      CALL SPLIN1(RFW,KFW,MFW,RFWI,KFWI)
      GO TO 26
   24 CALL SPLINN(RFW,KFW,MFW,RFWI,KFWI)
```

```
 26 FRFW = 9.972222E-02 * KFWI * D2W**2 * FAW * SQRT(HWFW * RHOW1)
    L = L + 1
    IF(L.GT.100) GO TO 75
    EPS = ABS(FRFW - FRW1)
    IF(EPS.GT.1.0E-06) GO TO 205
    GO TO 34
 75 WRITE(6,80)
 80 FORMAT(T25,'MORE THAN 100 ITERATIONS FOR WATER FLANGE TAPS -- LATE
   *ST VALUES PRINTED'/)
 34 FRDW = FRFW
    M = 0
300 FRW2 = FRDW
    RDWI = 15.2784 * FRDW/(D1W * GMUW)
    IF (RDWI.LE.1.0E 06) GO TO 36
    KDWI = KDW(MDW)
    GO TO 38
 36 IF(M.GT.0) GO TO 37
    CALL SPLIN1(RDW,KDW,MDW,RDWI,KDWI)
    GO TO 38
 37 CALL SPLINN(RDW,KDW,MDW,RDWI,KDWI)
 38 FRDW = 9.972222E-02 * KDWI * D2W**2 * FAW * SQRT(HWDW * RHOW1)
    M = M + 1
    IF(M.GT.100) GO TO 85
    EPS1 = ABS(FRDW - FRW2)
    IF(EPS1.GT.1.0E-06) GO TO 300
    GO TO 499
 85 WRITE(6,90)
 90 FORMAT(T25,'MORE THAN 100 ITERATIONS FOR WATER     D   TAPS -- LATE
   *ST VALUES PRINTED'/)
499 WRITE(6,500)
500 FORMAT( T65,'AIR',T98,'WATER',/,T51,'-------------------------------
   *--', T85,'------------------------------')
    WRITE (6,501)
501 FORMAT( T52, 'FLANGE TAPS', T71, 'D TAPS', T86, 'FLANGE TAPS',
   *T105, 'D TAPS'/)
    WRITE(6,600) HMFA,HMDA,HMFW,HMDW
600 FORMAT(T25, 'PRESSURE DROP', T49, F9.4, T59,'IN.H2O', T66,F9.4, T7
   *6, 'IN.H2O',T83, F9.4, T93, 'IN.HG', T100, F9.4, T110, 'IN.HG')
    WRITE(6,601) RFAI,RDAI,RFWI,RDWI
601 FORMAT( T25, 'REYNOLDS NUMBER', T47, 1P4D17.6)
    WRITE(6,602)KFAI,KDAI,KFWI,KDWI
602 FORMAT( T25, 'DISCHARGE COEFFICIENT' T47, 0P4D17.6)
    WRITE(6,603) FRFA,FRDA,FRFW,FRDW
603 FORMAT( T25, 'MASS FLOW RATE (LBM/SEC)', T49, F11.6, T66, F11.6,
   *T83, F11.6,  T100, F11.6)
C
C
C
```

```
C     LOCKHART-MARTINELLI TWO-PHASE PRESSURE DROP PREDICTION
C
      PI = 3.1415926
      D = DT/12.0
      A = PI * D*D/4.0
      G = 32.174
      FRL = (FRFW + FRDW)/2.0
      FRG = (FRFA + FRDA)/2.0
      GMUL = VISCOW(TTFW)
      GMUG = VISCCA(TTFA)
C
C     SPECIFIC GRAVITY OF WATER IN TEST SECTION
      GH2OT = SPGRW(TTFW)
      RHOWT = GH2CT  * 62.42732
      TTA = TTFA + 459.69
      RHOAT = 144.0 * PT/(R * TTA)
      RLM = 4.0 * FRL/(PI * D * GMUL)
      RGM = 4.0 * FRG/(PI * D * GMUG)
      VL = FRL/(RHOWT * A)
      VG = FRG/(RHOAT * A)
C
C     FL = FRICTION FACTOR = FG
      FL = 0.024
      FG = 0.024
C
      PDROPL = RHOWT * FL * LT * VL**2/(G * D * 2.0)
      PDROPG = RHOAT * FG * LT * VG**2/(G * D * 2.0)
      IF(PDROPL.GT.0.0.AND.PDROPG.GT.0.0) GO TO 255
      IF(PDROPL.GT.0.0) GO TO 235
      WRITE (6,220) PDROPG
  220 FORMAT( T44, 'NO LIQUID FLOW - AIR PRESSURE DROP (LB/SQFT) =',
     *T52,1PE10.4,/)
      GO TO 755
  235 WRITE (6,245) PDROPL
  245 FORMAT( T44, 'NO AIR FLOW - LIQUID PRESSURE DROP (LB/SQFT) =',
     *T52,E10.4,/)
      GO TO 755
  255 XI = SQRT(PDROPL/PDROPG)
      CALL SPLIN1 (XG,FGTT,MG,XI,FGTTI)
      CALL SPLIN1 (XG,FGTV,MG,XI,FGTVI)
      CALL SPLIN1 (XG,FGVT,MG,XI,FGVTI)
      CALL SPLIN1 (XG,FGVV,MG,XI,FGVVI)
      CALL SPLIN1 (XL,FLTT,ML,XI,FLTTI)
      CALL SPLIN1 (XL,FLTV,ML,XI,FLTVI)
      CALL SPLIN1 (XL,FLVT,ML,XI,FLVTI)
      CALL SPLIN1 (XL,FLVV,ML,XI,FLVVI)
      TPPD1 = FGTTI**2 * PDROPG/144.0
      TPPD2 = FGTVI**2 * PDROPG/144.0
```

```
      TPPD3 = FGVTI**2 * PDROPG/144.0
      TPPD4 = FGVVI**2 * PDROPG/144.0
      TPPD5 = FLTTI**2 * PDROPL/144.0
      TPPD6 = FLTVI**2 * PDROPL/144.0
      TPPD7 = FLVTI**2 * PDROPL/144.0
      TPPD8 = FLVVI**2 * PDROPL/144.0
      WRITE (6,390)
      WRITE (6,391)
      WRITE (6,340)
      WRITE (6,341)
      WRITE (6,411) D, LT, TTFW, TTFA, PT
      WRITE (6,341)
      WRITE (6,510)
  510 FORMAT(T43, 'LOCKHART-MARTINELLI TWO-PHASE PRESSURE DROP PREDICTIO
     *N',//, T77, 'WATER', T92, 'AIR',/, T75, '-----------', T89, '-----
     *------')
      WRITE (6,511) RHOWT,RHOAT,RLM,RGM,VL,VG,PDROPL,PDROPG
      IF (RLM.GE.2.0E 03.AND.RGM.GE.2.0E 03) GO TO 405
      IF (RLM.GE.2.0E 03.AND.RGM.LT.2.0E 03) GO TO 425
      IF (RLM.LT.2.0E 03.AND.RGM.GE.2.0E 03) GO TO 450
      IF (RLM.LT.2.0E 03.AND.RGM.LT.2.0E 03) GO TO 475
  405 WRITE (6,410)
      WRITE (6,512) FLTTI,FGTTI,TPPD5,TPPD1
      GO TO 755
  425 WRITE (6,435)
      WRITE (6,512) FLTVI,FGTVI,TPPD6,TPPD2
      GO TO 755
  450 WRITE (6,460)
      WRITE (6,512) FLVTI,FGVTI,TPPD7,TPPD3
      GO TO 755
  475 WRITE (6,485)
      WRITE (6,512) FLVVI,FGVVI,TPPD8,TPPD4
  410 FORMAT (T40,'THE FLOW IS TURBULENT-TURBULENT'/)
  435 FORMAT (T40,'THE FLOW IS TURBULENT-VISCOUS'/)
  460 FORMAT (T40,'THE FLOW IS VISCOUS-TURBULENT'/)
  485 FORMAT (T40,'THE FLOW IS VISCOUS-VISCOUS'/)
  411 FORMAT( T46,'TEST SECTION DIAMETER (FT)          =', 1PE12.4,/, T46
     *, 'TEST SECTION LENGTH (FT)           =',  E12.4,/, T46,'TEST SECT
     *ION WATER TEMP. (DEG.F.)  =',  E12.4,/, T46,'TEST SECTION AIR TEMP
     *. (DEG.F.)     =',  E12.4,/, T46,'TEST SECTION PRESSURE (PSIA)
     *  =',  E12.4,/)
  511 FORMAT( T40, 'DENSITY (LBM/CU-FT)                =',1P2E14.5,/, T40,
     *'REYNOLDS NUMBER                   =',  2E14.5,/, T40,'VELOCITY (FT/S
     *EC)                =',  2E14.5,/, T40,'FICT. PRESS. DROP (PSF/10FT)
     *  =',  2E14.5/)
  512 FORMAT( T40, 'CORRELATION PARAMETER              =',  2E14.5,/, T40,
     *'PREDICTED TWO-PHASE PRESSURE',/,T53,'DROP (PSI/10FT)    =',2E14.5/
     *)
```

```
C
C
C     CHENOWETH-MARTIN CORRELATICN COMPUTATIONS
C
C
C
  755 RLC = D * (FRL + FRG)/(GMUL * A)
      RGC = D * (FRL + FRG)/(GMUG * A)
      FLC = 0.0241
      FGC = 0.0232
      PDLC = FLC * LT/D
      PDGC = FGC * LT/D
      CORPAR = PDGC * RHOWT/(PDLC * RHCAIR)
      VLC = (FRL + FRG)/(RHOWT * A)
      PDRLC = RHOWT * FLC * LT * VLC**2/(G * D * 2.0)
C
C     VOLUMETRIC FLOW RATIO -- LIQUID/GAS
      VFR = (FRL * RHOAT)/(FRG * RHOWT)
C
C     LIQUID VOLUME FRACTION
      LVOLFR = 1.0/(1.0 + 1.0/VFR)
      WRITE (6,341)
      WRITE (6,805)
  805 FORMAT(     T48,'CHENOWETH-MARTIN TWO-PHASE FLOW CALCULATIONS'/)
      WRITE (6,905) RLC,RGC,PDLC,PDGC,CORPAR,VFR,PDRLC,LVOLFR
      WRITE (6,390)
  905 FORMAT(/T46,'REYNOLDS NUMBER (LIQUID)          =', 1PE15.6,/,
     *T46,'REYNOLDS NUMBER (GAS)             =', E15.6,/, T46,'DIM.-LESS GR
     *OUP (ALL LIQUID)    =',  E15.6,/, T46,'DIM.-LESS GROUP (ALL GAS)
     *    =', E15.6,/,T46,'CORRELATION PARAMETER              =',E15.6,/,T46,
     *'VOLUMETRIC FLOW RATIC (LQ/GS)  =', E15.6,/,T46, 'FICT. ALL-LIQ. P
     *RESS.DROP(PSF) =',  E15.6,/,T46,    'LIQUID VOLUME FRACTION
     * =', E15.6//)
      STOP
      END
```

```
      FUNCTION EXPFAC(B,DP,P,G)
      EXPFAC = 1.0 - (0.41 + 0.35 * B**4) * DP/(P * G)
      RETURN
      END


      SUBROUTINE SPLIN1(X,Y,M,XINT,YINT)                                SPLIN045
      IMPLICIT REAL*8 (A-H),REAL*8 (O-Z)                                SPLIN046
      DIMENSION X(M),Y(M),C(4,300)                                      SPLIN047
      CALL SPLICO(X,Y,M,C)                                              SPLIN048
      K=1                                                               SPLIN049
      ENTRY SPLINN(X,Y,M,XINT,YINT)                                     SPLIN050
    3 IF(XINT-X(1)) 70,1,2                                              SPLIN051
   70 K=1                                                               SPLIN052
      GO TO 7                                                           SPLIN053
    1 YINT=Y(1)                                                         SPLIN054
      RETURN                                                            SPLIN055
    2 IF(XINT-X(K+1))6,4,5                                              SPLIN056
    4 YINT=Y(K+1)                                                       SPLIN057
      RETURN                                                            SPLIN058
    5 K=K+1                                                             SPLIN059
      IF(M-K) 71,71,3                                                   SPLIN060
   71 K=M-1                                                             SPLIN061
      GO TO 7                                                           SPLIN062
    6 IF(XINT-X(K))13,12,11                                             SPLIN063
   12 YINT=Y(K)                                                         SPLIN064
      RETURN                                                            SPLIN065
   13 K=K-1                                                             SPLIN066
      GO TO 6                                                           SPLIN067
    7 PRINT 101,XINT                                                    SPLIN068
  101 FORMAT(8H0XINT = D18.9,32H, OUT OF RANGE FOR INTERPOLATION)       SPLIN069
   11 YINT=(X(K+1)-XINT)*(C(1,K)*(X(K+1)-XINT)**2+C(3,K))               SPLIN070
      YINT=YINT+(XINT-X(K))*(C(2,K)*(XINT-X(K))**2+C(4,K))              SPLIN071
      RETURN                                                            SPLIN072
      END                                                               SPLIN073
```

```
      SUBROUTINE SPLICO(X,Y,M,C)                                        SPLIN074
      IMPLICIT REAL*8 (A-H),REAL*8 (O-Z)                                SPLIN075
      DIMENSION X(M),Y(M),C(4,300),D(300),P(300),E(300),A(300,3),B(300),SPLIN076
     1Z(300)                                                            SPLIN077
      MM=M-1                                                            SPLIN078
      DO 2 K=1,MM                                                       SPLIN079
      D(K)=X(K+1)-X(K)                                                  SPLIN080
      P(K)=D(K)/6.                                                      SPLIN081
    2 E(K)=(Y(K+1)-Y(K))/D(K)                                           SPLIN082
      DO 3 K=2,MM                                                       SPLIN083
    3 B(K)=E(K)-E(K-1)                                                  SPLIN084
      A(1,2)=-1.-D(1)/D(2)                                              SPLIN085
      A(1,3)=D(1)/D(2)                                                  SPLIN086
      A(2,3)=P(2)-P(1)*A(1,3)                                           SPLIN087
      A(2,2)=2.*(P(1)+P(2))-P(1)*A(1,2)                                 SPLIN088
      A(2,3)=A(2,3)/A(2,2)                                              SPLIN089
      B(2)=B(2)/A(2,2)                                                  SPLIN090
      DO 4 K=3,MM                                                       SPLIN091
      A(K,2)=2.*(P(K-1)+P(K))-P(K-1)*A(K-1,3)                           SPLIN092
      B(K)=B(K)-P(K-1)*B(K-1)                                           SPLIN093
      A(K,3)=P(K)/A(K,2)                                                SPLIN094
    4 B(K)=B(K)/A(K,2)                                                  SPLIN095
      Q=D(M-2)/D(M-1)                                                   SPLIN096
      A(M,1)=1.+Q+A(M-2,3)                                              SPLIN097
      A(M,2)=-Q-A(M,1)*A(M-1,3)                                         SPLIN098
      B(M)=B(M-2)-A(M,1)*B(M-1)                                         SPLIN099
      Z(M)=B(M)/A(M,2)                                                  SPLIN100
      MN=M-2                                                            SPLIN101
      DO 6 I=1,MN                                                       SPLIN102
      K=M-I                                                             SPLIN103
    6 Z(K)=B(K)-A(K,3)*Z(K+1)                                           SPLIN104
      Z(1)=-A(1,2)*Z(2)-A(1,3)*Z(3)                                     SPLIN105
      DO 7 K=1,MM                                                       SPLIN106
      Q=1./(6.*D(K))                                                    SPLIN107
      C(1,K)=Z(K)*Q                                                     SPLIN108
      C(2,K)=Z(K+1)*Q                                                   SPLIN109
      C(3,K)=Y(K)/D(K)-Z(K)*P(K)                                        SPLIN110
    7 C(4,K)=Y(K+1)/D(K)-Z(K+1)*P(K)                                    SPLIN111
      RETURN
      END                                                               SPLIN112
```

TWO-PHASE FLOW TEST RIG

NAVAL POSTGRADUATE SCHOOL

JUNE 1969

MASS FLOW RATE DETERMINATION

SQUARE-EDGE CONCENTRIC ORIFICE

ASME STANDARD

	AIR	WATER
PIPE DIAMETER (IN.)	2.0872	3.0862
ORIFICE DIAMETER (IN.)	1.4602	2.1597
BETA (D2/D1)	0.6996	0.6998
TEMPERATURE IN PIPE (DEG.F.)	100.0000	100.0000
TEMPERATURE OF ATM. (DEG.F.)	68.0000	68.0000
PRESSURE IN PIPE (PSIA)	50.0000	

	AIR		WATER	
	FLANGE TAPS	D TAPS	FLANGE TAPS	D TAPS
PRESSURE DROP	23.4100 IN.H2O	23.0455 IN.H2O	15.0364 IN.HG	14.7972 IN.HG
REYNOLDS NUMBER	2.011906D 05	2.027541D 05	3.777007D 05	3.778586D 05
DISCHARGE COEFFICIENT	0.698388D 00	0.703752D 00	0.695378D 00	0.701270D 00
MASS FLOW RATE (LBM/SEC)	0.350282	0.353005	35.000793	35.015427

```
                    TWO-PHASE FLOW TEST RIG
                  NAVAL POSTGRADUATE SCHOOL
                          JUNE 1969
-----------------------------------------------------------------------

      TEST SECTION DIAMETER (FT)              =  2.5883E-01
      TEST SECTION LENGTH (FT)                =  1.0000E 01
      TEST SECTION WATER TEMP. (DEG.F.)       =  1.0000E 02
      TEST SECTION AIR TEMP. (DEG.F.)         =  1.0000E 02
      TEST SECTION PRESSURE (PSIA)            =  5.0000E 01
-----------------------------------------------------------------------

    LOCKHART-MARTINELLI TWO-PHASE PRESSURE DROP PREDICTION

                                         WATER          AIR
                                      -----------   -----------
   DENSITY (LBM/CU-FT)            =   6.19934E 01   2.41153E-01
   REYNOLDS NUMBER                =   3.75389E 05   1.35731E 05
   VELOCITY (FT/SEC)              =   1.07323E 01   2.77127E 01
   FICT. PRESS. DROP (PSF/10FT)   =   1.02893E 02   2.66875E 00

   THE FLOW IS TURBULENT-TURBULENT

   CORRELATION PARAMETER          =   0.20454D 01   0.12647D 02
   PREDICTED TWO-PHASE PRESSURE
              DROP (PSI/10FT)     =   0.29894E 01   0.29645E 01
-----------------------------------------------------------------------

        CHENOWETH-MARTIN TWO-PHASE FLOW CALCULATIONS

      REYNOLDS NUMBER (LIQUID)          =   3.791598E 05
      REYNOLDS NUMBER (GAS)             =   1.364849E 07
      DIM.-LESS GROUP (ALL LIQUID)      =   9.311010E-01
      DIM.-LESS GROUP (ALL GAS)         =   8.963295E-01
      CORRELATION PARAMETER             =   2.474706E 02
      VOLUMETRIC FLOW RATIO (LQ/GS)     =   3.872697E-01
      FICT. ALL-LIQ. PRESS.DROP(PSF)    =   1.054082E 02
      LIQUID VOLUME FRACTION            =   2.791597E-01
```

LIST OF REFERENCES

1. U. S. Navy Marine Engineering Laboratory Research and Development Report 358/66, A Preliminary Parametric Study of a Water-Augmented Air-Jet for High-Speed Ship Propulsion, by R. K. Muench and T. G. Keith, Jr., February 1967.

2. Davison, W. R., and Sadowski, T. J., "Water-Augmented Turbofan Engine," AIAA Journal of Hydronautics, v. 2, n. 1, p. 14-20, January 1968.

3. Quandt, E. R., On the Theory of One Type of Air-Water Jet (Mist-Jet) for Ship Propulsion, Naval Ship Research and Development Center, Annapolis, Maryland (personal communication).

4. Knudson, T. C., Theoretical Optimization of a Water-Augmented Turbofan Marine Propulsion System, Master's Thesis, Naval Postgraduate School, Monterey, California, 1968.

5. Keenan, J. H., and Keyes, F. G., Thermodynamic Properties of Steam, Wiley, 1936.

6. Lockhart, R. W., and Martinelli, R. C., "Proposed Correlation of Data for Isothermal Two-Phase, Two-Component Flow in Pipes," Chemical Engineering Progress, v. 45, n. 1, p. 39-48, January 1949.

7. Chenoweth, J. M., and Martin, M. W., "Turbulent Two-Phase Flow," Petroleum Refiner, v. 34, n. 10, p. 151-155, October 1955.

8. Reese, B. A., and Richard, L. P., "Equilibrium Between Phases in Converging-Diverging Nozzles," Progress in Astronautics and Rocketry, v. 6, "Detonation and Two-Phase Flow," p. 209-240, Academic Press, 1962.

9. Dukler, A. E., Wicks, W., III, and Cleveland, R. G., "Frictional Pressure Drop in Two-Phase Flow: A. A Comparison of Existing Correlations for Pressure Loss and Holdup," A.I.Ch.E.Journal, v. 10, n. 1, p. 38-43, January 1964.

10. Power Test Codes Supplement, Chapter 4, "Flow Measurement-Instruments and Apparatus," PTC 19.5, v. 4, part 5, American Society of Mechanical Engineers, 1959.

11. Muench, R. K., and Ford, A. E., A Water-Augmented Air-Jet for the Propulsion of High Speed Marine Vehicles, AIAA Paper No. 69-405, presented at AIAA 2nd Advanced Marine Vehicles and Propulsion Meeting, Seattle, Washington, 21-23 May 1969.

INITIAL DISTRIBUTION LIST

		No. Copies
1.	Defense Documentation Center Cameron Station Alexandria, Virginia 22314	20
2.	Library, Code 0212 Nava Postgraduate School Monterey, California 93940	2
3.	Commander, Naval Air Systems Command Navy Department Washington, D. C. 20360	1
4.	Mr. R. F. Lawson Naval Applications Office of Naval Research Pasadena, California 91101	1
5.	Mr. R. K. Muench Power and Propulsion Department Naval Ship Research and Development Laboratory Annapolis, Maryland 21402	1
6.	Dean of Research Administration Naval Postgraduate School Monterey, California 93940	2
7.	Chairman, Department of Aeronautics Naval Postgraduate School Monterey, California 93940	1
8.	Professor M. H. Vavra Department of Aeronautics Naval Postgraduate School Monterey, California 93940	1
9.	Professor R. D. Zucker Department of Aeronautics Naval Postgraduate School Monterey, California 93940	1
10.	LT. Randolph G. Watson, USN c/o O. E. Heathman RR No. 1, Penfield, Illinois 61862	1

DOCUMENT CONTROL DATA - R & D

(Security classification of title, body of abstract and indexing annotation must be entered when the overall report is classified)

1. ORIGINATING ACTIVITY *(Corporate author)* Naval Postgraduate School Monterey, California 93940	2a. REPORT SECURITY CLASSIFICATION Unclassified
	2b. GROUP

3. REPORT TITLE
Computer Optimization of Water-Augmented Turbofan Concept and Development of a Test Facility for Two-Phase Flow

4. DESCRIPTIVE NOTES *(Type of report and inclusive dates)*
Aeronautical Engineer's Thesis; (June 1969)

5. AUTHOR(S) *(First name, middle initial, last name)*
Randolph Grant Watson

6. REPORT DATE	7a. TOTAL NO. OF PAGES	7b. NO. OF REFS
June 1969	109	11

8a. CONTRACT OR GRANT NO.	9a. ORIGINATOR'S REPORT NUMBER(S)
b. PROJECT NO.	
c.	9b. OTHER REPORT NO(S) *(Any other numbers that may be assigned this report)*
d.	

10. DISTRIBUTION STATEMENT
Distribution of this document is unlimited.

11. SUPPLEMENTARY NOTES	12. SPONSORING MILITARY ACTIVITY
	Naval Postgraduate School Monterey, California 93940

13. ABSTRACT

A turbofan engine propulsion system in which large amounts of water are injected into the fan discharge duct is investigated with the goal of increasing both the thrust and propulsive efficiency while retaining the light-weight qualities of a standard turbofan engine. A parametric computer analysis is used to examine the effect of several variables, including water-to-gas generator air ratio, water injection velocity, fan duct pressure loss, and fan duct thermal and dynamic nonequilibrium, upon thrust and propulsive efficiency. In addition, the design parameters of fan pressure ratio and fan bypass ratio are examined for their optimum values, and optimum operating combinations of water-to-gas ratio and water injection velocity are determined.

A test apparatus is developed for the direct measurement of wall friction force in two-phase flows. A computer program is presented to reduce experimental data and compare with pressure drop predicted by two empirical correlations.

Security Classification

14. KEY WORDS	LINK A		LINK B		LINK C	
	ROLE	WT	ROLE	WT	ROLE	WT
MARINE PROPULSION						
TWO-PHASE FLOW						
WATER-AUGMENTED TURBOFAN						

DD FORM 1 NOV 65 1473 (BACK)

S/N 0101-807-6821

Security Classification

A-31409